Freshwater microbialites from Laguna Bacalar, Quintana Roo, Mexico: effects controlling their growth.

by

Set Ismael Castro

A thesis submitted in partial fulfillment of the requirements for the degree of

Master of Science

Department of Earth and Atmospheric Sciences
University of Alberta

ABSTRACT

Microbialites are among the oldest direct evidence of life on Earth. They reached their greatest abundance and diversity during the Proterozoic and decline thereafter. The decline has been attributed to grazing and/or burrowing by metazoan, to changes in ocean chemistry leading to a drop in carbonate saturation, or to substrate and elemental competition with other organisms capable of precipitating calcium carbonate ($CaCO_3$). Here we examine the freshwater microbialites of Laguna Bacalar (Mexico) in hope of better understanding the various factors controlling their growth, and internal fabric. It was concluded that microbialite growth was controlled by the supersaturation of water with regards to $CaCO_3$, however, the laminated (stromatolitic) and clotted (thrombolitic) fabric were dependent on sediment transport and availability. The presence of gastropods and bivalves appeared not to influence growth due to the fast growth rate employed by microbialites as well as to the endolithic growth of the cyanobacteria present.

Dedicada a mi Dios por todas sus bendiciones. A mi Tata, a mi Nita y al mejor hermano que Dios me pudo dar *Saulo Manuel Castro Contreras* por todo su apoyo y amor.

ACKNOWLEDGMENTS

First and foremost I would like to thank by advisors Dr. Kurt O. Konhauser and Dr. Murray K. Gingras for their support and guidance through out my MSc. but also for their belief in me. They opened their lab and had the patience to teach me, and guide me throughout my MSc.

I would also like to thank my Dr. John-Paul Zonneveld the input he provided regarding my thesis, and his support as a committee member and defense chair.

Additionally I am grateful for the opportunity to collaborating with Dr. Greg Dick, Dr. Pecoits, Dr. Noah Planavsky, Natalie Aubet, and my brother Saulo Manuel Castro-Contreras. Working with each of them has truly been a pleasure.

Sincere thanks are extended to Dr. Tom Chacko (Associate Chair) for his support. Thanks also to Dr. Sergei Matveev for his assistance with the electron microprobe, to Mark Labbe and the thin section lab for all their work, to Guangcheng Chen for his geochemical analyses, and to Dr. George Owttrim who opened up his lab for me to work on cyanobacterial samples.

I would like to thank all my friends, and family who have supported me throughout this time. Thanks to Nestor (El Viejo), Natta (la que sabe TODO), Luis (Sammy), Kelsey, Newton (my writing buddy), Jaime, Aleks, Vir, Jose, Anita (la gallega), Nur , the Torhjelms, the Winklers, the Glovers, the Gerbrands, the Garretts, and the Chartrands.

TABLE OF CONTENTS

LIST OF TABLES

LIST OF FIGURES

CHAPTER 2

CHAPTER 3

APPENDIX 1

LIST OF ABBREVIATIONS AND NOMENCLATURE

DNA – deoxyribonucleic acid
DOC – dissolved organic carbon
DOI – digital object identifier
DIC – dissolved inorganic carbon
EDTA – ethylenediaminetetraacetic acid
EPS – extracellular polymeric substance
IC – ion chromatograph
ICDD – International center for diffraction data
ICP-MS – inductively coupled plasma mass spectrometry
ICSD – Inorganic crystal structure database
PAR – photosynthetic active radiation
PPL – plain polarized light
RNA – ribonucleic acid
SEM – scanning electron microscope
SMOW – vienna standard mean ocean water
UV – ultra violet
V-PDB – vienna pee dee belemnite
XPL – cross polarized light
XRD – x-ray diffraction

Chapter 1: Introduction

Microbialites have been identified as some of the earliest evidence for life, first observed ca. 3.5 Ga in the Strelley Pool formation, Australia and in the Swaziland Supergroup, South Africa (Lowe, 1980; Walter et al., 1980; Awramik et al., 1983; Lowe, 1983; Byerly et al., 1986; Awramik, 1991; Schopf, 1993; Hofmann et al., 1999; Hofmann, 2000; Allwood et al., 2006; Schopf, 2006; Allwood et al., 2007; Allwood et al., 2009). Microbialites form through the trapping, binding, and/or precipitation of calcium carbonate by benthic bacteria (Burne and Moore, 1987), and display a vast number of outer morphologies that included domes, laterally hemispheroidal, cones and columns – both branched and coniform (Logan et al., 1964; Awramik and Sprinkle, 1999; Awramik and Grey, 2005; Schopf, 2006; Altermann, 2008). They are differentiated into different groups (stromatolites, thrombolites, dendrolites, and leiolites) based on their internal fabric of which stromatolites and thrombolites have historically received the most attention (Aitken, 1967; Awramik and Margulis, 1974; Riding, 1991; Riding, 2000; Riding, 2011)

Kalkowsky (1908) first introduce the term ‘stromatolite’ in order to describe the laminated domal and columnar carbonates from the oolitic beds of the Lower Buntsandstein formation near the Harz Mountain. The definition had a biogenic implication that would henceforth become contentious when describing and defining such structures. This difficulty is, in part, due to absence of well-preserved bacteria in many fossil stromatolites, but also to their similarities with abiogenic structures (Read, 1976; Thrailkill, 1976; Walter, 1976; Semikhatov et al., 1979; Grotzinger and Knoll, 1999; Riding, 1999). The occurrence of biologically mediated modern stromatolites having both structural and morphological similarities to fossil samples (Dill et al., 1986; Knoll and Golubic, 1992; Reid et al., 2003; Andres and Pamela Reid, 2006; Bosak et al., 2013) and the discovery of preserved bacteria within fossilized stromatolites (Schopf and Blacic, 1971) has allowed the assumption of a biogenic formation of these structures.

Thrombolites were first defined by Aitken (1967) in describing the Cambro-Ordovician examples from the southern Canadian Rocky Mountains. The samples, while similar to stromatolites, lacked internal lamination, and instead displayed internal clotting. These were still regarded as biogenically mediated structures, however, what constituted 'clotting' would become contentious as the description appeared to be directly associated with the scale the sample was described with. Many would attempt to better define the scale and type of structure related to 'thrombolites', however, it would not be until Shapiro (2000) and the introduction of meso- and macro-structures in describing the different types of textures, that microbialite samples could begin to be better characterized.

Microbialites have been pervasive throughout Earth's history, spanning the geological record from the Archean through to the modern, despite several interruptions in their record (Awramik, 1991; Visscher et al., 1998; Grotzinger and Knoll, 1999; Dupraz et al., 2009). During the Archean, environmental conditions were much different than at present. The atmosphere lacked oxygen and mostly comprised of nitrogen, methane and carbon dioxide (Wiechert, 2002; Westall, 2006), and the oceans are thought to have been supersaturated with regards to calcium carbonate ($CaCO_3$)(Arp et al., 1999; Grotzinger and Knoll, 1999; Arp et al., 2001). The predominant microbialites during this time were stromatolites, and their formation appears to have been limited to shallow-marine evaporitic basins, while morphologically they appear less complex than their Proterozoic counterparts (Altermann, 2008). To date only 48 different morphotypes have been described (Schopf, 2006). In contrast the Proterozoic microbialites saw their greatest abundance and diversity during this period, and display more than 1000 different forms, colonizing silicicalstic and carbonate platform settings, as well as epicontinental alkaline lakes and rivers (Buck, 1980; Beukes, 1987; Awramik, 1992; Awramik and Sprinkle, 1999; Schieber, 1999). Such diversification of microbialites began in the Paleoproterozoic (2500-1650 Ma), and reached its peak during the Mesoproterozoic (1350-1000 Ma)(Awramik, 1992). Such diversification appeared to coincide with more favorable environmental changes. The atmosphere became oxic (around 2400 Ma), while the formation of an ozone layer allowed the attenuation of UV radiation. A warm Mezoproterozic (Jenkins, 2003) was followed by global glaciation (snowball Earth) during the Neoproterozoic (Bodiselitsch et al., 2005), and what is assumed to be a corresponding change in ocean chemistry. A decrease in the saturation state of oceans with regards to calcium carbonates during this time saw the suppression of stromatolites yet the prominent appearance of thrombolites (Grotzinger, 1989; Grotzinger, 1990; Grotzinger and Knoll, 1999; Riding, 2011.

A decline in microbialite abundance and diversity has been observed in the Neoproterozoic, the cause of which remains a matter of debate. Garrett (1970) attributed their decline to correlate with the evolution of metazoans and their ability to graze and burrow into microbialites, thereby causing their destruction at a faster rate than these could overcome. The observed ability of modern gastropods to feed and destroy algal mats in marine environments would support such a notion (Fenchel, 1998). Further evidence supporting such a hypothesis has come from the extreme environments (e.g. hypersaline, thermal, arid, or turbulent) that most modern microbialites are found in, as grazing and burrowing organisms are limited, therefore allowing microbialite growth (Mata and Bottjer, 2012). However, the onset of metazoans do not appear to directly coincide with the decline of microbialites (Grotzinger, 1990; Awramik and Sprinkle, 1999; Riding, 2006), suggesting that other factors may have caused, or contributed to the decline.

Microbialite growth is a result of the ability of cyanobacteria to precipitate calcium carbonate, as well as trap and bind grains through the use of extracellular polymeric substance (EPS). The supersaturation of water with regards to $CaCO_3$ is, therefore, an important factor influencing growth. The photosynthetic activity of cyanobacteria causes a shift in the carbonate saturation state of the water as a result of the uptake of CO_2 for carbon fixation, which, in turn, causes a local increase in pH and carbonate ion concentrations, facilitating carbonate precipitatino (Simkiss and Wilbur, 1989; Riding, 2006; Planavsky and Ginsburg, 2009). Temperature and pCO_2 decreases in seawater as a result of glaciation during the Neoproterozoic, in conjunction with the proposed decrease in ocean carbonate saturation state, would have had an adverse effect on microbialite growth, and potentially be the cause of their decline (Grotzinger, 1990; Grotzinger, 1994; Riding, 1997; Grotzinger and Knoll, 1999; Ridgwell and Zeebe, 2005; Riding, 2011).

While the microbialite decline at the Precambrian/Phanerozoic boundary is the most noteworthy, microbialites have seen several periods of abundance and subsequent declines throughout their history (c.f. Riding, 2011, Fig. 14). During the Archean and Precambrian, competition for substrates and nutrients are thought to have been minimal. However, as algal and other invertebrate organisms evolved the ability to form exoskeletons, a decrease in microbialites from the Ordovician onward, appears to be directly linked to the competition for limited carbonate ions in the oceans (Fischer, 1965; Pratt, 1979; Riding and Liang, 2005; Riding, 2011). During the Mesozoic, microbialites would see resurgence across a vast rage of environments (e.g.fresh water, deep shelf), and become important reef-builds, particularly in the case of thrombolites. This has been presumed to be a direct result of the mass extinction event that occurred at the Permian/Triassic boundary and the corresponding elimination of organisms previously outcompeting microbialites for substrates and nutrients (Schubert and Bottjer, 1992; Kershaw et al., 2002; Hips and Haas, 2006; Riding, 2011; Mata and Bottjer, 2012). However, a resurgence of microbialites following other mass extinction events (End-Ordovician, End-Triassic, and End-Cretaceous)(Riding, 2006) has not always been observed, suggesting that the controlling factors influencing microbialite growth are likely to be more complex, and multidimensional.

The ability to better understand microbialites and the factors influencing their growth and diversity was largely aided by the discovery of modern samples. The work by Black (1933) and Ginsburg (1955) on modern microbialites led to further discoveries which include the localities of Hamelin Pool, Lagoa Salgada, Cuatro Cienegas, Lake Pavillion and Kelley lake. The already vast knowledge from the fossil record was available to be compared with and complemented by the research on these modern microbialites. At present more than 30 locations of modern microbialites have been found in several environments, from freshwater to marine (Tbl. 1). Some microbialites, as previously stated, thrive in extreme environments thought to restrict the presence of burrowing and grazing organisms. However, some have been found to grow and thrive in conditions where microbialite co-existence with grazing and burrowing organisms is possible. One such location is Laguna Bacalar, a freshwater lake connected to the Xul-ha sinkhole, and the locality where some of the largest microbialites are found. Microbialites have been observed on the western shore of the lake, as well as on the riverbank and the main channel of the river connecting the lake to the Xul-ha sinkhole, the primary source of fresh water.

The Laguna Bacalar microbialites display both thrombolitic, and stromatolitic meso-structures, and form predominantly with a domal morphology, coalescing with each other to form larger formations. The water chemistry of the lake and river have been found to be supersaturated with regards to $CaCO_3$, most likely the result of the degassing of karstic waters surfacing at the Xul-ha sinkhole, favoring microbialite growth. However, there also seems to be a limiting factor controlling growth, as they only colonize the southern most part of the lake, and disappearing past the town Bacalar. The supersaturation of the water with respect to $CaCO_3$, the ability to co-exist with gastropods, while overcoming bivalve colonization of their surfaces, provides us with new insights into the various mechanisms that regulate microbialite growth. The results herein have the ability to shed light on the factors that influence microbialite growth and the formation of two distinctive textures, but may also shed light on the cause of the Proterozoic microbialite decline observed in the geological record.

ABED, R.M.M., GOLUBIC, S., GARCIA-PICHEL, F., CAMOIN, G.F., and SPRACHTA, S., 2003, Characterization of microbialite-forming cyanobacteria in a tropical lagoon: Tikehau Atoll, Tuamotu, French Polynesia: Journal of Phycology, v. 39, p. 862-873.

AITKEN, J.D., 1967, Classification and environmental significance of cryptalgal limestones and dolomites with illustrations from Cambrian and Ordovician of southwestern Alberta: Journal of Sedimentary Petrology, v. 37, p. 1163-1178.

ALLWOOD, A.C., GROTZINGER, J.P., KNOLL, A.H., BURCH, I.W., ANDERSON, M.S., COLEMAN, M.L., and KANIK, I., 2009, Controls on development and diversity of Early Archean stromatolites: Proceedings of the National Academy of Sciences of the United States of America, v. 106, p. 9548-9555.

ALLWOOD, A.C., WALTER, M.R., BURCH, I.W., and KAMBER, B.S., 2007, 3.43 billion-year-old stromatolite reef from the Pilbara Craton of Western Australia: Ecosystem-scale insights to early life on Earth: Precambrian Research, v. 158, p. 198-227.

ALLWOOD, A.C., WALTER, M.R., KAMBER, B.S., MARSHALL, C.P., and BURCH, I.W., 2006, Stromatolite reef from the Early Archaean era of Australia: Nature, v. 441, p. 714-718.

ALTERMANN, W., 2008, Accretion, trapping and binding of sediment in Archean stromatolites - Morphological expression of the antiquity of life: Space Science Reviews, v. 135, p. 55-79.

ANDRES, M.S., and PAMELA REID, R., 2006, Growth morphologies of modern marine stromatolites: A case study from Highborne Cay, Bahamas: Sedimentary Geology, v. 185, p. 319-328.

ARP, G., REIMER, A., and REITNER, J., 1999, Calcification in cyanobacterial biofilms of alkaline salt lakes: European Journal of Phycology, v. 34, p. 393-403.

ARP, G., REIMER, A., and REITNER, J., 2001, Photosynthesis-induced biofilm calcification and calcium concentrations in phanerozoic oceans: Science, v. 292, p. 1701-1704.

ARP, G., REIMER, A., and REITNER, J., 2003, Microbialite formation in seawater of increased alkalinity, Satonda crater lake, Indonesia: Journal of Sedimentary Research, v. 73, p. 105-127.

AWRAMIK, S.M., 1991, Archaean and Proterozoic stromatolites, *in* Riding, R., ed., Calcareous Alae and Stromatolites: Springer-Verlag, New York, p. 571.

AWRAMIK, S.M., 1992, The History and Significance of Stromatolites, *in* Schidlowski, M., Golubic, S., Kimberley, M.M., McKirdy, D.M., and Trudinger, P.A., eds., Early Organic Evolution: Springer Berlin Heidelberg, p. 435-449.

AWRAMIK, S.M., and GREY, K., 2005, Stromatolites: biogenicity, biosignatures, and bioconfusion, in Hoover, R.B., Levin, G.V., Rozanov, A.Y., and Gladstone, G.R. eds.: SPIE, San Diego, CA, USA, p. 59060P-9.

Awramik, S.M., and Margulis, L., 1974, Definiton of stromatolite, Stromatolite Newsletter, p. 5.

Awramik, S.M., Schopf, J.W., and Walter, M.R., 1983, Filamentous Fossil Bacteria from the Archean of Western Australia, *in* B. Nagy, R.W.J.C.G., and Schidlowski, M., eds., Developments in Precambrian Geology: Elsevier, p. 249-266.

Awramik, S.M., and Sprinkle, J., 1999, Proterozoic stromatolites: The first marine evolutionary biota: Historical Biology, v. 13, p. 241-253.

Beukes, N.J., 1987, Facies relations, depositional-environments and diagenesis in a major early Proterozoic stromatolitic carbonate platform to basinal sequence, Campbellrand Subgroup, Transvaal Supergroup, Southern-Africa: Sedimentary Geology, v. 54, p. 1-46.

Black, M., 1933, The algal sediments of Andros Island, Bahamas: Philosophical Transactions of the Royal Society of London Series B-Containing Papers of a Biological Character, v. 222, p. 165-U50.

Bodiselitsch, B., Koeberl, C., Master, S., and Reimold, W.U., 2005, Estimating duration and intensity of Neoproterozoic snowball glaciations from Ir anomalies: Science, v. 308, p. 239-242.

Bosak, T., Liang, B., Wu, T.D., Templer, S.P., Evans, A., Vali, H., Guerquin-Kern, J.L., Klepac-Ceraj, V., Friedman, J., Sim, M.S., and Mui, J., 2013, Cyanobacterial diversity and activity in modern conical microbialites (vol 10, pg 384, 2012): Geobiology, v. 11, p. 100-100.

Braithwaite, C.J.R., Casanova, J., Frevert, T., and Whitton, B.A., 1989, Recent stromatolites in landlocked pools on Aldabra, Western Indian ocean: Palaeogeography, Palaeoclimatology, Palaeoecology, v. 69, p. 145-165.

Braithwaite, C.J.R., and Zedef, V., 1994, Living hydromagnesite stromatolites from Turkey: Sedimentary Geology, v. 92, p. 1-5.

Braithwaite, C.J.R., and Zedef, V., 1996, Hydromagnesite stromatolites and sediments in an alkaline lake, Salda Golu, Turkey: Journal of Sedimentary Research, v. 66, p. 991-1002.

Buck, S.G., 1980, Stromatolite and ooid deposits within the fluvial and lacustrine sediments of the Precambrian Ventersdorp Supergroup of South-Africa: Precambrian Research, v. 12, p. 311-330.

Burne, R.V., and Moore, L.S., 1987, Microbialites: organosedimentary deposits of benthic microbial communities: Palaios, v. 2, p. 241-254.

Burne, R.V., 1995, Microatoll microbialites of Lake Clifton, Western-Australia - the morphological analogs of cryptozoon Proliferum Hall, the first formally named stromatolite - reply: Facies, v. 32, p. 257-257.

Byerly, G.R., Lower, D.R., and Walsh, M.M., 1986, Stromatolites from the 3,300-3,500-Myr Swaziland Supergroup, Barberton Mountain Land, South-Africa: Nature, v. 319, p. 489-491.

Camoin, G.F., Gautret, P., Montaggioni, L.F., and Cabioch, G., 1999, Nature and environmental significance of microbialites in Quaternary reefs: the Tahiti paradox: Sedimentary Geology, v. 126, p. 271.

Charpyroubaud, C.J., Charpy, L., and Cremoux, J.L., 1990, Nutrient budget of the lagoonal waters in an open central South-Pacific atoll (Tikehau, Tuamotu, French-Polynesia): Marine Biology, v. 107, p. 67-73.

Defarge, C., Trichet, J., Maurin, A., and Hucher, M., 1994, Kopara in polynesian atolls - early stages of formation of calcareous stromatolites: Sedimentary Geology, v. 89, p. 9-23.

Dill, R.F., Shinn, E.A., Jones, A.T., Kelly, K., and Steinen, R.P., 1986, Giant subtidal stromatolites forming in normal salinity waters: Nature, v. 324, p. 55-58.

Duane, M.J., and Al-Zamel, A.Z., 1999, Syngenetic textural evolution of modern sabkha stromatolites (Kuwait): Sedimentary Geology, v. 127, p. 237-245.

Dupraz, C., Reid, R.P., Braissant, O., Decho, A.W., Norman, R.S., and Visscher, P.T., 2009, Processes of carbonate precipitation in modern microbial mats: Earth-Science Reviews, v. 96, p. 141-162, doi: 10.1016/J.Earscirev.2008.10.005.

Ferris, F.G., Thompson, J.B., and Beveridge, T.J., 1997, Modern Freshwater Microbialites from Kelly Lake, British Columbia, Canada: Palaios, v. 12, p. 213-219.

Fenchel, T., 1998, Formation of laminated cyanobacterial mats in the absence of benthic fauna: Aquatic Microbial Ecology, v. 14, p. 235-240.

Fischer, A.G., 1965, Fossils early life and atmospheric history: Proceedings of the National Academy of Sciences of the United States of America, v. 53, p. 1205-1213.

Frost, J.G., 1974, Subtidal algal stromatolites from Florida backreef environment: Journal of Sedimentary Petrology, v. 44, p. 532-537.

Gautret, P., Camoin, G., Golubic, S., and Sprachta, S., 2004, Biochemical control of calcium carbonate precipitation in modern lagoonal microbialites, Tikehau atoll, French Polynesia: Journal of Sedimentary Research, v. 74, p. 462-478.

Garrett, P., 1970, Phanerozoic stromatolites: noncompetitive ecologic restriction by grazing and burrowing animals: Science, v. 169, p. 171-173.

Ginsburg, R.N., 1955, Recent Stromatolitic Sediments from South-Florida: Journal of Paleontology, v. 29, p. 723-724.

Gischler, E., Gibson, M.A., and Oschmann, W., 2008, Giant Holocene freshwater microbialites, Laguna Bacalar, Quintana Roo, Mexico: Sedimentology, v. 55, p. 1293-1309.

Golubic, S., and Focke, J.W., 1978, Phormidium-Hendersonii Howe - identity and significance of a modern stromatolite building microorganism: Journal of Sedimentary Petrology, v. 48, p. 751-764.

Greinert, J., Bohrmann, G., and Elvert, M., 2002, Stromatolitic fabric of authigenic carbonate crusts: result of anaerobic methane oxidation at cold seeps in 4,850 m water depth: International Journal of Earth Sciences, v. 91, p. 698-711.

Grotzinger, J.P., 1989, Facies and evolution of Precambrian carbonate depositional systems: emergence of the modern platform archetype.

Grotzinger, J.P., 1990, Geochemical model for Proterozoic stromatolite decline: American Journal of Science, v. 290A, p. 80-103.

Grotzinger, J.P., 1994, Trends in Precambrian carbonate sediments and their implication for understanding evolution, *in* Bengtson, S., ed., Nobel Symposium; Early life on earth, p. 245-258.

Grotzinger, J.P., and Knoll, A.H., 1999, Stromatolites in Precambrian carbonates: evolutionary mileposts or environmental dipsticks?: Annual Review of Earth and Planetary Sciences, v. 27, p. 313-358.

Grotzinger, J.P., and Knoll, A.H., 1999, Stromatolites in Precambrian carbonates: evolutionary mileposts or environmental dipsticks?: Annual Review of Earth and Planetary Sciences, v. 27, p. 313-358.

Hips, K., and Haas, J., 2006, Calcimicrobial stromatolites at the Permian-Triassic boundary in a western Tethyan section, Bukk Mountains, Hungary: Sedimentary Geology, v. 185, p. 239-253.

Hofmann, H., 2000, Archean stromatolites as microbial archives, *in* Riding, R.A., S. M., ed., Microbial sediments: Springer Verlag, New York, p. 315-327.

Hofmann, H.J., Grey, K., Hickman, A.H., and Thorpe, R.I., 1999, Origin of 3.45 Ga coniform stromatolites in Warrawoona Group, Western Australia: Geological Society of America Bulletin, v. 111, p. 1256-1262.

Javor, B.J., and Castenholz, R.W., 1981, Laminated microbial mats, Laguna Guerrero Negro, Mexico: Geomicrobiology Journal, v. 2, p. 237-273.

Jenkins, G.S., 2003, GCM greenhouse and high-obliquity Solutions for early Proterozoic glaciation and middle Proterozoic warmth: Journal of Geophysical Research: Atmospheres (1984–2012), v. 108.

Kalkowsky, E., 1908, Oolith und stromatolith im norddeutschen Buntsandstein: Zeitschrift der deutschen geologischen Gesells-chaft, v. 60, p. 68-125.

Kazmierczak, J., and Kempe, S., 2004, Microbialite formation in seawater of increased alkalinity, Satonda Crater Lake, Indonesia - Discussion: Journal of Sedimentary Research, v. 74, p. 314-317.

Kazmierczak, J., Kempe, S., Lopez-Garcia, P., Tavera, R., Kremer, B.,, and Moreira, D., 2008, Modern and sub-recent carbonate microbialites from the alkaline crater lake Alchichica, Mexico, in Reitner, J. ed., Internationales Kalkowsky-Symposium: University of Göttingen, Göttingen, p. 87.

Kempe, S., and Kazmierczak, J., 1990, Chemistry and stromatolites of the sea-linked Satonda Crater Lake, Indonesia - a recent model for the Precambrian sea: Chemical Geology, v. 81, p. 299-310.

Kempe, S., Kazmierczak, J., Landmann, G., Konuk, T., Reimer, A., and Lipp, A., 1991, Largest known microbialites discovered in Lake Van, Turkey: Nature, v. 349, p. 605-608.

Kershaw, S., Guo, L., Swift, A., and Fan, J.S., 2002, Microbialites in the Permian-Triassic boundary interval in Central China: Structure, age and distribution: Facies, v. 47, p. 83-89.

Knoll, A.H., and Golubic, S., 1992, Proterozoic and Living Cyanobacteria, *in* Schidlowski, M., Golubic, S., Kimberley, M.M., McKirdy, D.M., and

Trudinger, P.A., eds., Early Organic Evolution: Springer-Verlag, Belin, p. 450-462.

Kobluk, D.R., and Crawford, D.R., 1990, A modern hypersaline organic mud and gypsum-dominated basin and associated microbialites: Palaios, v. 5, p. 134-148.

Konishi, Y., Prince, J., and Knott, B., 2001, The fauna of thrombolitic microbialites, Lake Clifton, Western Australia: Hydrobiologia, v. 457, p. 39-47.

Laval, B., Cady, S.L., Pollack, J.C., McKay, C.P., Bird, J.S., Grotzinger, J.P., Ford, D.C., and Bohm, H.R., 2000, Modern freshwater microbialite analogues for ancient dendritic reef structures: Nature, v. 407, p. 626-629.

Logan, B.W., Rezak, R., and Ginsburg, R.N., 1964, Classification and Environmental Significance of Algal Stromatolites: The Journal of Geology, v. 72, p. 68-83.

Love, F.G., Simmons, G.M., Parker, B.C., Wharton, R.A., and Seaburg, K.G., 1983, Modern conophyton-like microbial mats discovered in Lake Vanda, Antarctica: Geomicrobiology Journal, v. 3, p. 33-48.

Lowe, D.R., 1980, Stromatolites 3,400-Myr old from the archean of western-australia: Nature, v. 284, p. 441-443.

Lowe, D.R., 1983, Restricted shallow-water sedimentation of Early Archean stromatolitic and evaporitic strata of the Strelley Pool Chert, Pilbara Block, Western Australia: Precambrian Research, v. 19, p. 239-283.

Mann, C.J., and Nelson, W.M., 1989, Microbialitic structures in Storr's Lake, San Salvador Island, Bahama Islands: Palaios, v. 4, p. 287-293.

Mata, S.A., and Bottjer, D.J., 2012, Microbes and mass extinctions: paleoenvironmental distribution of microbialites during times of biotic crisis: Geobiology, v. 10, p. 3-24.

Mcmaster, R.L., and Conover, J.T., 1966, Recent algal stromatolites from Canary Islands: Journal of Geology, v. 74, p. 647-&.

Nicholson, J.A.M., Stolz, J.F., and Pierson, B.K., 1987, Structure of a microbial mat at Great Sippewissett Marsh, Cape-Cod, Massachusetts: Fems Microbiology Ecology, v. 45, p. 343-364.

Parker, B.C., Simmons, G.M., Jr., Love, F.G., Wharton, R.A., Jr., and Seaburg, K.G., 1981, Modern stromatolites in Antarctic Dry Valley Lakes: BioScience, v. 31, p. 656-661.

Petrash, D.A., Lalonde, S.V., Pecoits, E., Gingras, M.K., and Konhauser, K.O., 2010, Microbially-catalyzed cementation of modern gypsum-dominated thrombolites: Geochimica Et Cosmochimica Acta, v. 74, p. A811-A811.

Planavsky, N., and Ginsburg, R.N., 2009, Taphonomy of Modern Marine Bahamian Microbialites: Palaios, v. 24, p. 5-17, doi: Doi 10.2110/Palo.2008.P08-001r.

Pratt, B.R., 1979, Early Cementation and Lithification in Inter-Tidal Cryptalgal Structures, Boca Jewfish, Bonaire, Netherlands Antilles: Journal of Sedimentary Petrology, v. 49, p. 379-386.

Pringault, O., de Wit, R., and Camoin, G., 2005, Irradiance regulation of photosynthesis and respiration in modern marine microbialites built by benthic cyanobacteria in a tropical lagoon (New Caledonia): Microb Ecol, v. 49, p. 604-16.

Rasmussen, K.A., Macintyre, I.G., and Prufert, L., 1993, Modern stromatolite reefs fringing a brackish coastline, Chetumal Bay, Belize: Geology, v. 21, p. 199-202.

Read, J.F., 1976, Chapter 3.1 Calcretes and Their Distinction from Stromatolites, *in* Walter, M.R., ed., Developments in sedimentology: Elsevier, p. 55-71.

Reid, R.P., James, N.P., Macintyre, I.G., Dupraz, C.P., and Burne, R.V., 2003, Shark Bay stromatolites: Microfabrics and reinterpretation of origins: Facies, v. 49, p. 299-324.

Reid, R.P., Macintyre, I.G., Browne, K.M., Steneck, R.S., and Miller, T., 1995, Modern marine stromatolites in the Exuma-Cays, Bahamas - uncommonly common: Facies, v. 33, p. 1-17.

Reid, R.P., Visscher, P.T., Decho, A.W., Stolz, J.F., Bebout, B.M., Dupraz, C., Macintyre, L.G., Paerl, H.W., Pinckney, J.L., Prufert-Bebout, L., Steppe, T.F., and DesMarais, D.J., 2000, The role of microbes in accretion, lamination and early lithification of modern marine stromatolites: Nature, v. 406, p. 989-992.

Reitner, J., 1993, Modern cryptic microbialite/metazoan facies from Lizard Island (Great Barrier Reef, Australia) formation and concepts: Facies, v. 29, p. 3-39.

Richert, L., Golubic, S., Le Guedes, R., Herve, A., and Payri, C., 2006, Cyanobacterial populations that build 'kopara' microbial mats in Rangiroa, Tuamotu Archipelago, French Polynesia: European Journal of Phycology, v. 41, p. 259-279.

Ridgwell, A., and Zeebe, R.E., 2005, The role of the global carbonate cycle in the regulation and evolution of the Earth system: Earth and Planetary Science Letters, v. 234, p. 299-315.

Riding, R., 1991, Classification of microbial carbonates, *in* Riding, R., ed., Calcareous Algae and Stromatolites: Springer-Verlag, Berlin, p. 21-51.

Riding, R., 1997, Stromatolite decline: a brief reassessment: Facies, v. 36, p. 227-230.

Riding, R., 1999, The term stromatolite: towards an essential definition: Lethaia, v. 32, p. 321-330.

Riding, R., 2000, Microbial carbonates: the geological record of calcified bacterial-algal mats and biofilms: Sedimentology, v. 47, p. 179-214.

Riding, R., 2006, Cyanobacterial calcification, carbon dioxide concentrating mechanisms, and Proterozoic-Cambrian changes in atmospheric composition: Geobiology, v. 4, p. 299-316.

Riding, R., 2006, Microbial carbonate abundance compared with fluctuations in metazoan diversity over geological time: Sedimentary Geology, v. 185, p. 229-238.

Riding, R., 2011, Microbialites, stromatolites, and thrombolites, in Reitner, J., and Thiel, V. eds., Encyclopedia of Geobiology: Springer, Netherlands, p. 635-654.

Riding, R., and Liang, L.Y., 2005, Geobiology of microbial carbonates: metazoan and seawater saturation state influences on secular trends during the Phanerozoic: Palaeogeography Palaeoclimatology Palaeoecology, v. 219, p. 101-115.

Sabater, S., 2000, Structure and architecture of a stromatolite from a Mediterranean stream: Aquatic Microbial Ecology, v. 21, p. 161-168.

Sabater, S., Guasch, H., Romani, A., and Munoz, I., 2000, Stromatolitic communities in Mediterranean streams: adaptations to a changing environment: Biodiversity and Conservation, v. 9, p. 379-392.

Shen, J.W., and Wang, Y., 2008, Modern microbialites and their environmental significance, Meiji reef atoll, Nansha (Spratly) Islands, South China Sea: Science in China Series D-Earth Sciences, v. 51, p. 608-617.

Schieber, J., 1999, Microbial mats in terrigenous clastics: the challenge of identification in the rock record: Palaios, v. 14, p. 3-12.

Schopf, J.W., 1993, Microfossils of the Early Archean Apex Chert - New Evidence of the Antiquity of Life: Science, v. 260, p. 640-646.

Schopf, J.W., 2006, Fossil evidence of Archaean life: Philosophical Transactions of the Royal Society B-Biological Sciences, v. 361, p. 869-885.

Schopf, J.W., and Blacic, J.M., 1971, New Microorganisms from the Bitter Springs Formation (Late Precambrian) of the North-Central Amadeus Basin, Australia: Journal of Paleontology, v. 45, p. 925-960.

Schubert, J.K., and Bottjer, D.J., 1992, Early Triassic Stromatolites as Post Mass Extinction Disaster Forms: Geology, v. 20, p. 883-886.

Semikhatov, M.A., Gebelein, C.D., Cloud, P., Awramik, S.M., and Benmore, W.C., 1979, Stromatolite Morphogenesis - Progress and Problems: Canadian Journal of Earth Sciences, v. 16, p. 992-1015.

Shapiro, R.S., 2000, A comment on the systematic confusion of thrombolites: Palaios, v. 15, p. 166-169.

Simkiss, K., and Wilbur, K.M., 1989, Biomineralization : cell biology and mineral deposition: Academic Press, San Diego, xiv, 337 p.

Stolz, J.F., B. Nagy, R.W.J.C.G., and Schidlowski, M., 1983, Fine structure of the stratified microbial community at Laguna Figueroa, Baja California, Mexico. I. Methods of in situ study of the laminated sediments, Developments in Precambrian Geology: Elsevier, p. 371-384.

Thrailkill, J., 1976, Chapter 3.2 Speleothems, *in* Walter, M.R., ed., Developments in sedimentology: Elsevier, p. 73-86.

Vasconcelos, C., Warthmann, R., McKenzie, J.A., Visscher, P.T., Bittermann, A.G., and van Lith, Y., 2006, Lithifying microbial mats in Lagoa Vermelha, Brazil: Modern Precambrian relics?: Sedimentary Geology, v. 185, p. 175-183.

Visscher, P.T., Reid, R.P., Bebout, B.M., Hoeft, S.E., Macintyre, I.G., and Thompson, J.A., 1998, Formation of lithified micritic laminae in modern marine stromatolites (Bahamas): the role of sulfur cycling: American Mineralogist, v. 83, p. 1482-1493.

WALTER, M.R., 1976, Chapter 3.3 Geyserites of Yellowstone National Park: An Example of Abiogenic "Stromatolites", *in* Walter, M.R., ed., Developments in sedimentology: Elsevier, p. 87-112.

WALTER, M.R., BUICK, R., and DUNLOP, J.S.R., 1980, Stromatolites 3,400-3,500 Myr Old from the North-Pole Area, Western-Australia: Nature, v. 284, p. 443-445.

WESTALL, F., DE RONDE, C.E.J., SOUTHAM, G., GRASSINEAU, N., COLAS, M., COCKELL, C.S., and LAMMER, H., 2006, Implications of a 3.472-3.333 Gyr-old subaerial microbial mat from the Barberton greenstone belt, South Africa for the UV environmental conditions on the early Earth: Philosophical Transactions of the Royal Society B-Biological Sciences, v. 361, p. 1857-1875

WIECHERT, U.H., 2002, Earth's early atmosphere: Science, v. 298, p. 2341-2342.

WINSBOROUGH, B.M., and GOLUBIC, S., 1987, The role of diatoms in stromatolite growth - Two examples from modern fresh-water settings: Journal of Phycology, v. 23, p. 195-201.

A

Occurrence	**Microbialite size**	**Water depth**	**Depositional environment**	**Microbialite shapes; texture**	**Organisms**	**Mineralogy, cements**	**Type of accretion**	**Grazers present**
Shark Bay (arid) Australia[a]	-0.5m	Intertidal to shallow sub-tidal, -4m	Marine bay	Heads; laminated	*Schizothrix,* *Entophysalis major,* Solentia	Aragonite	Trapping and binding, precipitation	No
Exumas, (sub-tropical) Bahamas[b]	>2 m	Sub-tidal 7 to 8m	Marine	Heads; laminated well-laminated stromatolites to unlaminated thrombolites	*Schizothrix, Solentia,* diatoms, *Batophora, Acetabularia, Sargassum*	Aragonite Mg-calcite	Trapping, precipitation	Rare
	See Tbl. 1 from Reid et al. for depth, max height, shape, & surface community							
Kopara (tropical sub-tropical) Polynesia[c]	10s of cm	<1 m	Atoll	Crusts; laminated	*Phormidium*	Mg calcite, (aragonite)	Precipitates	Rare
Reef Cavities (tropical, sub-tropical) Australia[d]	Several cm Thrombolite 3-6cm thick	Sub-tidal	Marine caves	Thrombolite crusts (pillars); laminated, clotted Cryptic Microbialite	Bacteria (?)	Mg calcite	Org.-induced precipitates	Rare
Lagoa Vermelha (semi-arid w/in tropical) Brazil[e]	-3cm thick		Lagoon	Microbial mats	*Gloeocapsa, Spirulina* & *Microcoleus*. S^{2-} oxidizers. Eubacteria & Archea	Mg calcite	Org.-induced precipitates	No
Laguna Pirata Venezuela[f]	-0.7m	-1.5m	Lagoon	Heads, thrombolitic	Bacteria (?) Diatoms	Gypsum, calcite	Org.-induced precipitates	No
Tikehau - Tuamotu Archipelago (tropical) French Polynesia[g]	1m [2] -15cm, 5cm high[2] -20cm,10cm high[3]	9-25m[1] 5-15m[2] 5-26m[3]	Lagoon	Horizontally spreading microbial mats[1],Cobweb-like soft gelatinous masses[2], and Hemispherical to spherical domes[3]	*Phormidium laysanens*[2] *Phormidium, Symploca, Schizothrix*[3]	Mg calcite	trapping, precipitation	
Laguna Guerrero Negro (arid), Mexico[h]	0.3-2 cm		Lagoon	Mats Pinnacles	Microcoleus chthonoplastes Chromatium sp.	Mg calcite, (aragonite)	Trapping, precipitation	

South Florida (Tropical) U.S.A[i]	20-40mm (diameter) 4-10mm high	Intertidal zone intermittently floodedmud flats		Blue-green algae Depressed, convexoconcave hemispheroid		Calcite		
Al Khiran (sabkhas) Kuwait[j]	5-10cm		Sabknas Tidal creek	stromatolite bioherms Irregular hemispherical masses Type 1: 'cinder' stromatolite Type 2: 'polygonal' stromatolite	*Microcoleus chthonaplastees, Lyngbya eastuarii, Lynbya limnetica, Oscillatoria*	Mg-calcite, aragonite	Org.-induced precipitates	No
Aleutian accretional margin[k]	50-200mm diameter 5-70mm thick	4,850m	Downward growing crust-shaped stromatolites	Crust-like precipitations. Top and bottow different in appearance. One side is wavy, smooth and strongly cemented, the other rough and covered by uncemented to partly cemented sediment.	Bacteria, Archaea, *Clayptogena phaseoliformis, Pogonophora, Vestimentifera,* Acharax shells.	Mg-calcite aragonite	Binding, carbonate precipitation	some
Salda Golu (Mediteranean) Turkey[l]	-1m -5m vertical	-6m	Lake	Botryoidal (coliflower-like) Mounds	Diatoms, cyanobacteria, protozoans, nematodes	Hydromagnesite	` precipitates	No
Great Sippewissett Salt Marsh (tropical) Cape Cod[m]	-1cm thick	sandy/silty flats, several inches of water	Salt marsh	Microbial mats	*Lyngbya, Nostoc*, diatoms, *Phormidium, Amoebobacter,* Thiocapsa, Chromatium, Thiocysts, Thiocapsa pfennigii, Prosthecochloris		sediment binding	
Meiji atoll - Nansha island. South China Sea[n]	decimeter (domes) meter size (mats) mm (hairy microb.)	-15 m	Atoll	Hairy microbialites, gelatinous masses, mats. Filamentous cyanobacteria arranged in linear trichomes.	Phormidium laysonense		Org.-induced precipitates	

Aldabra (arid) Indian Ocean[o]	-70 cm	-2m	Landlocked pools	Columnar, dome	*Cardisoma, Geograpsus, Lyngbya, Phormidium, Schizothrix, Spirulina, Pleurocasns,* diatoms, *Cladophora, Shizoclonium*	Calcite, cements hard to identify. High-magnesium calcite	Org.-induced	yes
Barra barrida de olas Gran Ganaria Shelf[p]	0.5-10.0 cm	Above 100-125	Marine	Multicoloured spheroidal structures (red, green, white)	*Goniolithon accretum,* Porolithon, *Zonaria tournefotii,*	Calcite, aragonite (26.7%)		yes
Storr's Lake (sub-tropical) San Salvador Island[q]	1-15cm (stromatolites) 20-40cm (pinnacle)	-1.2m	Marine lake	Thrombilitic microbialites 'pie' mounds. Stromatolitic microbialites crumbly calcareous knobs; hard calcareous table-type. Stromatoliic pinnacle mounds	*Phormidium hendersonii* (Thrombolites)			

Modern microbialites found in saline environments. **a**. Reid et al., 2003; **b.** Dill et al., 1986; Reid et al., 1995; Visscher et al., 1998; Reid et al., 2000; Andres and Reid, 2006; **c.** Defarge et al., 1994; **d.** Reitner, 1993, **e.** Vasconcelos et al., 2006; **f.** Petrash, 2010; **g.** Charpyroubaud et al., 1990; Abed et al., 2003; Gautret et al., 2004; **h.** Javor and Castenholz, 1981; **i.** Ginsburg, 1955; Frost, 1974; Golubic and Focke, 1978; **j.** Duane and Al-Zamel, 1999; **k.** Greinert et al., 2002; **l.** Braithwaite and Zedef, 1994; Braithwaite and Zedef, 1996; **m.** Nicholson et al., 1987; **n.** Shen and Wang, 2008; **o.** Braithwaite et al., 1989; **p.** Mcmaster and Conover, 1966; **q.** Mann and Nelson, 1989; Dupraz et al., 2009;

B

Occurrence	**Microbialite size**	**Water depth**	**Depositional environment**	**Microbialite shapes; texture**	**Organisms**	**Mineralogy, cements**	**Type of accretion**	**Grazers present**
Laguna Bacalar (sub-tropical) Mexico[a]	-3m	-3 m	Lagoon	Heads, oncolites	*Homeothrix, Leptoxyngbya* diatoms, molluscs	Calcite	Precipitates, baffling	Yes
Cuatro Cienegas (arid) Mexico[b]	-0.2m	shallow	Lake	Heads, mats, oncolites; Laminated	*Homoeothrix, Schizothrix* diatoms	Calcite	Precipitates	Yes
Lake Clifton (arid) Australia[c]	-1.5m	shallow	Lake	Heads, mats; thrombolitic, (stromatolitic)	*Scytonema*, diatoms	Aragonite	Mainly precipitates	Yes
Pavilion Lake (temperate) Canada[d]	-3m	10 to >30 m	Lake	Digitate heads; dentritic	*Synechococcus*, Fischerella, Oscillatoria	Calcite	Trapping	Yes
Lake Van (temperate) Turkey[e]	-40m	10 to >100 m	Lake	Towers; irregular layering	*Pleurocapsa*, CFB group, diatoms	Aragonite, calcite	Precipitation	Yes
Satonda Crater (tropical) Indonesia[f]	-1m	-23 m	Alkaline	Cemented mats	*Pleurocapsa* group, red algae green algae,	Aragonite, Mg calcite	Biol.-induced calcification	Yes
Laguna Figueroa Baja California Mexico[g]			Lagoon	Microbial mats	*Microcoleus, Chloroflexus, Ectothiorhodospira, Chromatium, Thiocapsa, Oscillatoria, Spirulin*	Calcite		
Alchichica Mexico[h]		-8m	Crater lake	Spongy, columnar tufa	*Nostocales, Chroococcales, Oscillatoriales, Pleurocapsales Acaryochloris*	Calcite	Org.-iduced precipitates.	

Kelly Lake (temporate) Canada[i]	1.0-2.0cm (diameter and height)	-0.5m	Lake	irregular clotted factrics,small laminated hemispherical domes	*Gloeocapsa* (found in both), *Synechococcus* (thrombolites),*Pseudanobaena* (found in both, *Oscillaorea* (Stromatolites) heterotrophic bactera, diatoms, *Calothrix, Fischerella*	Calcite	Org.-induced precipitates	
La Solana Spain[j]	3-9 mm thick				*Schizothrix* spp., *Rivularia biasolettiana, Hymenostyluim recurvirostrum, Zygnoma, Spirogyra*, Mougoetia, diatoms	Calcite		yes
Lanke Vanda Antarctica[k]	Cones were: 2-5cm high and 3-5cm wide	31m	Lake	Coniform	*Phormidium frigidum, Lyngbya martensiana, Tetracystis sp., Navicula spp., Caloneis ventricosa, Cymbella sp., Stauroneis anceps, Nitzschia frustulum, Hantzschia amphioxys, Bryum algens*	Calcite	Org. -induced	no

Modern fresh water microbialites. **a**. Gischler et al., 2008; **b**. Winsborough, 1994; **c**. Burne, 1995; Konishi et al., 2001; **d**. Laval et al., 2000; **e**. Kempe et al., 1991; **f**.Kempe and Kazmierczak, 1990; Arp et al., 2003; Kazmierczak and Kempe, 2004; **g**. Stolz et al., 1983; **h**. Kazmierczak et al., 2008; **i**. Ferris et al., 1997; **j**. Sabater, 2000; Sabater et al., 2000; **k**. Parker et al., 1981; Love et al., 1983.

C

Occurrence	Microbialite size	Water depth	Depositional environment	Microbialite shapes; texture	Organisms	Mineralogy, cements	Type of accretion	Grazers present
Chetumal Bay (sub-tropical) Mexico[a]	-1.5m	-1.5m	Marive bay	Heads, oncolites, laminar columnar	*Scytonema*, *Phormidium*, bivalves, diatoms	Calcite	Mostrly precipitation	Yes
Bonaire (semi-arid) Netherland Antille islands[b]	-2m across -0.5m high (linear structure)	-1.5m	Gotomeer channel	Dome linear structures	Brine shrimp, unidentified swimming worms. Cyanobacteria	Aragonite, gypsum, halite	Org. -induced	No
(Tropical) New Caledonia[c]	-20cm in diameter -8cm in height	20-25m	Lagoon	Dome	*Phormidium crosbyanum*, *Halimeda opuntia*, *Halophilda*	Calcite		
Rangiroa Atoll - Tuamotu Archipelago. (tropical) French Polynesiad[d]	20-50 cm	shallow	Ponds	Polygonal microbial mats	*Schizothirx*, *Scytonema cf. Myochrous*, *Calothrix*, *Lyngbya aestuarii*, *Oscillatoria*, *Leptolyngbya*. *Spirulina*, *Johannesbaptistia*, *Chroococcus*, *Aphanothece*, *Gloeocapsa*, *Xenococcus*	Calcite		

Modern microbialites found in brackish waters. **a**. Rasmussen et al., 1993**;** **b**. Golubic and Focke, 1978; Kobluk and Crawford, 1990; **c.** Richert et al., 2006; **d**. Pringault et al., 2005

Table 1.1 - Compitaltion of several modern microbialites. (A) Microbialites found in saline environments. (B) Microbialites found growthing in freshwater environments. (C) Microbialites found growing in brackish environments.

CHAPTER 2: TEXTURAL AND GEOCHEMICAL FEATURES OF FRESHWATER MICROBIALITES FROM LAGUNA BACALAR, QUINTANA ROO, MEXICO

2.1 Introduction

Microbialites are organo-sedimentary structures that form in modern marine and non-marine environments through the accretion of sediment by benthic microbial communities (e.g., Burne and Moore, 1987). Based on their internal fabric, microbialites are subdivided into two distinct groups as per Shapiro (2000): (1) stromatolites, which show internally laminated mesostructures (as originally defined by Kalkowsky, 1908), and (2) thrombolites, distinguished by their non-laminated and clotted mesostructrue (Aitken, 1967). Both form through a combination of trapping, binding, and/or authigenic precipitation by benthic microbial communities (Hofmann, 1973; Riding, 1999; Riding, 2011), and abiogenic processes (e.g., cementation).

Stromatolites, in particular, are amongst the oldest direct evidence of life, occurring in rocks as old as ca. 3.5 Ga (Hofmann, 1973; Allwood et al., 2009). Unlike the Archean, where stromatolites have been observed as being limited to shallow-marine evaporitic basins (Lowe, 1983; Allwood et al., 2006; Schopf, 2006), by the Proterozoic, they were present in siliciclastic nearshore, intertidal (Schieber, 1999), and carbonate platforms (Beukes, 1987), as well as in epicontinental alkaline lakes and rivers, where the mats were commonly dolomitized and silicified (Buck, 1980). Morphologically, these ranged from domes and simple columns to elaborately branched and bulbous structures. There were two major periods of diversification, the first during the Paleoproterozoic (2500-1650 Ma), and the second during the latter stages of the Mesoproterozoic (1350-1000 Ma).

By the late Neoproterozoic and early Paleozoic, there was a sharp decline in stromatolite diversity (Fischer, 1965; Awramik, 1971; Walter and Heys, 1985; Awramik, 1991; McNamara and Awramik, 1992; Schopf et al., 2007). The cause of the decline remains controversial but factors such as the grazing and burrowing of mats by metazoans, competition for nutrients, substrate competition, and compositional changes in seawater chemistry may all have been contributory factors (Fischer, 1965; Pratt, 1982; Riding, 1997). For instance, the decline is coincident with a major change in biota, the advent of grazing and burrowing organisms (Garrett, 1970), and the onset of calcifying metazoans (Wood et al., 2002). Moreover, as the carbonate saturation state of the oceans changed there was a simultaneous decrease in the efficiency by which the stromatolitic layers accreted. Thus, it is possible that the abundance and the environmental diversity of stromatolites in the rock record is directly linked to marine carbonate saturation states (Grotzinger, 1990; Grotzinger, 1994; Grotzinger and Knoll, 1999; Ridgwell and Zeebe, 2005).

At the end of the Precambrian, and into the early Phanerozoic, thrombolites became important, and in places, even the dominant type of microbialite. There are several, not necessarily mutually exclusive, models regarding the factors leading to the expansion of thrombolites. Walter and Heys (1985) first attributed the rise in their abundance to burrowing in pre-existing stromatolites, while others proposed a switch in modes to benthic microbial communities mediating carbonate precipitation and early diagenetic modification (Shapiro, 2000; Arp et al., 2001; Planavsky et al., 2009), and to the diversification and evolution of foraminifera (Bernhard et al., 2013). Microbialites, in general, were gradually replaced by reefs constructed of crustose red algae, calcareous sponges and/or coelenterates (Golubic, 1994), yet there are marine settings and short time periods where abundant microbialites persisted throughout the Phanerozoic.

An understanding of how modern microbialites grow, and what factors control their accretion, can provide us with a foundation from which to assess their changes in the rock record. The recently discovered microbialites from Laguna Bacalar, Quintana Roo, Mexico are some of the largest freshwater examples yet observed. Additionally, the microbialites display stromatolitic (internal lamination) and thrombolitic (internal clotting) fabrics, which affords a unique opportunity to explore the factors controlling both microbialite mesostructures. Lastly, these microbialites appear to be actively accreting alongside grazing animals. Little is known of these microbialites, as only the giant Holocene samples have been studied with the aim of assessing their ability to record accretionary rates (Gischler et al., 2008). The relationship that exists between microbialites and grazing organisms, and the lake conditions that facilitate such abundant growth, are yet to be determined. This paper considers the relationships between the environmental conditions of Laguna Bacalar and the composition of the microbialites, with the aim being to gain new insight into their Precambrian/Phanerozoic decline.

2.2 Study area

Laguna Bacalar is a lake located in the southeastern part of Quintana Roo, Yucatan Peninsula, Mexico (Fig. 1). The Peninsula is characterized by its massive carbonate platform composed of limestone, dolomite, and evaporites, and by its extensive underground karstic system (Perry et al., 2002). The age of the platform ranges from Cretaceous to Holocene with the bedrock becoming younger towards the north (Hodell et al., 2004; Perry et al., 2009; Bauer-Gottwein et al., 2011; Perez et al., 2011). The regional geology has been subdivided into six different hydrogeochemical/physiographical zones: (1) Chicxulub Sedimentary Basin; (2) Cenote Ring; (3) Pock-marked Terrain; (4) Ticul fault zone; (5) Holbox Fracture zone - Xel-Ha Zone; and (6) the Evaporite Region where Laguna Bacalar is found (Fig. 1; Perry et al., 2002).

Outcrops from Bacalar, and the banks of the Rio Hondo, are predominantly Miocene in age and separated by an Eocene ground fault, which is aligned sub-parallel to the southern Caribbean coast. The faulting was the result of distinct tectonic events during the Late Cretaceous and Pliocene period, and the formation of faulted basins (Fig.2) (Díaz, 2005; López, 2005; Bauer-Gottwein et al., 2011). Such basins are presently occupied by Laguna Bacalar, which is ~2 km wide, ~50 km long, an area of ~3.1 km^2, and an elevation of 1.5 meters above sea level (Gamboa-Perez and Schmitter-Soto, 1999; Conagua, 2002; Gischler et al., 2011). The lake receives an average annual precipitation of 1367 mm (SMN, 2000) and is fed from the north by karstic waters from the cenote Xul-Ha (Fig. 1). Microbialites are found predominantly on the western shores, spanning approximately 10 km from the northern end of Xul-Ha. No microbialites were found in Xul-Ha, or past Bacalar town.

2.3 Methods

2.3.1. Collection of samples

2.3.1.1. Sediment samples

A variety of microbialite samples, ranging in size and morphology, were collected from Laguna Bacalar during the summer of 2011 and winter of 2012. A microbialite core sample measuring 32 cm in length and 5 cm in diameter was collected with the use of a custom sediment corer. Lake sediments, and macrofauna (bivalves, and gastropods), were also collected.

2.3.1.2. Water samples

Water samples were collected directly from the lake using a 60 mL sterile syringe, and then filtered through a 0.2 μm micropore filter. Duplicate samples were stored in polycarbonate sample bottles and immediately refrigerated. From the duplicates, one sample was treated with analytical grade HNO_3 (8 N) to a final concentration of 10% v/v for cation analysis, while the other was left un-acidified for anion analysis. *In situ* pH measurements were taken with a Beakman Φ 295 pH-meter fitted with a Thermo Scientific Oron pH probe. Water hardness for each of the latter samples was determined *in situ* with a Hach Digital Titrator.

2.3.2. Aqueous geochemistry (analyses at the University of Alberta)

Cl^- analyses of the lake water were performed using a Dionex DX600 Ion Chromatograph (IC). Acidified water samples were analyzed using a Perkin-Elmer Elan6000 quadrupole ICP-MS. The parameters used were as follows: RF power 1200 W, peak hopping acquisition, and 50 ms dwell time. Results were calibrated against a standard containing 10 ppm of Br, In, and Sc. The relative standard deviations (2σ) were between 3% for Na and Fe, 0.35% for Al and Zn, and between 0.005 and 0.06% for most analyzed elements. Detection limits were between 10 ppb (e.g., Ru, Ga) and 0.31 ppm (e.g. Ca).

2.3.3. Solid phase mineralogical/geochemical analyses

All solid phase mineralogical and geochemical analyses were conducted in the laboratories at the University of Alberta

2.3.3.1. Major element geochemistry

The analyses of major elements were performed on polished sections (1 mm thick) using a JEOL 8900 Microprobe (15 kV accelerating voltage, 5 μm beam diameter, and 15 nA). The synthetic crystals used to calibrate the instrument included, sphalerite (S), apatite (P), dolomite (Ca:Mg), willemite (Mn), calcite

(Ca), barite (Ba), strontianite (Sr), siderite (Fe), and albite (Na) (as per Jarosewich, 2002).

2.3.3.2. Trace element geochemistry

Trace elements were analyzed *in situ* using a Perkin Elmer Elan600 quadrupol ICP-MS coupled to a New Wave UP-213 laser ablation system. Samples were ablated using identical parameters: spot size (30 μm), repetition rate (5 Hz), and energy density (~13 J/cm^2), RF power (1200 W), peak hopping acquisition, and dwell time (50 ms). Quantitative results were calibrated against the NIST SRM612 internal glass standard, and normalized to [Ca], previously determined by electroprobe analysis. Data reduction and concentration determination were obtained using GLITTER® laser ablation software.

2.3.3.3. Bulk trace element geochemistry

For each sample, a mass of 10 mg was ground and dissolved in screw-top Teflon® bombs (Savillex®) using HF and HNO_3. The samples were left to react at 130ºC for 48 hours. Subsequently the temperature was increased to 140ºC in order to completely dry the samples. These were then treated with HCL and HNO_3 for 24 hours at 130ºC, and dried at 140ºC. HNO_3 was then added and allowed to react with the samples at 130ºC for two hours. Samples were then analyzed using a Perkin-Elmer Elan 6000 quadrupol ICP-MS as above.

2.3.3.4. Stable C- and O-isotope analysis

Samples of both the stromatolitic and thrombolitic microbialites were analyzed, as well as lake sediment, gastropod, and bivalve shells. Samples were ground in an agar mortar and pestle, treated with H_2O_2 (50%) for 48 h to eliminate all organic matter, rinsed three times with ultrapure water, and dried overnight in a vacuum oven at 30ºC. Carbon and oxygen isotope compositions were determined through analysis of cryogenically extracted CO_2 produced by H_3PO_4 digestion (McCrea, 1950). The CO_2 was analyzed using an internal standard NBS90 in a Finnigan Mat 252 Mass Spectrometer. The results were reported in δ-notation with respect to V-PDB and SMOW for carbon and oxygen, respectively (Craig, 1957; Craig, 1961).

2.3.3.5. Scanning electron microscopy (SEM

Grain mounts were sputter coated with gold, and observed using a Zeiss EVO MA 15 and JEOL630F. The analyses were performed at accelerating voltages of 5 and 20 kV and a working distance ranging from 6 to 19 mm (see individual image for specifics). The textural relationship between the extracellular polymeric substance (EPS), and authigenic mineral phases, organisms present, and grain types and sizes were observed.

2.3.3.3.6. X-ray microtomography

One microbialite sample displaying internal lamination and dome morphology (5 cm in length, 2 cm in width and height) was analyzed using a SkyScan 1172 Desktop X-say Microtomograph with an X-ray microfocus tube operating at 110 kV and 250 μm, resulting in a 5 μm focal spot and a 33 μm resolution. The sample was scanned every 0.5º in its entirety and the images processed using the application CT-Analyzer. The relationship between the cyanobacteria and the internal laminae were documented.

2.3.3.7. XRD analyses

Five microbialite samples from different locations in Laguna Bacalar were powdered using an agar mortar and pestle. Powder was less than 10 μm from which 1-2 g were placed on the holders and analyzed using a Rigaku Ultima IV X-Ray diffractometer. Data was processed and minerals identified using JADE 9.1 software and the ICDD and ICSD databases.

2.3.4. Petrography

Petrographic thin sections of various microbialites displaying stromatolitic and thrombolitic textures were prepared and examined using transmitted light microscopy. The grain type and size, mineral and textural composition, and their relationship with the organisms present were recorded.

2.4. Results and Discussion

2.4.1. Lake water chemistry

Measured pH values of the surface waters of Laguna Bacalar varied between 7.7 and 8.2. The dominant cations in the lake waters were Ca^{2+} (332.5 ppm) and Mg^{2+} (80.8 ppm), while the average Cl^- concentration was 42.44 mg/L (see Table 1 for completer water chemistry). These values are in agreement with those reported by Gischler et al. (2008). They determined that the water originating from the Xul-Ha sinkhole was supersaturated with respect to calcium carbonate due the flow path of the karstic water through the carbonate bedrock of the Yucatan Peninsula, and the change in partial pressure of CO_2 due to degassing upon reaching the surface at Xul-Ha.

2.4.2. Microbialite composition and texture

Microbialites displayed a variety of sizes and morphologies, but in general can be classified into two groups based on their internal fabrics or mesostructures: (1) stromatolites and (2) thrombolitic-stromatolites. It is these textures that can provide us with insight into the various factors controlling microbialite growth.

2.4.2.1. Stromatolite texture

These microbialites are mainly observed on the outer surfaces of larger thrombolitic-stromatolites (Fig. 3A). They display a dark gray color and smooth domal morphology (Figs. 3A-B). Cross sections reveal very well defined laminae with an internal fibrous texture (Figs. 3C, D), presumed to be the result of filamentous cyanobacteria. Petrographically, stromatolites are composed entirely of calcite (see Appendix 1 for XRD analysis) and cyanobacteria filaments. The filaments (brown in color) were ~10-30 μm in width, with variable lengths (Fig. 4A), some of which still display internal structure and green pigmentation (Fig. 4B). Micrite-sized calcite is precipitated around the individual filaments resulting in the formation of molds ~20 μm thick (Fig. 4C). As the cyanobacteria within the molds begin to decompose, secondary precipitation occurs in the form of microspar infills. The existing micrite is used as a substrate from which growth is observed to occur inward, even while filaments are still present (Fig. 4D). Subsequently, the molds are cemented together by microspar as calcite precipitation continued (Fig. 4E). SEM images further show the highly calcified cyanobacterial filaments (Fig. 5A), as well as the individual molds that are composed of microspar (Fig. 5B) and micrite (Fig. 5C). Also of importance is the presence of abundant EPS covering calcite grains (Fig. 5D), cyanobacterial filaments (Fig. 5E), and diatoms (Figs. 5E & F).

Internal lamination results from the rhythmic layering of laminae containing higher abundances of cyanobacterial filaments/ molds (which we refer to here as P-lamina after Konhauser et al., 2004), preceded by laminae having greater porosity and lesser cyanobacterial abundance (called U-laminae) (Figs. 4E & 5G). Due to the continuous precipitation of calcite, the cyanobacteria must migrate upwards in order to obtain the necessary photosynthetic active radiation (generally between 400-700 nm wavelength; Howard, 2012). It is such migration that results in the generation of porosity, as seen in the U-laminae.

A lack of detrital grains suggests that growth was solely through the precipitation of calcite. This very much differs from modern marine stromatolites in the Bahamas in which cyanobacterial filaments are able to intertwine and incorporated detritus within their EPS to form a cohesive mat-like structure. There are several microbially-mediated processes that can drive carbonate precipitation (e.g., Simkiss and Wilbur, 1989; Riding, 2006; Planavsky et al., 2009). Photosynthetic CO_2 uptake can locally cause an increase in pH and the carbonate anion (CO_3^{2-}) concentration. This mode of carbonate precipitation is consistent with formation of filament molds within a cyanobacterial sheath. In other environments, anaerobic heterotrophy, such as bacterial sulfate reduction, plays an important role in generating alkalinity (eg., Visscher et al., 1998; Petrash et al., 2012). Indeed, in marine stromatolites much more calcium carbonate is precipitated within the aphotic zone of intertidal mats on cyanobacterial remains than in the euphotic zone dominated by living cyanobacteria (Chafetz and Buczynski, 1992). However, in Laguna Bacalar, there is minimal sulfate in the lake water. Additionally, the presence of EPS provides nucleation sites for mineral precipitation, while also potentially absorbing essential elements utilized by the cyanobacteria (Pentecost, 1978; Pentecost and Riding, 1986; Merz-Preifi, 2000; Braissant et al., 2003; Jones et al., 2005; Dupraz et al., 2009; Perri and Spadafora, 2011; Petrash et al., 2011). Collectively, these processes facilitate the formation of the cyanobacterial molds (e.g., Fig. 4C).

2.4.2.2. Thrombolitic-stromatolite textures

These microbialites tend to reach sizes up to several meters. They typically display domal morphology, having either a smooth or a pitted exterior (Figs. 6A-C). They appear light cream in coloration, although those sub-aerially exposed have a darker gray color (Fig. 6C). Their close proximity to each other often results in their coalescence (Fig. 6C). Bivalves (identified as *Dreissena* sp.) were found embedded on their outer surface (Fig. 6D), while gastropods (*Pomacea* sp.) lay dispersed around the microbialites (Fig. 6E). Microbialites were also observed utilizing several substrates for their growth, including mangrove roots (Fig. 6F). Internally, domal thrombolitic-stromatolites have both stromatolitic and thrombolitic mesostructures (Fig. 7B-D). Laminae, similar to that found in stromatolites, were observed predominantly at the base and uppermost parts of the sectioned samples (Figs. 7B-C). A green, 1.2 cm thick microbial mat was present in the upper part of the structure (see arrow with 'e'; Fig. 7B), but ~2-3 mm beneath the outer mineralization zone (i.e. endolithic growth). The porosity varied and was dependent on the internal texture: zones having stromatolitic textures were found to have lower porosity (Figs. C-E) compared to their thrombolitic counterparts (Fig. 7D). Bivalves were also seen cemented into the internal texture but exhibited no evidence of burrowing or boring (see arrow with 'b' Figs. 7B & E). Microbial molds similar to those in stromatolites were observed (Figs. 8A & B), as was internal lamination created by P- and U-laminae (Fig. 8C). Such internal texture is thought to be the result of growth exclusively through the precipitation of calcite.

In contrast, clotted laminae are composed primarily of rounded micrite grains that have no internal structure, and as such, are interpreted as peloids (McKee et al., 1969), and cemented bioclasts (see arrow with 'v'; Fig. 8D). The same rounded peloids were found in the lake sediment (Fig. 8E), suggesting that the peloids found in thrombolitic-stromatolites are transported and not formed *in situ*. Cyanobacterial filaments within the clotted laminae were sparse, and appeared less mineralized than those found in the stromatolitic laminae (Fig. 8F). The presence of detrital peloids and bioclasts, and the lack of cyanobacterial filament molds, suggests that growth is the result of binding and trapping of grains by cyanobacteria, with subsequent precipitation driven by heterotrophic processes.

Interestingly, all of the observed microbialites appear to begin as stromatolites: this is observed in the overturned stromatolite at the base of Bac 110113 (Fig. 7C). As stromatolites grow their surface area increases, thereby allowing for more sediment (if available) to be deposited on their surfaces, and ultimately trapped. Those trapped grains are then cemented together by microsparite, most likely the result of EPS induced precipitation. SEM images show the interaction between the individual grains and the EPS (Fig. 5 & 9), as well as the presence of calcite grains with dipyramid morphology (Fig. 9C) that have previously been reported to preferentially grow in the presence of EPS (Buczynski and Chafetz, 1991; Buczynski and Chafetz, 1993). As greater amounts of peloids are incorporated into the structure, the cyanobacteria migrate upwards in order to obtain the necessary light, causing further trapping and binding of grains, and subsequent migration. This results in internal clotting, and the elimination of banding, due to the constant cyanobacterial movement that prevents the continuous precipitation of micrite in the horizontal. Such lamination re-appears if sediment deposition decreases, either due to the decrease in current or due to the sheltering of the microbialite allowing time for micrite precipitation to occur (see arrow; Fig. 7D).

In summary, the textural and morphological differences observed between the microbialites can be attributed to the distinct growth mechanisms. Internal lamination is attributed to the precipitation of calcite by cyanobacteria while accretion occurs through the process of trapping and binding which results in internal clotting. These mechanisms, however, also appear to be dependent on the lake's current. Lamination is favored by calm lake conditions, in which no sediment is deposited upon the stromatolite's surface. Hence, calcite can be precipitated from the supersaturated waters, and lamination produced as the bacteria rhythmically migrate upwards. In contrast, internal clotting is favored during relatively high-energy conditions in which detrital sediments are transported and deposited by the lake currents on the surface of microbialites, yet are not immediately removed. Such conditions are confirmed by suspended sediment in the water causing poor visibility. This allows sediments to be trapped and bound by the bacteria, which in turn, become incorporated into the microbialite structure. As a consequence of the deposited detrital sediment on microbialites, bacteria are continuously forced to migrate upwards, further binding and trapping newly deposited sediment. This results in the clotted fabric, and prevents precipitation of calcite.

2.4.3. Microbialite geochemistry

Elemental maps obtained from the microprobe analysis of the various microbialites (stromatolites and thrombolitic-stromatolites) show low relative concentrations of Fe, S, Mn, Mg, and Si. Bulk ICP-MS values for individual samples were averaged and compared to those obtained through laser ablation. It was observed that the values differed depending on the analytical technique used (bulk vs. laser ablation; Fig. 10), but also whether or not they had been treated with or without H_2O_2 (Fig. 11). When stromatolites and thrombolitic-stromatolites were compared, similarities in their elemental patterns were observed, however, stromatolites were enriched in certain elements (Mg, Si, V, Cr, Fe, Ni, Mo, Fe, Ni)(Fig. 10). We believe such disparities can be linked to the presence of cyanobacteria.

It is known that certain elements are essential for microorganisms. Some are needed for the synthesis of particular enzymes, while others are utilized as nutrients (Silver, 1998; Silva and Williams, 2001; Baptista and Vasconcelos, 2006). Both types of microbialites found in Laguna Bacalar displaying very similar major and trace element patters, however, they do differ depending on the lake waters in which they grow (i.e., they show some elemental enrichment factors; Fig. 10). This is not surprising given that cyanobacteria filaments and EPS are present in the microbialites, both of which have highly reactive surfaces that can facilitate sorption reactions (see Konhauser, 2007 for details). Consequently the slight elemental differences between stromatolites and thrombolitic-stromatolites may be attributed to the duration the cyanobacteria and its EPS remain in a given place. Specifically, during precipitated mediated growth (i.e. laminated), higher concentrations of essential nutrients are absorbed by cyanobacterial EPS due to their constant presence and slow migration. However, as the growth mechanism changes to that of trapping and binding, cyanobacterial migration increases, causing their abundance at a given place and time to be become limited. Support for this idea comes from the observation that the microbialite samples containing organic matter have higher concentrations than those that had their organic content removed through the use of H_2O_2 (Fig. 11). Individual samples appear to have similar patterns that differ only in their concentrations, possibly in response to the presence or absence of cyanobacterial filaments. This suggests that while the elemental concentrations might differ as a consequence of cyanobacterial presence, the original signature is preserved in the microbialites even after the decomposition and disappearance of the bacteria and its EPS. As such the comparison of trace elements found in stromatolites, and in various sections of thrombolitic-stromatolites potentially allow us to attribute the internal clotting to cyanobacteria even though the cells are not always preserved.

Carbonate $\delta^{13}C$ isotope values can also provide insights into the role that different microbial processes played in driving calcium carbonate precipitation at Laguna Bacalar. Carbon and oxygen isotope data from microbialites, gastropods, bivalves, sediment, and lake water are presented in Table 2 and plotted in Figure 12. $\delta^{13}C_{PDB}$ isotope values of thrombolitic-stromatolites have a range between -0.30 and -1.53‰. Bulk stromatolite samples were slightly more depleted averaging -2.03‰. Lake sediment ranged between -1.46 and -1.55‰. Gastropods and bivalves had the lowest values averaging -6.15 and -4.40‰, respectively.

Cyanobacteria preferentially fix ^{12}C during photosynthesis due to the kinetic isotope effects during CO_2 uptake (Park and Epstein, 1961; O'Leary, 1981; McConnaughey et al., 1997; Schidlowski, 2000). Therefore, low $\delta^{13}C$ carbonate isotope values in microbialites, relative to the lake DIC values, are linked to precipitation in an environment with inorganic carbon derived from organic matter remineralization (e.g., Andres et al., 2006). Positive $\delta^{13}C$ isotope values suggest carbonate precipitation driven, in part, by significant photosynthetic CO_2 uptake, leaving behind a reservoir of positive $\delta^{13}C$ bicarbonate. Foremost, preferential uptake of ^{12}C-enriched carbon dioxide uptake creates a ^{13}C-enriched microenvironment with an elevated pH (for review see Riding, 2000, 2006).

We compared microbialite and bivalve carbonate $\delta^{13}C$ isotope values in order to gauge the effects that organic matter remineralization and photosynthetic carbon dioxide uptake played in driving carbonate precipitation. The bivalve carbonates can be assumed to have formed essentially synchronous with most of our microbialite samples (see discussion above), and hence, they track the lake DIC $\delta^{13}C$ values. Microbialite carbonates are consistently enriched relative to bivalves. Photosynthetic CO_2 uptake driving the carbonate precipitation is the simplest explanation for this difference in carbonate $\delta^{13}C$ values. It is important to note that when there are low concentrations of available CO_2 cyanobacteria will take up HCO_3^- instead, which causes little isotopic discrimination (Stal, 2000). This process makes it difficult to use the carbon isotopes to quantify microbial processes and to place constraints on the extent of CO_2 uptake needed to trigger carbonate precipitation.

2.4.4. Paleoenvironment implications

Based on our observations, we infer that varying sedimentation rates may similarly have been important in controlling the distribution of thrombolite-stromatolite packages in the geological record. It is possible that the diversification of carbonate biomineralization in the latest Neoproterozoic and earliest Phanerozoic could have increased the detrital carbonate sediment load on carbonate platforms. This higher detrital load could have led to a greater abundance of clotted microbialite textures – if the model outlined above for the formation of clotted textures at Laguna Bacalar is relevant to ancient thrombolites. Therefore, biological innovation that led to shifts in modes of carbonate formation could be another factor leading to an increase in thrombolite abundance in the Phanerozoic.

The results obtained from Laguna Bacalar microbialites suggest that water chemistry is the primary factor controlling microbialite growth. Supersaturation with regards to calcium carbonate facilitates organomineralization of calcium carbonate by cyanobacteria, and thus, formation of the microbialites. A reduction in the saturation state would likely result in the growth of a microbial mat, but they could not accrete to become microbialites. The water surfacing at the Xul-Ha sinkhole are supersaturated with regards to calcium carbonate (Gischler et al., 2008; Gischler et al., 2011), a consequence of its interaction with the carbonate bedrock in the karstic system and its degassing upon surfacing. As water flows northeast from the Xul-Ha sinkhole into Laguna Bacalar, the water depth decreases allowing for cyanobacteria to colonize the river bottom and begin the formation of microbialites. The microbialites are observed only in the southern part of the lake, decreasing in abundance to the north. They are completely absent at the town of Bacalar (some 14 km northeast of the Xul-Ha sinkhole). This suggests that Ca^{2+} and HCO_3^- ions are used in the formation of microbialites, and that as microbialites grow and utilize these ions, their concentration decreases to the point where calcium carbonate formation is no longer favorable. This model is supported by the observed northeastern depletion of Ca^{2+} and HCO_3^- in the lake water.

It is possible that similar changes during the Proterozoic would have caused a decrease in the calcification of microbialites, and decrease in their abundance and diversity. As to the cause of the possible changes to saturation state of the water, a decrease in CO_2, a decrease in temperature, or the competition by other calcifying organisms would have directly impacted microbialite growth (Fischer, 1965; Karhu and Epstein, 1986; Kasting, 1987; Riding and Liang, 2005; Kasting and Howard, 2006; Riding, 2006). A decrease in CO_2 was the result of enhanced silicate weathering and the subsequent reduction in greenhouse gasses and temperature (Riding, 1997; Riding, 2006), while calcium carbonate availability would have been reduced due to the ability of animals to form carbonate exoskeletons (Fischer, 1965).

Based on the discussion above, it also appears that the presence of bivalves and gastropods have no influence on microbialite growth. Bivalves only appear to use the microbialites as anchors, as is evident from their byssal threads (Fig. 7E) and the type of bivalve (*Dreissena* sp.), while showing no evidence of burrowing or grazing. The observed gastropods (*Pomacea* sp.), while having the ability to graze, showed no evidence of doing so, either due to the rapid growth or to the endolithic growth of the bacterial mat.

2.5. Conclusions

The growth and distribution of microbialites in Laguna Bacalar are controlled predominantly by the water carbonate chemistry. The supersaturation of the water with regards to calcium carbonate, and the photosynthetic activity of the cyanobacteria promote the precipitation of calcite, and the formation of large microbialites. However, the textural characteristics are the result of the different growth mechanisms that the benthic cyanobacterial communities employ. The presence of grazing gastropods (*Dreissena* sp.) appeared to have minimal, if any, influence on microbialite growth, likely due the fast growth rates and the unique protection that endolithic bacterial growth provides the cyanobacteria. Stromatolites are characterized by the precipitation of calcite, and formation of internal lamination, the result of rhythmic layering of lamina containing higher abundance of filaments, proceeded by those having higher porosity. In contrast, internal clotting is the result of bacterially induced trapping and binding of micritic peloids, which in combination with the laminated texture, form thrombolitic-stromatolites. Isotopically microbialite carbonates are consistently enriched in C^{13} relative to bivalves and gastropods, while cyanobacterial photosynthetic CO_2 uptake driving carbonate precipitation is the simplest explanation for such differences in the carbonate $\delta^{13}C$ values. Geochemically, both microbialites are similar, having enrichment of biologically essential elements, most likely as a result of metal sorption to the EPS present. However, the concentrations in stromatolites are slightly higher, and attributed to the longer presence of cyanobacteria and its EPS. These findings suggest that Laguna Bacalar microbialites may be valuable modern-day analogues to their Neoproterozoic and Phanerozoic counterparts, and provide support for the hypothesis that water chemistry is the main determinant in promoting the growth of such large biogenic structures.

2.6. References

AITKEN, J.D., 1967, Classification and environmental significance of cryptalgal limestones and dolomites with illustrations from Cambrian and Ordovician of southwestern Alberta: Journal of Sedimentary Petrology, v. 37, p. 1163-1178.

ALLWOOD, A.C., GROTZINGER, J.P., KNOLL, A.H., BURCH, I.W., ANDERSON, M.S., COLEMAN, M.L., AND KANIK, I., 2009, Controls on development and diversity of Early Archean stromatolites: Proceedings of the National Academy of Sciences of the United States of America, v. 106, p. 9548-9555.

ALLWOOD, A.C., WALTER, M.R., KAMBER, B.S., MARSHALL, C.P., AND BURCH, I.W., 2006, Stromatolite reef from the Early Archaean era of Australia: Nature, v. 441, p. 714-718.

ANDRES, M.S., SUMNER, D.Y., REID, R.P., AND SWART, P.K., 2006, Isotopic fingerprints of microbial respiration in aragonite from Bahamian stromatolites: Geology, v. 34, p. 973-976.

ARP, G., REIMER, A., AND REITNER, J., 2001, Photosynthesis-induced biofilm calcification and calcium concentrations in phanerozoic oceans: Science, v. 292, p. 1701-1704.

AWRAMIK, S.M., 1971, Precambrian columnar stromatolite diversity - reflection of metazoan appearance: Science, v. 174, p. 825-827.

AWRAMIK, S.M., 1991, Archaean and Proterozoic stromatolites, *in* Riding, R., ed., Calcareous Alae and Stromatolites: Springer-Verlag, New York, p. 571.

BAPTISTA, M.S., AND VASCONCELOS, M.T., 2006, Cyanobacteria metal interactions: requirements, toxicity, and ecological implications: Critical Reviews in Microbiology, v. 32, p. 127-137.

BAUER-GOTTWEIN, P., GONDWE, B., CHARVET, G., MARIN, L., REBOLLEDO-VIEYRA, M., AND MEREDIZ-ALONSO, G., 2011, Review: The Yucatan Peninsula karst aquifer, Mexico: Hydrogeology Journal, v. 19, p. 507-524.

BERNHARD, J.M., EDGCOMB, V.P., VISSCHER, P.T., MCINTYRE-WRESSNIG, A., SUMMONS, R.E., BOUXSEIN, M.L., LOUIS, L., AND JEGLINSKI, M., 2013, Insights into foraminiferal influences on microfabrics of microbialites at Highborne Cay, Bahamas: Proceedings of the National Academy of Sciences, v. 110, p. 9830-9834.

BEUKES, N.J., 1987, Facies relations, depositional-environments and diagenesis in a major early Proterozoic stromatolitic carbonate platform to basinal sequence, Campbellrand Subgroup, Transvaal Supergroup, Southern-Africa: Sedimentary Geology, v. 54, p. 1-46.

BRAISSANT, O., CAILLEAU, G., DUPRAZ, C., AND VERRECCHIA, A.P., 2003, Bacterially induced mineralization of calcium carbonate in terrestrial environments: the role of exopolysaccharides and amino acids: Journal of Sedimentary Research, v. 73, p. 485-490.

BUCK, S.G., 1980, Stromatolite and ooid deposits within the fluvial and lacustrine sediments of the Precambrian Ventersdorp Supergroup of South-Africa: Precambrian Research, v. 12, p. 311-330.

Buczynski, C., and Chafetz, H.S., 1991, Habit of bacterially induced precipitates of calcium-carbonate and the influence of medium viscosity on mineralogy: Journal of Sedimentary Petrology, v. 61, p. 226-233.

Buczynski, C., and Chafetz, H.S., 1993, Habit of bacterially induced precipitates of calcium carbonate: examples from laboratory experiments and recent sediments, *in* Rezak, R., and Lavoie, D.L., eds., Carbonate Microfabrics: Springer-Verlag, New York, p. 105-116.

Burne, R.V., and Moore, L.S., 1987, Microbialites: organosedimentary deposits of benthic microbial communities: PALAIOS, v. 2, p. 241-254.

Chafetz, H.S., and Buczynski, C., 1992, Bacterially induced lithification of microbial mats: PALAIOS, v. 7, p. 277-293.

Conagua, 2002, Determinación de la disponibilidad de agua en el acuífero Peninsula de Yucatán, estado de Yucatán: Gerencia de Aguas Subterráneas p. 20.

Craig, H., 1957, Isotopic standards for carbon and oxygen and correction factors for mass-spectrometric analysis of carbon dioxide: Geochimica Et Cosmochimica Acta, v. 12, p. 133-149.

Craig, H., 1961, Standard for reporting concentrations of deuterium and oxygen-18 in natural waters: Science, v. 133, p. 1833-1834.

Díaz, J.E.H., 2005, Decreto por el cual se establece el programa de ordenamineto ecologico territorial de al región de Laguna Bacalar, Quintana Roo, México, Periodico Oficial, p. 126.

Dupraz, C., Reid, R.P., Braissant, O., Decho, A.W., Norman, R.S., and Visscher, P.T., 2009, Processes of carbonate precipitation in modern microbial mats: Earth-Science Reviews, v. 96, p. 141-162.

Fischer, A.G., 1965, Fossils early life and atmospheric history: Proceedings of the National Academy of Sciences of the United States of America, v. 53, p. 1205-1213.

Gamboa-Perez, H.C., and Schmitter-Soto, J.J., 1999, Distribution of cichlid fishes in the littoral of Lake Bacalar, Yucatan Peninsula: Environmental Biology of Fishes, v. 54, p. 35-43.

Garrett, P., 1970, Phanerozoic stromatolites: noncompetitive ecologic restriction by grazing and burrowing animals: Science, v. 169, p. 171-173.

Gischler, E., Gibson, M.A., and Oschmann, W., 2008, Giant Holocene freshwater microbialites, Laguna Bacalar, Quintana Roo, Mexico: Sedimentology, v. 55, p. 1293-1309.

Gischler, E., Golubic, S., Gibson, M., Oschmann, W., and Hudson, J.H., 2011, Microbial mats and microbialites in the freshwater Laguna Bacalar, Yucatan Peninsula, Mexico, Advances in Stromatolite Geobiology: Springer Berlin Heidelberg, p. 187-205.

Golubic, S., 1994, The continuing importance of cyanobacteria, *in* Bengtson, S., ed., Nobel Symposium; Early life on earth, p. 334-340.

Grotzinger, J.P., 1990, Geochemical model for Proterozoic stromatolite decline: American Journal of Science, v. 290A, p. 80-103.

Grotzinger, J.P., 1994, Trends in Precambrian carbonate sediments and their implication for understanding evolution, *in* Bengtson, S., ed., Nobel Symposium; Early life on earth, p. 245-258.

Grotzinger, J.P., and Knoll, A.H., 1999, Stromatolites in Precambrian carbonates: evolutionary mileposts or environmental dipsticks?: Annual Review of Earth and Planetary Sciences, v. 27, p. 313-358.

Hodell, D.A., Quinn, R.L., Brenner, M., and Kamenov, G., 2004, Spatial variation of strontium isotopes (Sr-87/Sr-86) in the Maya region: a tool for tracking ancient human migration: Journal of Archaeological Science, v. 31, p. 585-601.

Hofmann, H.J., 1973, Stromatolites: characteristics and utility: Earth-Science Reviews, v. 9, p. 339-373.

Howard, A., 2012, Cyanobacteria (blue-green algae), *in* Bengtsson, L., Herschy, R., and Fairbridge, R., eds., Encyclopedia of Lakes and Reservoirs: Springer Netherlands, p. 174-175.

Jarosewich, E., 2002, Smithsonian microbeam standards: Journal of Research of the National Institute of Standards and Technology, v. 107, p. 681-686.

Jones, B., Renaut, R.W., and Konhauser, K.O., 2005, Genesis of large siliceous stromatolites at Frying Pan Lake, Waimangu geothermal field, North Island, New Zealand: Sedimentology, v. 52, p. 1229-1252.

Kalkowsky, E., 1908, Oolith und stromatolith im norddeutschen Buntsandstein: Zeitschrift der deutschen geologischen Gesells-chaft, v. 60, p. 68-125.

Karhu, J.A., and Epstein, S., 1986, The implication of the oxygen isotope records in coexisting cherts and phosphates: Geochimica Et Cosmochimica Acta, p. 867-870.

Kasting, J.F., 1987, Theoretical Constraints on Oxygen and Carbon-Dioxide Concentrations in the Precambrian Atmosphere: Precambrian Research, v. 34, p. 205-229.

Kasting, J.F., and Howard, M.T., 2006, Atmospheric composition and climate on the early Earth: Philosophical Transactions of the Royal Society B-Biological Sciences, v. 361, p. 1733-1741.

Konhauser, K., 2007, Introduction to geomicrobiology: Blackwell Pub., Oxford, x, 425 p.

Konhauser, K.O., Jones, B., Phoenix, V., Ferris, G., and Renaut, R., 2004, The microbial role in hot spring silicification: Ambio, v. 33, p. 552-558.

López, Z.L., Lugo, F.A., Pita, M.R.S., 2005, Chetumal E16-4-7, Carta Geológico-Minera: Servicio Geológico Mexicano

Lowe, D.R., 1983, Restricted shallow-water sedimentation of Early Archean stromatolitic and evaporitic strata of the Strelley Pool Chert, Pilbara Block, Western Australia: Precambrian Research, v. 19, p. 239-283.

McConnaughey, T., Burdett, J., Whelan, J., and Paull, C., 1997, Carbon isotopes in biological carbonates: respiration and photosynthesis: Geochimica Et Cosmochimica Acta, v. 61, p. 611-622.

McCrea, J., 1950, On the isotopic chemistry of carbonates and a paleotemperature scale: Journal of Chemical Physics, v. 18, p. 849-857.

McKee, E.D., Gutschick, R.C., and Skipp, B., 1969, History of the Redwall Limestone of northern Arizona: Geological Society of America.

McNamara, K.J., and Awramik, S.M., 1992, Stromatolites - a key to understanding the early evolution of life: Science Progress, v. 76, p. 345-364.

Merz-Preifi, M., 2000, Calcification in cyanobacteria, *in* Riding, R., Awramik, S.M., ed., Microbial sediments: Springer-Verlag Berlin Heidelberg, New York, p. 50.

O'Leary, M.H., 1981, Carbon isotope fractionation in plants: Phytochemistry, v. 20, p. 553-567.

Park, R., and Epstein, S., 1961, Metabolic fractionation of C13 & C12 in plants.: Plant physiology, v. 36, p. 133-138.

Pentecost, A., 1978, Blue-green algae and freshwater carbonate deposits: Proceedings of the Royal Society B: Biological Sciences, v. 200, p. 43-61.

Pentecost, A., and Riding, R., 1986, Calcification in cyanobacteria, *in* Leadbeater, B.S.C., and Riding, R., eds., Biomineralization of Lower Plants and Animals: Clarendon Press, Oxyford, p. 73-90.

Perez, L., Bugja, R., Lorenschat, J., Brenner, M., Curtis, J., Hoelzmann, P., Islebe, G., Scharf, B., and Schwalb, A., 2011, Aquatic ecosystems of the Yucatan Peninsula (Mexico), Belize, and Guatemala: Hydrobiologia, v. 661, p. 407-433.

Perri, E., and Spadafora, A., 2011, Evidence of microbial biomineralization in modern and ancient stromatolites, *in* Tewari, V.C., Seckbach, J., ed., Stromatolites: Interaction of Microbes with Sediments: Springer Dordrecht Heidelberg, New York, p. 633-649.

Perry, E., Paytan, A., Pedersen, B., and Velazquez-Oliman, G., 2009, Groundwater geochemistry of the Yucatan Peninsula, Mexico: constraints on stratigraphy and hydrogeology: Journal of Hydrology, v. 367, p. 27-40.

Perry, E., Velazquez-Oliman, G., and Marin, L., 2002, The hydrogeochemistry of the karst aquifer system of the northern Yucatan Peninsula, Mexico: International Geology Review, v. 44, p. 191-221.

Petrash, D.A., Gingras, M.K., Lalonde, S.V., Orange, F., Pecoits, E., and Konhauser, K.O., 2012, Dynamic controls on accretion and lithification of modern gypsum-dominated thrombolites, Los Roques, Venezuela: Sedimentary Geology, v. 245–246, p. 29-47.

Petrash, D.A., Lalonde, S.V., Raudsepp, M., and Konhauser, K.O., 2011, Assessing the importance of organic matrix materials in biofilm chemical reactivity: insights from proton and cadmium adsorption onto the commercially available biopolymer alginate: Geomicrobiology Journal, v. 28, p. 266-273.

Planavsky, N.J., Reid, R.P., Lyons, T.W., Myshrall, K.L., and Visscher, P.T., 2009, Formation and diagenesis of modern marine calcified cyanobacteria: Geobiology, v. 7, p. 566-576.

Pratt, B.R., 1982, Stromatolite decline - a reconsideration: Geology, v. 10, p. 512-515.

Ridgwell, A., and Zeebe, R.E., 2005, The role of the global carbonate cycle in the regulation and evolution of the Earth system: Earth and Planetary Science Letters, v. 234, p. 299-315.

Riding, R., 1997, Stromatolite decline: a brief reassessment: Facies, v. 36, p. 227-230.

Riding, R., 1999, The term stromatolite: towards an essential definition: Lethaia, v. 32, p. 321-330.

Riding, R., 2006, Cyanobacterial calcification, carbon dioxide concentrating mechanisms, and Proterozoic-Cambrian changes in atmospheric composition: Geobiology, v. 4, p. 299-316.

Riding, R., 2006, Microbial carbonate abundance compared with fluctuations in metazoan diversity over geological time: Sedimentary Geology, v. 185, p. 229-238.

Riding, R., 2011, The nature of stromatolites: 3,500 million years of histroy and a century of research, *in* Reitner, J., Quéric, N-VB, Arp, G., ed., Advances in Stromatolite Geobiology: Springer, Heidelberg, p. 29-74.

Riding, R., and Liang, L.Y., 2005, Geobiology of microbial carbonates: metazoan and seawater saturation state influences on secular trends during the Phanerozoic: Palaeogeography Palaeoclimatology Palaeoecology, v. 219, p. 101-115.

Schidlowski, M., 2000, Carbon isotopoes and microbial sediments, *in* Riding, R., and Awramik, S.M., eds., Microbial sediments: Springer-Verlag, Berlin, p. 84-95.

Schieber, J., 1999, Microbial mats in terrigenous clastics: the challenge of identification in the rock record: PALAIOS, v. 14, p. 3-12.

Schopf, J.W., 2006, Fossil evidence of Archaean life: Philosophical Transactions of the Royal Society B-Biological Sciences, v. 361, p. 869-885.

Schopf, J.W., Kudryavtsev, A.B., Czaja, A.D., and Tripathi, A.B., 2007, Evidence of archean life: stromatolites and microfossils: Precambrian Research, v. 158, p. 141-155.

Shapiro, R.S., 2000, A comment on the systematic confusion of thrombolites: PALAIOS, v. 15, p. 166-169.

Silva, J.J.R.F.s.d., and Williams, R.J.P., 2001, The biological chemistry of the elements : the inorganic chemistry of life: Oxford University Press, Oxford ; New York, xvii, 575 p. p.

Silver, S., 1998, Genes for all metals - a bacterial view of the periodic table - the 1996 thom award lecture: Journal of Industrial Microbiology & Biotechnology, v. 20, p. 1-12.

Simkiss, K., and Wilbur, K.M., 1989, Biomineralization : cell biology and mineral deposition: Academic Press, San Diego, xiv, 337 p.

SMN, 2000, Normales climatógicas de San Felipe Bacalar, Quintana Roo: Servicio Meteorologico Nacional

Stal, L.J., 2000, Cyanobacterial mats and stromatolites, *in* Whitton, B.A., Potts, M., ed., The Ecology of Cyanobacteria Their Diversity in Time and Space: Kluwer Academic Publisher, Dordrecht, p. 61-120.

VISSCHER, P.T., REID, R.P., BEBOUT, B.M., HOEFT, S.E., MACINTYRE, I.G., AND THOMPSON, J.A., 1998, Formation of lithified micritic laminae in modern marine stromatolites (Bahamas): the role of sulfur cycling: American Mineralogist, v. 83, p. 1482-1493.

WALTER, M.R., AND HEYS, G.R., 1985, Links between the rise of the metazoa and the decline of stromatolites: Precambrian Research, v. 29, p. 149-174.

WOOD, R.A., GROTZINGER, J.P., AND DICKSON, J.A.D., 2002, Proterozoic modular biomineralized metazoan from the Nama Group, Namibia: Science, v. 296, p. 2383-2386.

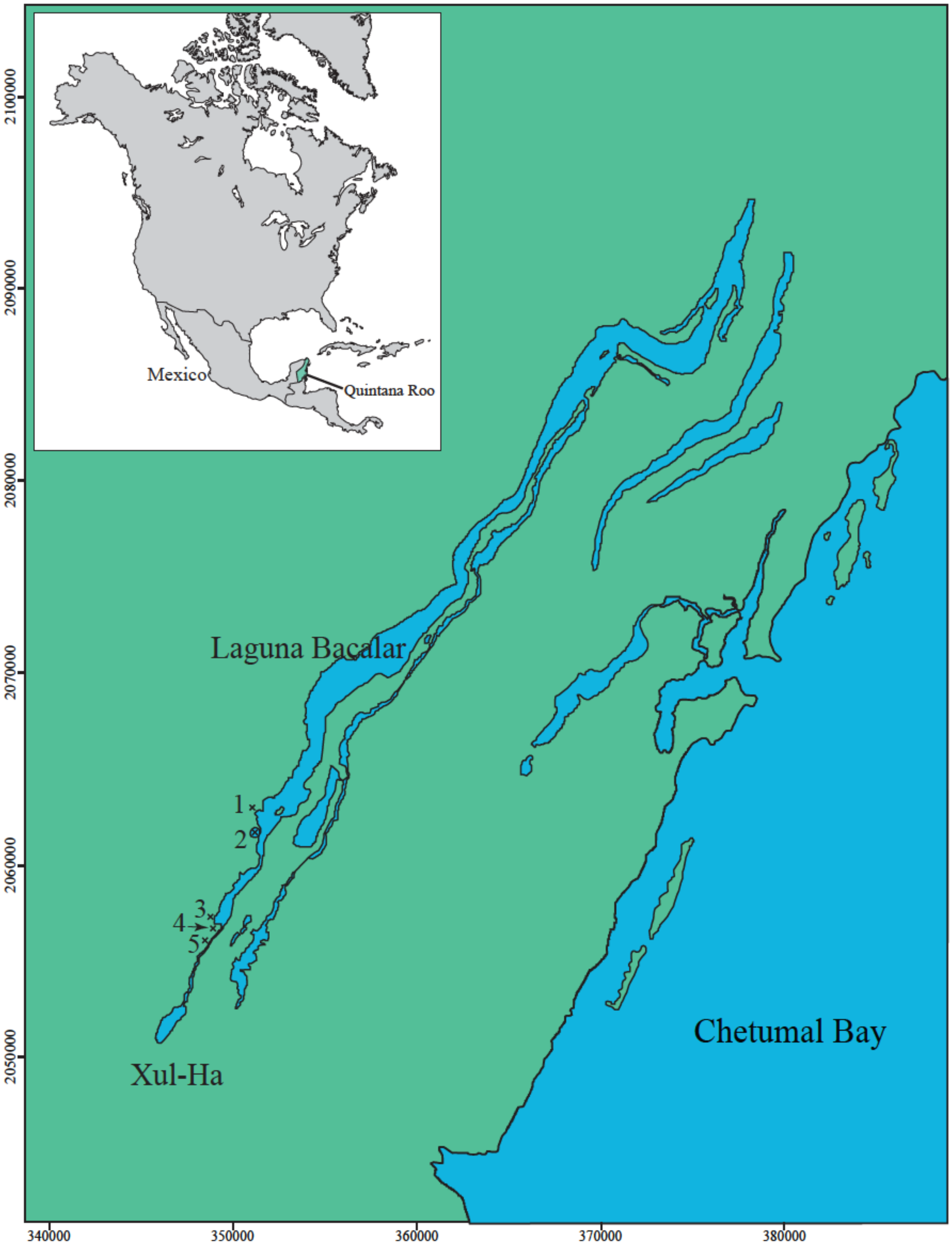
Mexico
Quintana Roo
Laguna Bacalar
Chetumal Bay
Xul-Ha
1
2
3
4
5
2100000
2090000
2080000
2070000
2060000
2050000
340000
350000
360000
370000
380000

FIGURE 2.1 — Map of the study area, Laguna Bacalar located in the South-east corner of the state of Quintana Roo, Mexico. Freshwater microbialites were found on the western shore of the lake, spanning some 10 km starting at the northern part of Xul Ha. Sampling locations are shown with a ‘x’. Samples Bac 110113, Th-St1 and stromatolite were collected from location 1. Water samples were collected from various locations; the cenote samples come from location 2 (Cenote Azul), samples R1-4 samples came from location 3, samples spring, and vent came from location 4, and RM1 and RM2 were come from location 5. The core samples Th-St2 were collected from location 3.

CHETUMAL E16-4-7

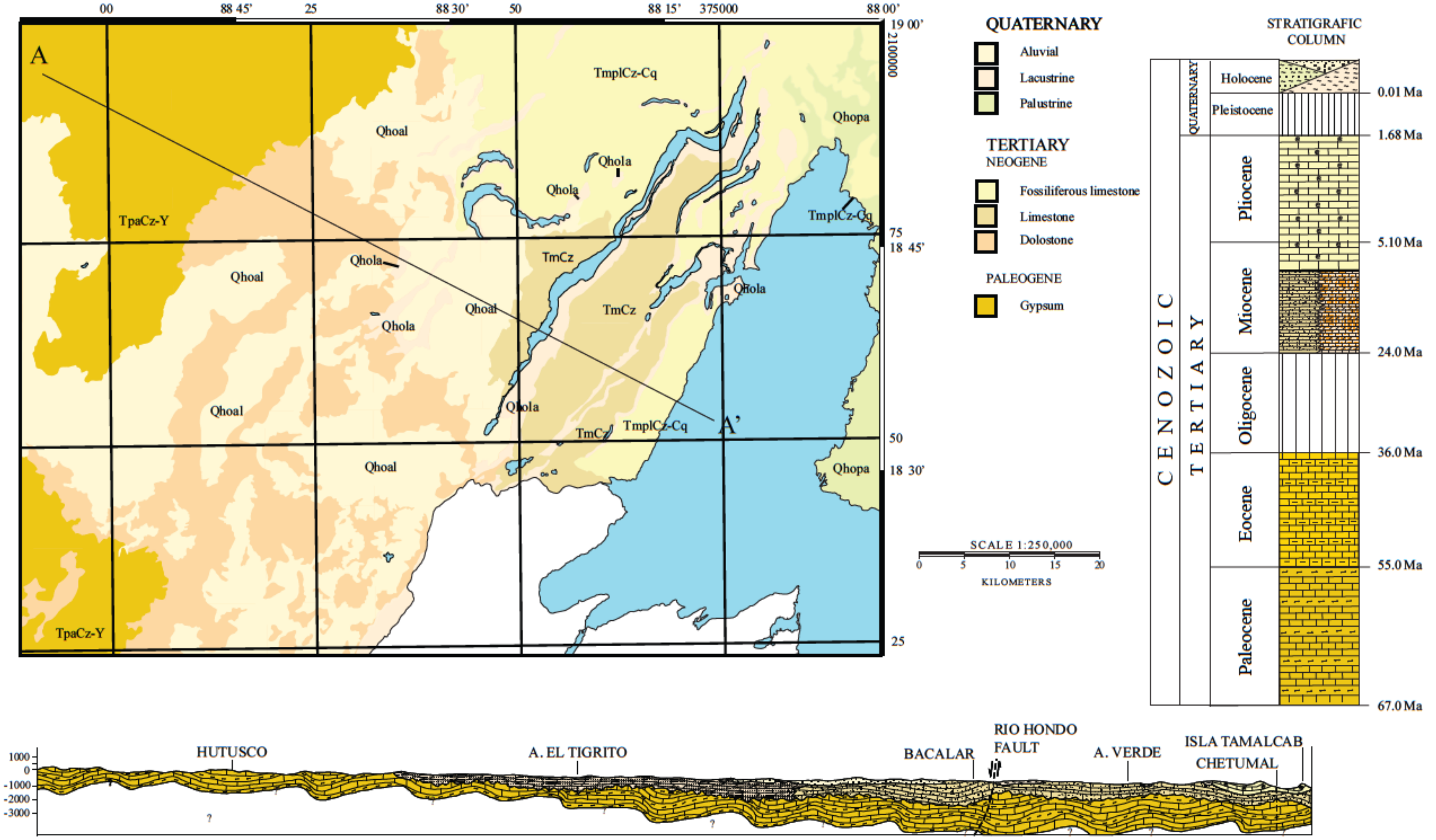

FIGURE 2.2 — Geological map of Southern Quintana Roo with cross section through Laguna Bacalar, modified from SGM, 2005. Carta Geologica 1:25000, hoja E16-4 (Chetumal). Mexico: Servicio Geológico Mexicano.

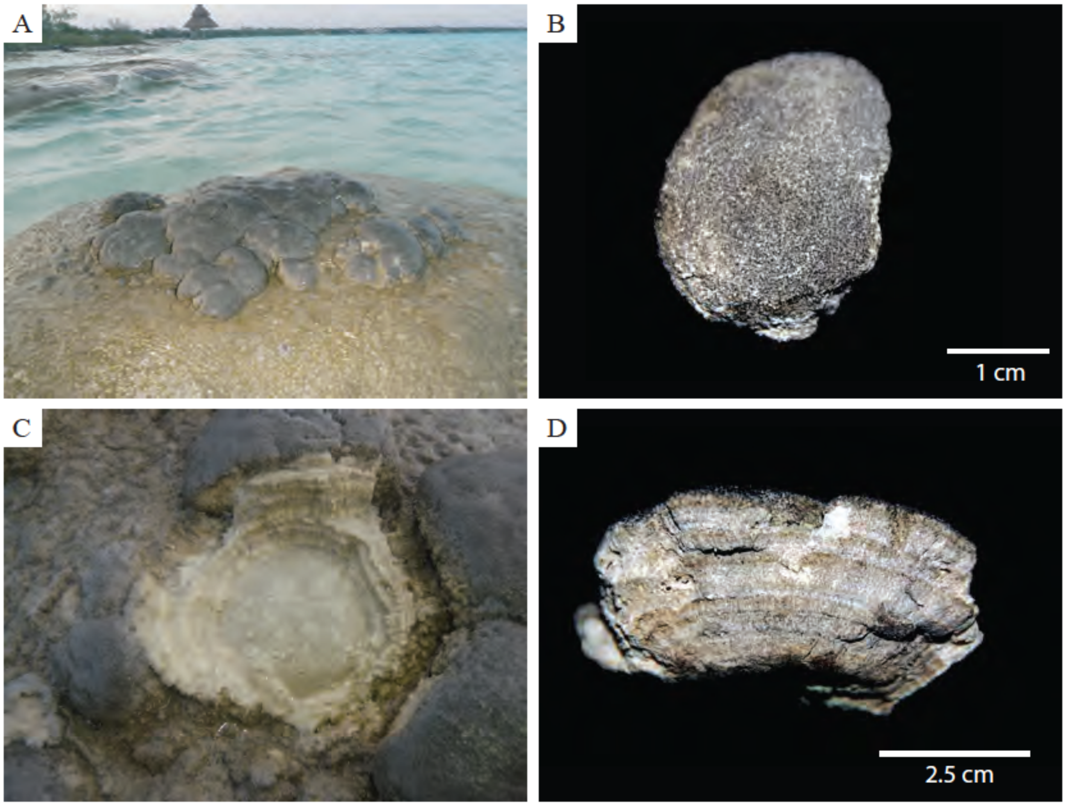

FIGURE 2.3 — Stromatolite images, hand and field samples. (A) Stromatolites found growing on top of the larger thrombolitic-stromatolites coalescing together forming larger structures and appearing to be imbedded on the larger thrombolitic-stromatolites (image contrast and brightness were modified). (B) Domal stromatolites displaying a dark grey coloration, and a smooth outer exterior. (C) Stromatolite removed from the larger thrombolitic-stromatolites display internal lamination, and fibrous texture. (D) Cross-section of stromatolite with distinct internal lamination made up of dark and light bands, fibrous texture can also be observed.

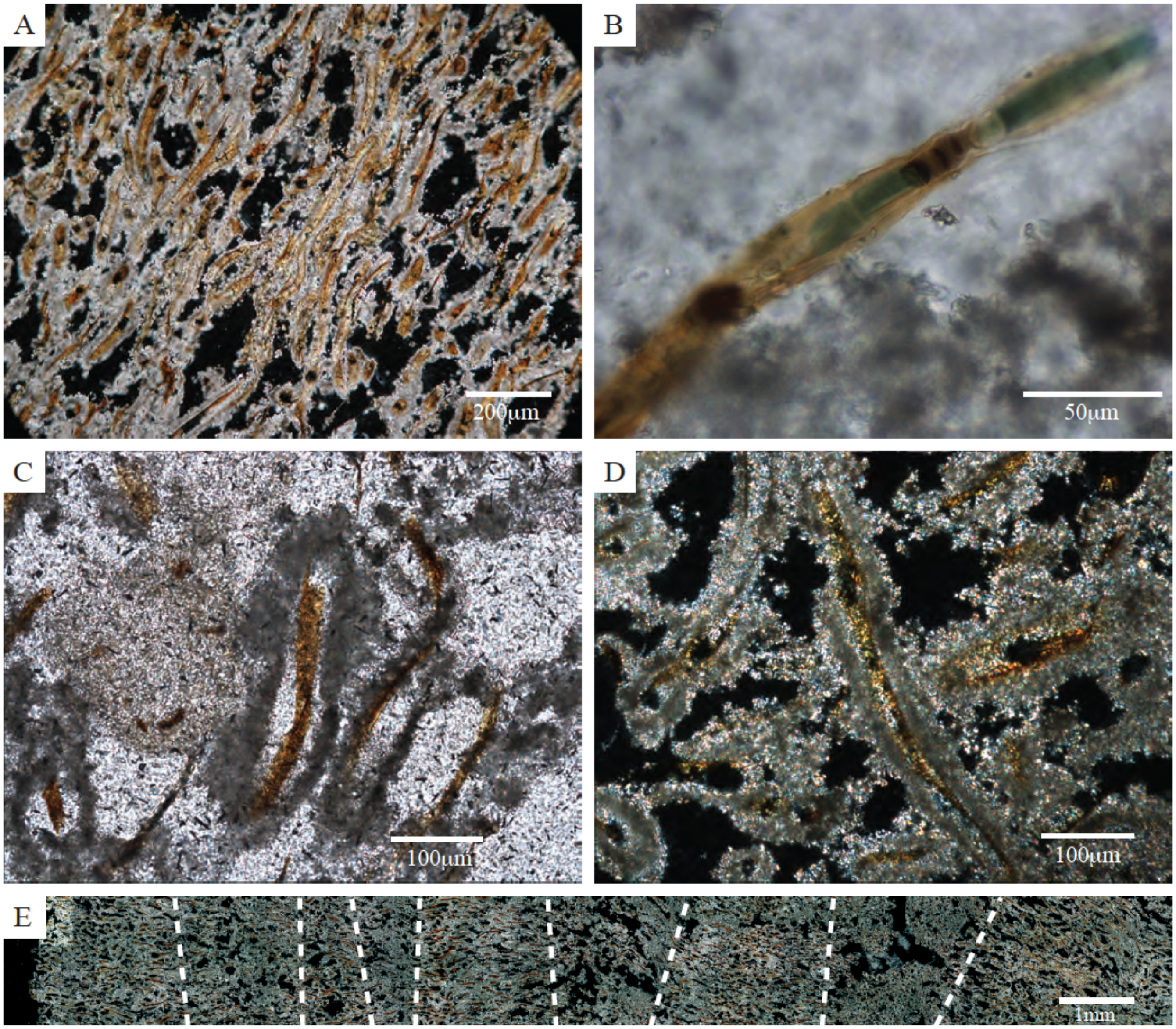

Figure 2.4 — Petrographic images of stromatolites under cross- (XPL) and plain-polarized light (PPL). (A) Microbial filaments under XPL displaying brownish coloration. Lengths of the filaments are variable, and the widths average between 10-30 m. Individual filaments are surrounded by calcite, predominantly micrite, and cemented together by microspar. The void formed by the decomposition of the bacterial filaments are infilled by varying degrees of microspar, always doing so inwardly. (B) Bacterial filament under PPL still retaining internal segmentation and green pigmentation. (C) Microbial filament under PPL surrounded by micrite (grey translucent appearance). (D) Microbial filament under XPL, displaying brownish coloration, surrounded by micrite, and infilled by microspar creating microbialite molds. (E) Petrographic cross-section of entire stromatolite under XPL. Banding is observed to be the result of sections having high abundance of bacterial filaments/molds and little porosity (designated as P-lamina), preceded by sections with higher porosity and much lesser bacterial abundance (designated as U-lamina).

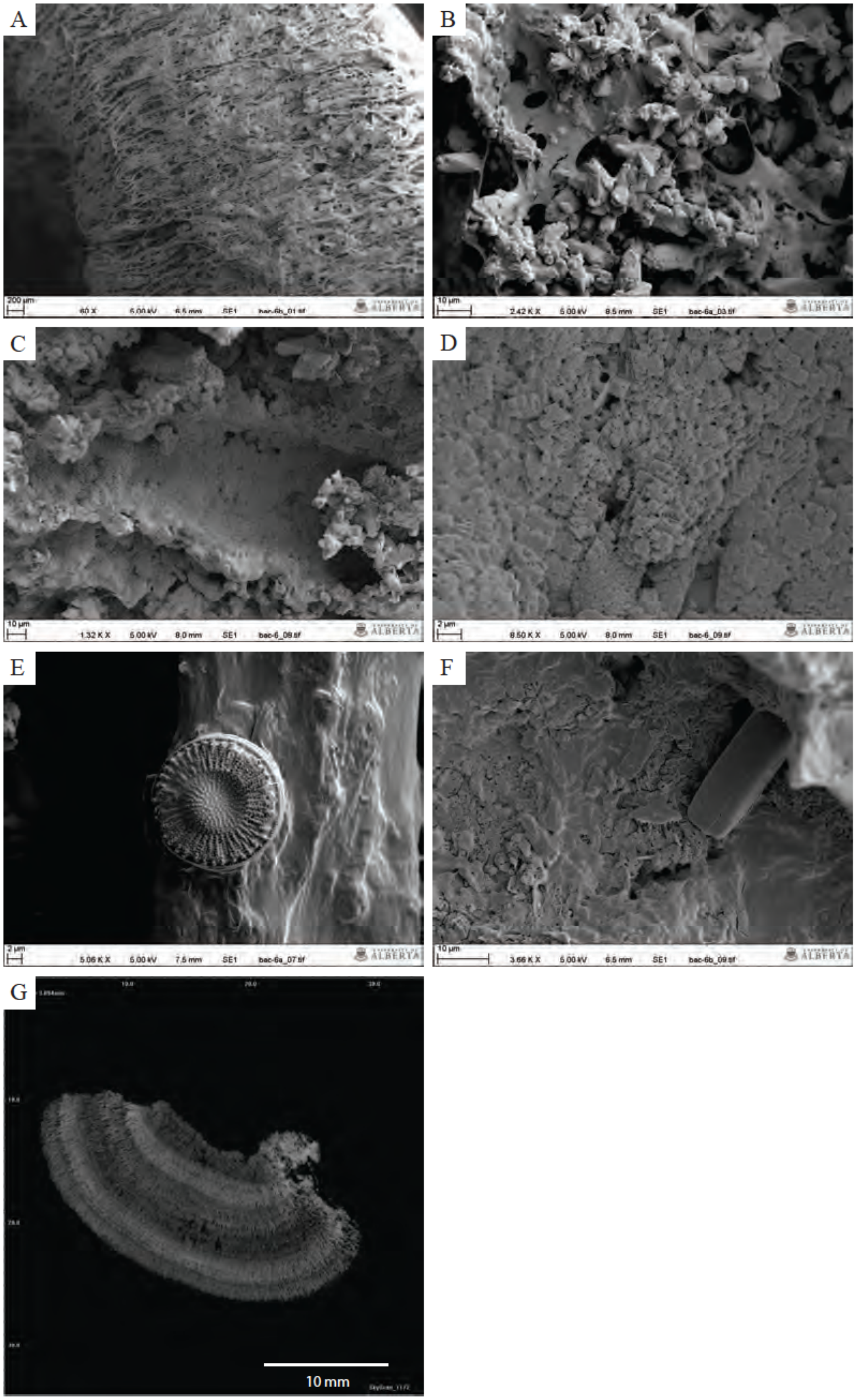
A
200 µm
60 X
5.00 kV
6.5 mm
SE1
bac-6b_01.tif
B
10 µm
2.42 K X
5.00 kV
8.5 mm
SE1
bac-6a_03.tif
C
10 µm
1.32 K X
5.00 kV
8.0 mm
SE1
bac-6_08.tif
D
2 µm
8.50 K X
5.00 kV
8.0 mm
SE1
bac-6_09.tif
E
2 µm
5.06 K X
5.00 kV
7.5 mm
SE1
bac-6a_07.tif
F
10 µm
3.66 K X
5.00 kV
6.5 mm
SE1
bac-6b_09.tif
G
10.0
20.0
30.0
10 mm

FIGURE 2.5 — SEM images of stromatolites. (A) High density of microbial filaments highly mineralized. (B) Calcite grains surrounded by EPS. (C) Bacterial mold having a smooth interior composed of very small calcite grains, presumably micrite. (D) Micrite grains smaller than 2 μm composing interior of bacterial mold. (E) Microbial filament surrounded by EPS with imbedded diatom. (F) Diatom cell in the presence of EPS and calcite grains. (G) X-ray microtomography of a complete stromatolite. Distinct layers can be observed, with varying densities of filamentous filaments and porosity.

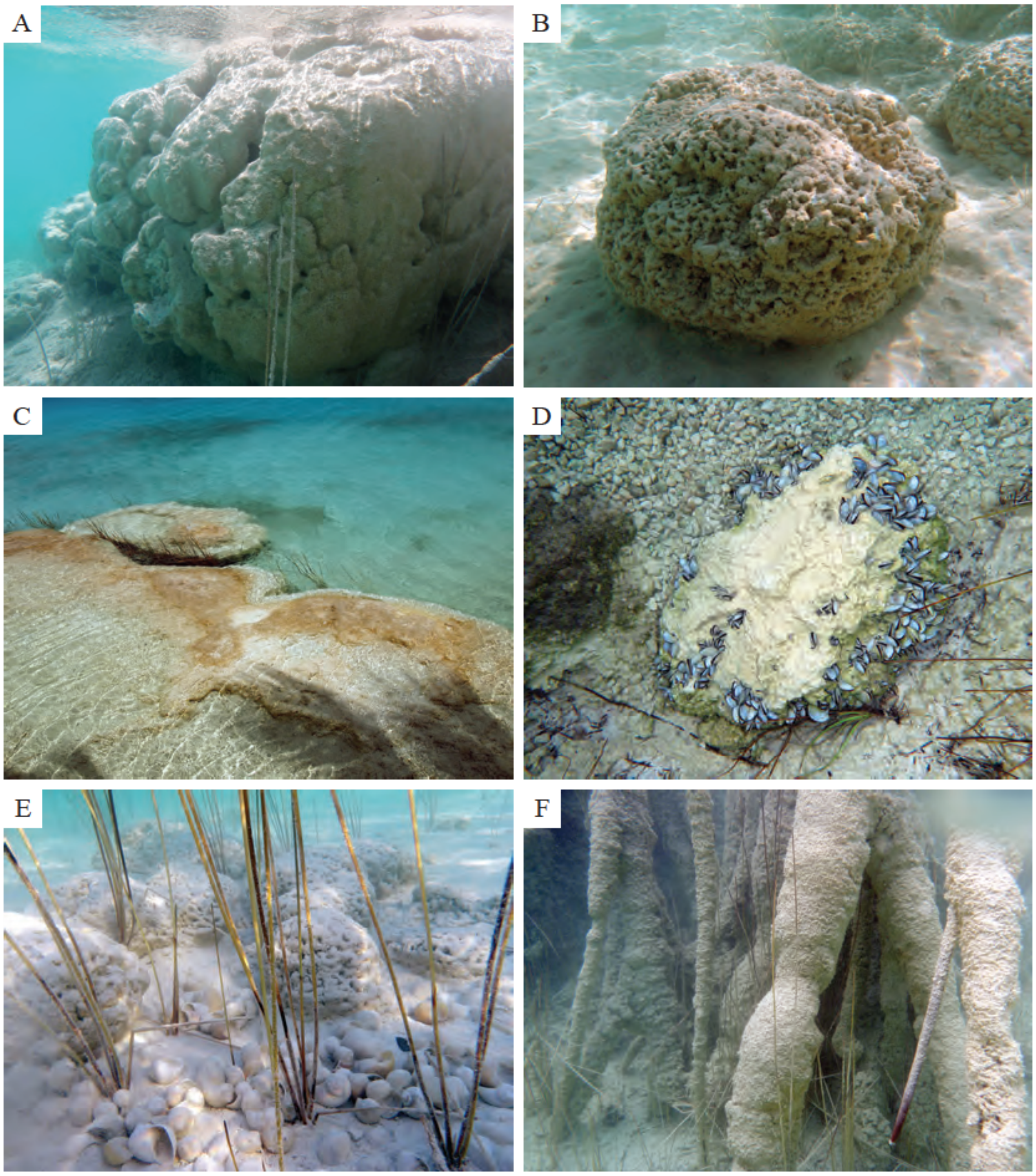
A
B
C
D
E
F

FIGURE 2.6 — Field images of various thrombolitic-stromatolites found in Laguna Bacalar (contrast and brightness modified). (A) thrombolitic-stromatolites displaying domal morphology and a smooth exterior, with a cream coloration similar to that of lake sediment. (B) Dome shaped sample with a pitted outer texture. (C) Meter size thrombolitic-stromatolites coalescing together to form larger structures. They also display domal morphology, and have a darker coloration where sub-aerially exposed. (D) Bivalves found embedded on the outer surface of thrombolitic-stromatolites. (E) thrombolitic-stromatolites found growing in the presence of surrounding gastropods, and mangrove shoots. (F) Mangrove roots on the western shore being used as substrates for the growth of microbialites.

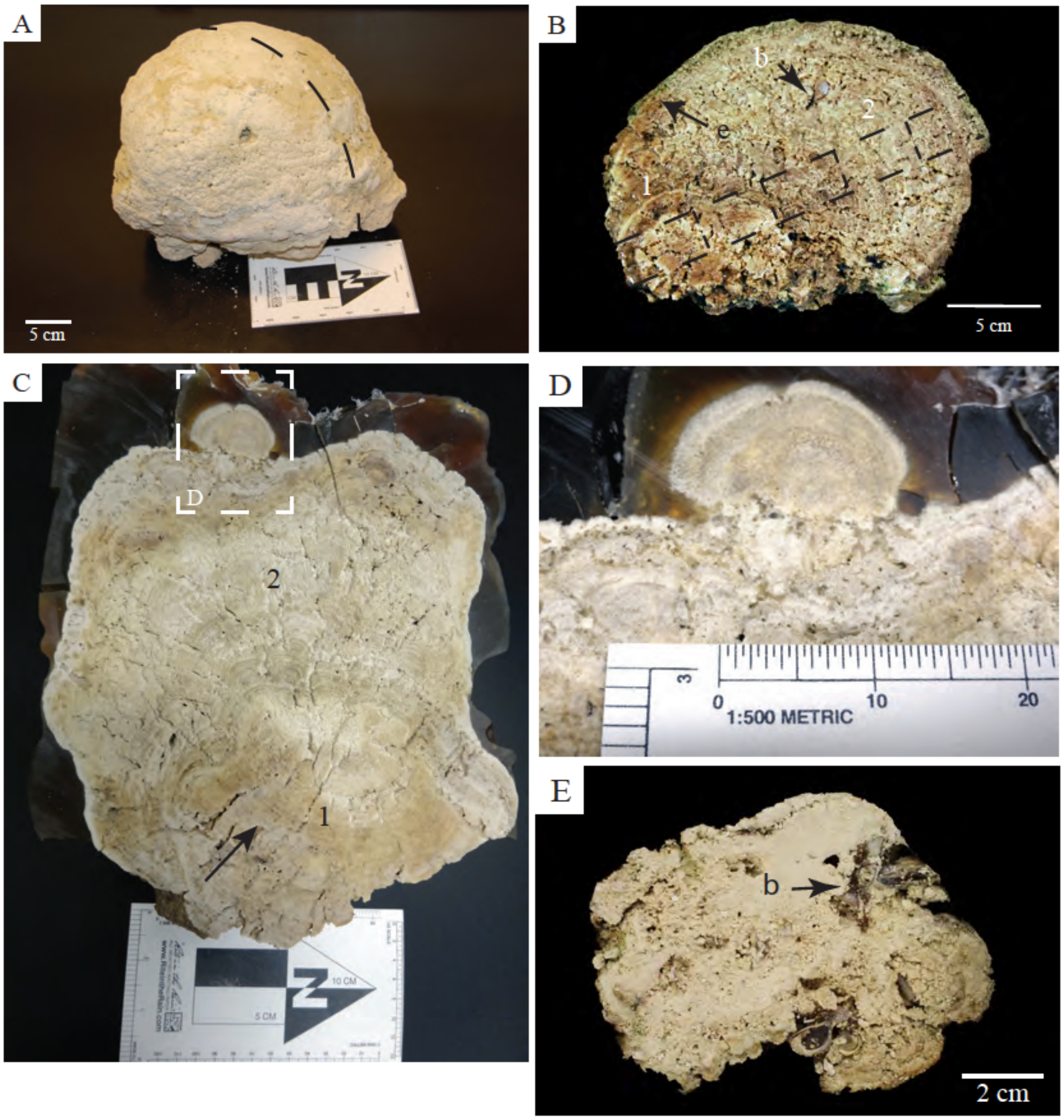
A
5 cm
B
b
e
2
1
5 cm
C
D
2
1
10 CM
5 CM
D
3
0
10
20
1:500 METRIC
E
b
2 cm

FIGURE 2.7 — Microbialite displaying domal morphologies, with internal stromatolitic and thrombolitic texture. (A) Domal thrombolitic-stromatolites with a smooth exterior. (B) Cross-section of latter microbialite. Internal stromatolitic lamination can be observed at the bottom-left (1) and top section (2). The middle section displays thrombolitic textures as well as cemented bivalve shells (see arrow with 'b'). A green endolithic algal mat is located at the top of the microbialite (see arrow with 'e'). Dashed lines display location from where thin and thick sections were made from. (C) Cross section of larger microbialite displaying stromatolitic (1) and thrombolitic (2) textures. Arrow indicates overturned stromatolite with concave laminations. Also present at the top of the sample are two apparent stromatolites that have coalesced and display complete internal lamination. (D) Small microbialite containing internal laminations, with dark and light bands, found at the top of sample C. (E) thrombolitic-stromatolites displaying domal morphology and a number of bivalves, including the byssal threads (see arrow with 'b').

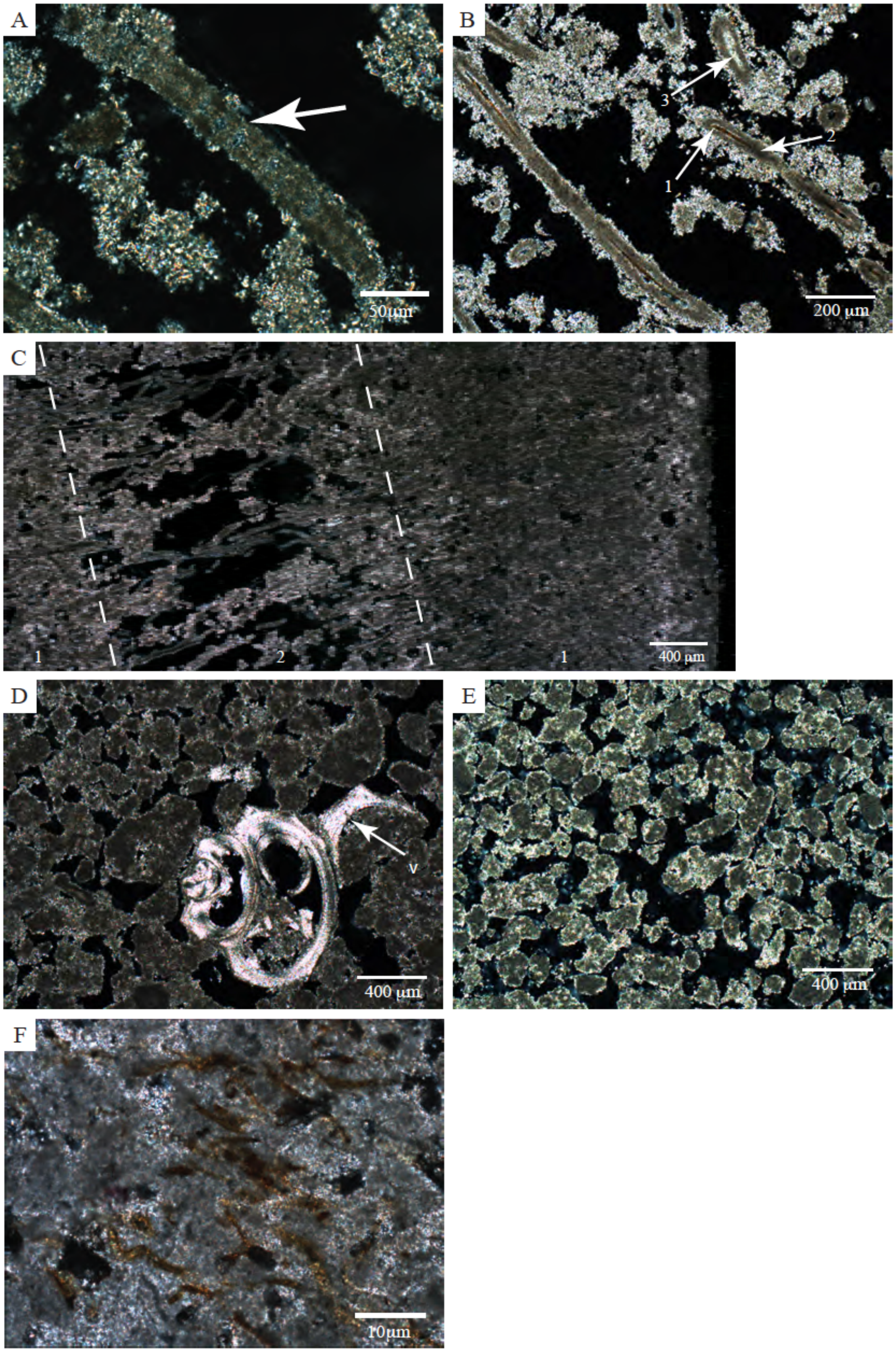
A
50µm
B
3
2
1
200 µm
C
1
2
1
400 µm
D
v
400 µm
E
400 µm
F
10µm

FIGURE 2.8 — Thrombolitic-stromatolite petrographic images. (A) Petrographic image of microbial mold under cross-polarized light (XPL). Internal structure is still visible, and has been replaced by micrite (grey translucent appearance, individual grains indistinguishable). Microspar (high birefringence grains) calcite is observed infilling parts of the mold, as well as precipitating on the outer surface of the mold. (B) Image under XPL showing microbial filaments (arrow with '1') with a dark brown coloration, surrounded by micrite (arrow with '2') and infilled by microspar (arrow with '3'), which is also cementing together the bacterial filament molds. (C) Transect of part of thrombolitic-stromatolites under XPL displaying lamination. Lamina are observed having a high density of cyanobacterial filaments/molds (P-lamina)(1), preceded by a lamina having greater porosity and a lesser abundance of cyanobacterial filaments/molds (U-lamina)(2). (D) Micrite peloids under XPL cemented together by secondary microspar. Also observed to be present is a bioclasts sell (arrow with 'v'). (E) Microbial filaments under XPL displaying brownish coloration and much lesser mineralization.

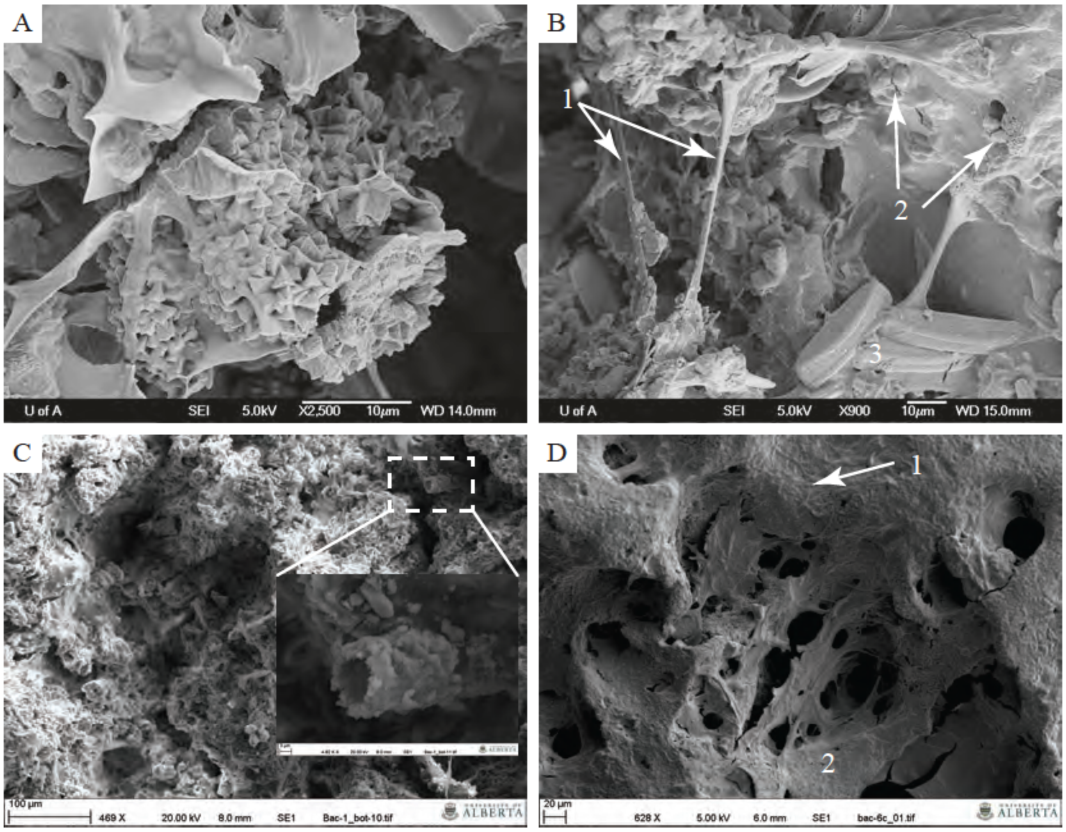

FIGURE 2.9 — SEM images of thrombolitic-stromatolites. (A) Present are tetrahedral dipyramid calcite crystals. (B) Observed is the presence of bacterial filaments with attached calcite grains (see arrow with ‘1’), calcite grains covered by a layer of EPS (see arrows with ‘2’), and diatoms partially covered with EPS (see ‘3’). (C) Image of the calcite grains composing the microbialite, as well as a filament molds void of the filament. (D) An abundance of EPS (2) covering individual filaments (1) as well as calcite grains.

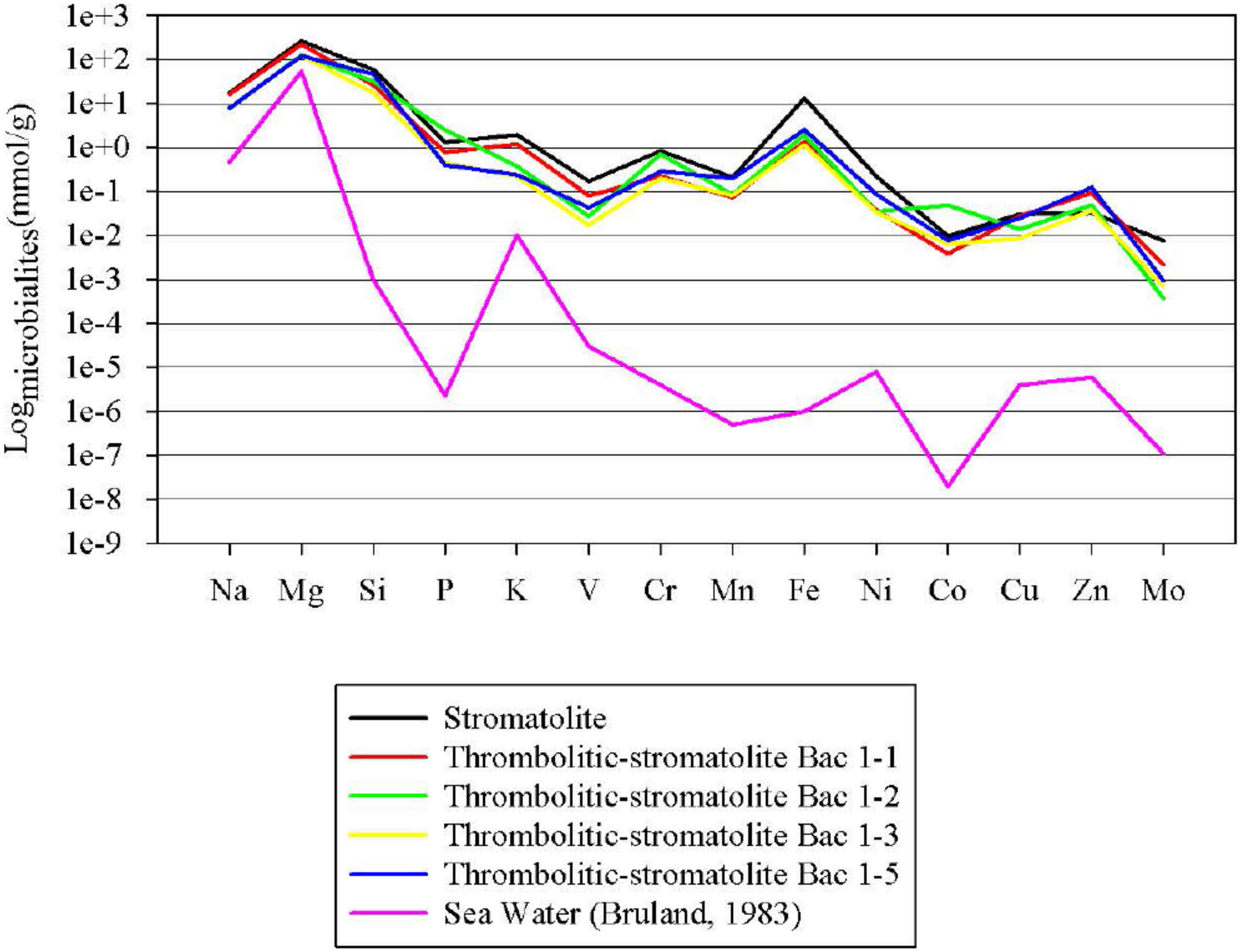
1e+3
1e+2
1e+1
1e+0
1e-1
1e-2
1e-3
1e-4
1e-5
1e-6
1e-7
1e-8
1e-9
Log$_{\text{microbialites}}$(mmol/g)
Na
Mg
Si
P
K
V
Cr
Mn
Fe
Ni
Co
Cu
Zn
Mo
Stromatolite
Thrombolitic-stromatolite Bac 1-1
Thrombolitic-stromatolite Bac 1-2
Thrombolitic-stromatolite Bac 1-3
Thrombolitic-stromatolite Bac 1-5
Sea Water (Bruland, 1983)

FIGURE 2.10 — Elemental graphs (A) Elemental comparison of a stromatolite sample vs. thrombolitic-stromatolites sample (four samples). Patterns appear to be similar. (B) Essential elements of stromatolites compared to those of thrombolitic-stromatolites sample, sea water, and Laguna Bacalar water.

A

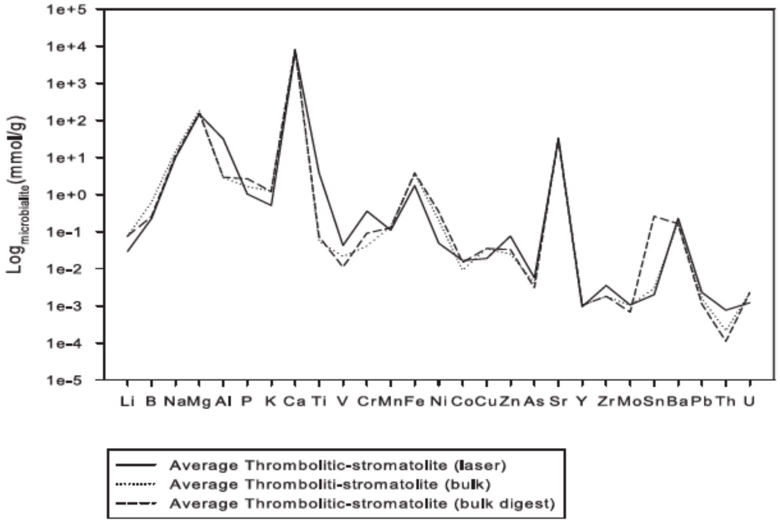
1e+5
1e+4
1e+3
1e+2
1e+1
1e+0
1e-1
1e-2
1e-3
1e-4
1e-5
Log$_{microbialite}$(mmol/g)
Li B NaMg Al P K Ca Ti V CrMnFe Ni CoCuZn As Sr Y ZrMoSnBaPbTh U
Average Thrombolitic-stromatolite (laser)
Average Thromboliti-stromatolite (bulk)
Average Thrombolitic-stromatolite (bulk digest)

B

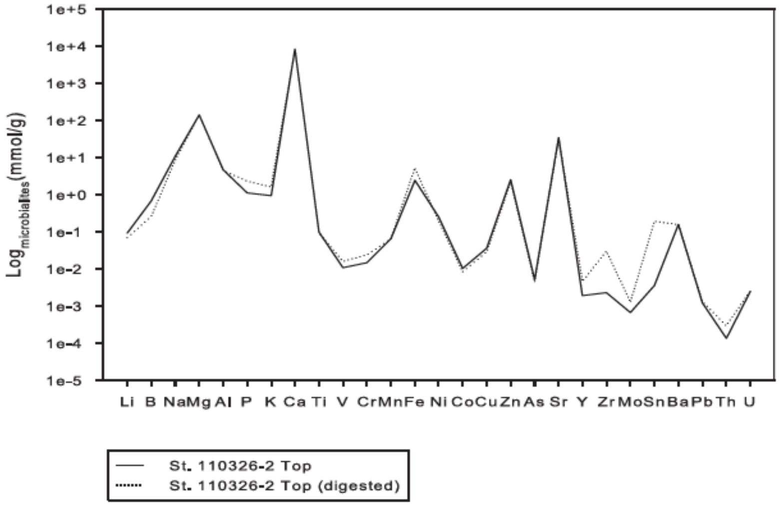
1e+5
1e+4
1e+3
1e+2
1e+1
1e+0
1e-1
1e-2
1e-3
1e-4
1e-5
Log$_{microbialites}$(mmol/g)
Li B NaMg Al P K Ca Ti V CrMnFe Ni CoCuZn As Sr Y ZrMoSnBaPbTh U
St. 110326-2 Top
St. 110326-2 Top (digested)

C

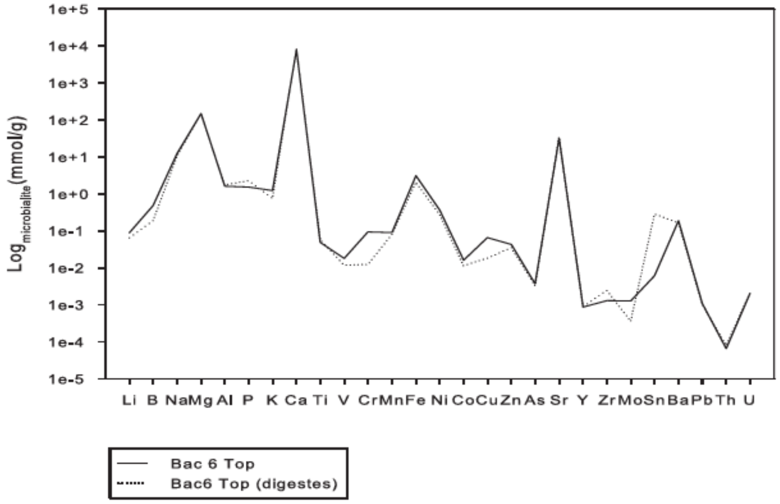
1e+5
1e+4
1e+3
1e+2
1e+1
1e+0
1e-1
1e-2
1e-3
1e-4
1e-5
Log$_{microbialite}$(mmol/g)
Li B NaMg Al P K Ca Ti V CrMnFe Ni CoCuZn As Sr Y ZrMoSnBaPbTh U
Bac 6 Top
Bac6 Top (digestes)

FIGURE 2.11 — Elemental graphs of stromatolites and thrombolitic-stromatolites. (A) Average measurements of thrombolitic-stromatolites sample obtained from laser ICP-MS, bulk ICP-MS, and digested bulk ICP-MS. (B) Thrombolitic-stromatolites (St. 10326) comparison between digested and undigested bulk ICP-MS measurements. (C) Thrombolitic-stromatolites (Bac 6) comparison between digested and undigested bulk ICP-MS measurements.

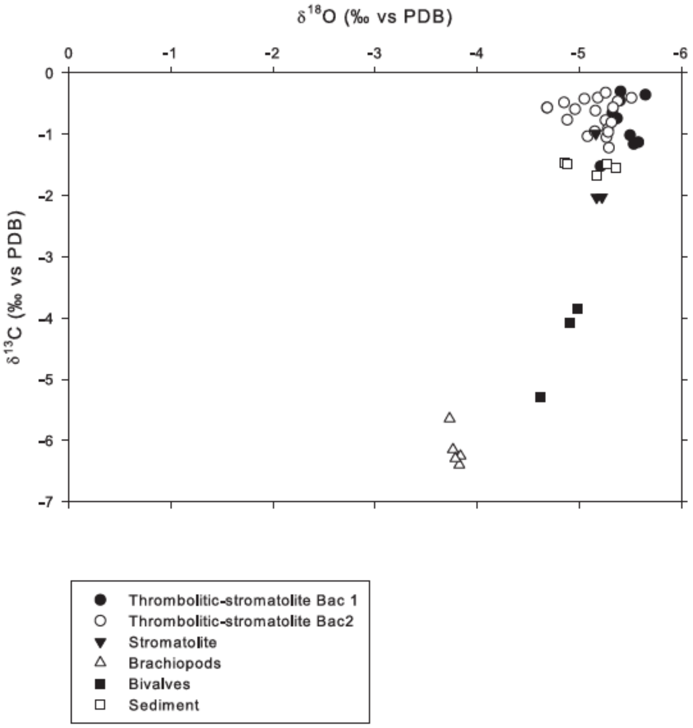

FIGURE 2.12 — Oxygen vs. carbon isotope measurements of thrombolitic-stromatolites, stromatolites, lake sediment, bivalves, and gastropods.

Analyte	Li	Na	Mg	Al	Si	K	Ca	Ti	V	Cr	Fe
Detection Limits (DL)	0.00005	0.0005	0.002	0.0002	0.005	0.006	0.031	0.00009	0.00005	0.00005	0.0037
Units	ppm	ppm	ppm	ppm	ppm	ppm	ppm	ppm	ppm	ppm	ppm
Sample											
RM1	0.0254	35.2	79.8	0.0054	13.0	3.02	317	0.0183	0.00865	0.00288	0.0218
RM2	0.0275	35.3	80.6	0.0051	13.2	3.23	323	0.0182	0.00817	0.00252	0.0533
R1	0.0285	35.0	79.2	0.0028	12.6	2.86	332	0.0187	0.00606	0.00151	0.0220
R2	0.0303	33.9	74.7	0.0035	11.6	2.85	335	0.0190	0.00414	<DL	<DL
R3	0.0332	33.3	74.4	0.0019	11.4	2.75	334	0.0187	0.00415	0.00079	<DL
R4	0.0366	33.1	73.3	0.0028	11.1	3.27	339	0.0174	0.00385	0.00088	<DL
Cenote	0.0415	34.5	79.9	0.0026	10.2	3.31	385	0.0185	0.00347	0.00027	<DL
Spring	0.0394	40.8	77.4	0.0022	11.4	3.01	349	0.0165	0.00409	0.00112	0.0082
Vent	0.0382	34.8	75.8	0.0140	11.1	3.31	338	0.0163	0.00515	0.00080	<DL
Vent duplicate	0.0378	35.1	76.2	0.0137	11.4	3.35	341	0.0163	0.00686	0.00127	<DL

Analyte	Mn	Co	Ni	Cu	Zn	Ge	As	Se	Rb
Detection Limits	0.00003	0.00003	0.00006	0.00003	0.00008	0.00002	0.00006	0.0002	0.00004
Units	ppm	ppm	ppm	ppm	ppm	ppm	ppm	ppm	ppm
Sample									
RM1	0.00036	0.00073	0.00360	0.00133	0.0161	0.00009	0.00169	<DL	0.00690
RM2	0.00037	0.00069	0.00287	0.00132	0.0201	0.00009	0.00156	<DL	0.00479
R1	0.00022	0.00065	0.00282	0.00111	0.0160	0.00011	0.00118	<DL	0.00440
R2	0.00031	0.00071	0.00514	0.00144	0.0149	0.00011	0.00085	<DL	0.00440
R3	0.00019	0.00058	0.00381	0.00100	0.0154	0.00011	0.00104	<DL	0.00420
R4	0.00026	0.00055	0.00429	0.00128	0.0152	0.00008	0.00110	<DL	0.00429
Cenote	0.00031	0.00062	0.00514	0.00242	0.0176	0.00008	0.00143	<DL	0.00412
Spring	0.00564	0.00063	0.00378	0.00178	0.0192	0.00008	0.00179	<DL	0.00411
Vent	0.00076	0.00055	0.00314	0.00197	0.0230	0.00007	0.00176	<DL	0.00431
Vent duplicate	0.00075	0.00049	0.00153	0.00172	0.0241	0.00006	0.00227	<DL	0.00436

Analyte	Sr	Y	Zr	Mo	Ru	Sb	Cs	Ba	La	Ce
Detection Limits	0.00003	0.00002	0.00009	0.00002	0.00001	0.00001	0.00002	0.00003	0.00003	0.00003
Units	ppm	ppm	ppm	ppm	ppm	ppm	ppm	ppm	ppm	ppm
Sample										
RM1	8.16	0.00004	<DL	0.0122	0.00086	0.00016	0.00009	0.0170	<DL	0.00003
RM2	7.90	0.00004	<DL	0.0119	0.00075	0.00016	0.00007	0.0166	<DL	<DL
R1	8.09	0.00004	<DL	0.0117	0.00091	0.00013	0.00005	0.0167	<DL	<DL
R2	8.16	0.00004	<DL	0.0114	0.00104	0.00013	0.00005	0.0167	<DL	<DL
R3	8.06	0.00004	<DL	0.0112	0.00106	0.00011	0.00005	0.0166	<DL	<DL
R4	8.22	0.00003	<DL	0.0114	0.00102	0.00016	0.00005	0.0165	<DL	<DL
Cenote Azul	8.36	0.00004	<DL	0.0123	0.00113	0.00016	0.00004	0.0162	<DL	<DL
Spring	8.32	0.00008	<DL	0.0127	0.00106	0.00010	0.00005	0.0176	0.00005	0.00005
Vent	8.13	0.00006	0.00020	0.0120	0.00100	0.00031	0.00006	0.0163	0.00004	0.00006
Vent duplicate	8.15	0.00005	0.00037	0.0124	0.00084	0.00033	0.00006	0.0164	0.00004	0.00006

Analyte	Au	Tl	Pb	U	Cl^-
Detection Limits (DL)	0.00001	0.00005	0.00003	0.00003	
Units	ppm	ppm	ppm	ppm	mg/L
Sample					
RM1	0.00108	0.00022	0.00021	0.00288	41.60
RM2	0.00084	0.00022	0.00021	0.00294	41.50
R1	0.00063	0.00021	<DL	0.00295	42.00
R2	0.00051	0.00019	0.00006	0.00303	41.31
R3	0.00039	0.00018	0.00002	0.00298	41.69
R4	0.00038	0.00019	0.00021	0.00298	41.44
Cenote Azul	0.00031	0.00017	0.00045	0.00314	42.75
Spring	0.00029	0.00017	0.00010	0.00309	47.59
Vent	0.00025	0.00020	0.00029	0.00286	43.08
Vent duplicate	0.00025	0.00020	0.00029	0.00291	

TABLE 2.1 — Trace element concentrations of lake water.

	Sample no.	**Description**	**Weight**	**δ^{13}C (‰ vs. PDB)**	**δ^{18}O (‰ vs. PDB)**	**δ^{18}O (‰ vs. SMOW)**
Thrombolitic-stromatolite 1	Th-St1-TL1	Top left	18.5	-0.304	-5.406	25.336
	Th-St1-TL2	Top left	12.2	-0.359	-5.650	25.086
	Th-St1-TR1	Top right	13.7	-1.016	-5.498	25.242
	Th-St1-TR2	Top right	-	-1.133	-5.580	25.158
	Th-St1-M1	Middle	-	-0.655	-5.325	25.420
	Th-St1-M2	Middle right	12.1	-0.744	-5.371	25.373
	Th-St1-MR2	Middle right	11.9	-1.163	-5.535	25.204
	Th-St1-TSM	Middle banding	10.6	-0.451	-5.400	25.343
	Th-St1-B	Base	-	-1.527	-5.210	25.539
Thrombolitic-stromatolite-2	Th-St2-35	core bottom at 35cm from top	18.7	-0.483	-4.851	25.909
	Th-St2-33	core bottom at 33cm from top	18.7	-0.765	-4.884	25.875
	Th-St2-30	core bottom at 30cm from top	15.8	-0.568	-4.686	26.080
	Th-St2-26	core bottom at 26cm from top	14.8	-1.035	-5.083	25.670
	Th-St2-24	core bottom at 24cm from top	19.3	-0.464	-5.378	25.366
	Th-St2-22	core bottom at 22cm from top	16.5	-0.567	-4.687	26.078
	Th-St2-20	core bottom at 20cm from top	13.2	-0.593	-4.961	25.796
	Th-St2-18	core bottom at 18cm from top	13.4	-1.221	-5.291	25.455
	Th-St2-18a	core bottom at 18cm from top	23.4	-1.052	-5.269	25.478
	Th-St2-16	core bottom at 16cm from top	13	-0.423	-5.051	25.703
	Th-St2-14	core bottom at 14cm from top	12.1	-0.954	-5.153	25.598
	Th-St2-12	core bottom at 12cm from top	18.5	-0.617	-5.160	25.591
	Th-St2-10	core bottom at 10cm from top	12.8	-0.774	-5.258	25.490
	Th-St2-8	core bottom at 8cm from top	16.5	-0.916	-5.282	25.465
	Th-St2-6	core bottom at 6cm from top	25.6	-0.408	-5.513	25.227
	Th-St2-6a	core bottom at 6cm from top	19.1	-0.406	-5.183	25.567
	Th-St2-6b	core bottom at 6cm from top	22.3	-0.324	-5.261	25.487
	Th-St2-4	core bottom at 4cm from top	22.1	-0.810	-5.317	25.428
	Th-St2-2	core bottom at 2cm from top	25.6	-0.566	-5.333	25.412
	Th-St2-0	core bottom at 0cm from top	12.4	-0.966	-5.286	25.460

Stromatolite	St-1	Stromatolite 1	10.9	-0.994	-5.165	25.585
	St-2	Stromatolite 2	12.7	-2.036	-5.171	25.579
	St-2	Stromatolite 2	14.1	-2.03	-5.223	25.525
Gastropods	Gr-1	Gastropod 1	32.2	-6.253	-3.838	26.953
	Gr-1a	Gastropod 1	15.8	-6.398	-3.827	26.965
	Gr-2	Gastropod 2	37.6	-6.15	-3.763	27.031
	Gr-2a	Gastropod 2	28.1	-6.296	-3.787	27.006
	Gr-3	Gastropod 3	20.8	-5.645	-3.731	27.063
Bivalves	Bv-22	Imbedded in Th-St2 at 19cm	22.6	-5.286	-4.621	26.147
	Bv-29	Imbedded in Th-St2 at 6cm	23.7	-4.082	-4.911	25.847
	Bv-29a	Imbedded in Th-St2 at 6cm	18.4	-3.84	-4.983	25.773
Sediment	Sed-1-09	Lake sediment		-1.46	-4.853	25.907
	Sed-2-09	Lake sediment		-1.674	-5.177	25.573
	Sed-3-09	Lake sediment		-1.492	-4.879	25.88
	Sed-1-11	Lake sediment		-1.498	-5.273	25.474
	Sed-2-11	Lake sediment		-1.549	-5.364	25.381
Water	Wt-1	Water sample 1				-3.152552
	Wt-2	Water sample 2				-2.930288
					Water average	-3.04142

TABLE 3.2 — Carbon and oxygen isotope data for microbialites, gastropods, bivalves, sediments and water.

CHAPTER 3: FACTORS CONTROLLING GROWTH AND MORPHOLOGY OF THE FRESHWATER MICROBIALITES OF LAGUNA BACALAR, QUINTANA ROO, MEXICO

3.1. Introduction

Microbialites are biogenic sedimentary structures formed through the trapping, binding, and/or precipitation of calcium carbonate by benthic microbial communities (Burne and Moore, 1987). They are amongst the oldest evidence of life, first appearing some ca. 3.5 Ga (Hofmann, 1977; Lowe, 1980; Walter et al., 1980; Byerly et al., 1986; Hofmann et al., 1999; Allwood et al., 2006; Allwood et al., 2009), and have existed throughout much of Earth's history (85%)(Awramik, 1991). In modern settings, microbialites have been reported from both marine (subtidal to supratidal, hypersaline and normal conditions) and non-marine settings (streams, lakes, thermal springs, frozen lakes) (McNamara and Awramik, 1992), forming domes, columns, and mounds (Wray, 1977), but their diversity and abundance are incomparable to those of the Proterozoic (Awramik, 1991; Awramik, 1992).

Microbialites are subdivided into two distinct groups based on their internal fabric (Shapiro, 2000): (1) those containing internal lamination have been described as stromatolite macrostructures (Kalkowsky, 1908), (2) whereas the presence of internal clotting and poorly defined or absent lamination have been described as thrombolite macrostructures (Aitken, 1967). The formation of both, even though distinct, has been ascribed to the benthic microbial communities present in such structures (Hofmann, 1973; Riding, 1999; Riding, 2011), along with other abiogenic processes (e.g., cementation).

When microbialites first appeared during the Archean their abundance was restricted, with only 48 known occurrences reported, displaying 40 different morphotypes (Schopf et al., 2007). These were predominantly stromatolitic in nature, resulting from the biogenic precipitation of calcium carbonate, within shallow-marine and possibly evaporitic basins (Awramik and Sprinkle, 1999; Schieber, 1999; Altermann, 2008). In the Proterozoic, microbialites would reach their greatest abundance and diversity (Hofmann, 1973; Awramik, 1991; Awramik and Grey, 2005), colonizing siliciclastic and carbonate platforms settings (Beukes, 1987; Schieber, 1999), as well as epicontinental alkaline lakes and rivers (Buck, 1980). Microbialite diversification occurred in two stages, the first during the Paleoproterozoic (2500-1650 Ma) and the second during the Mesoproterozoic (1350-1000 Ma), resulting in some 800 different morphologically different taxa (Awramik, 1992). However by the late Neoproterozoic and early Paleozoic microbialites abundance and diversity drastically declined (Fischer, 1965; Awramik, 1971; Walter and Heys, 1985; Awramik, 1991; McNamara and Awramik, 1992; Schopf et al., 2007). The cause of the decline is still controversial, and thought to have been due to the changes in ocean chemistry, grazing and burrowing of mats by metazoans, spatial/substrate competition, or due to competition for nutrients with other organisms (Pratt, 1982; Riding, 1997). Thrombolitic microbialites became proportionally more important near the end of the Precambrian, and early Phanerozoic. However, both stromatolites and thrombolites suffer a decrease in their abundance, as they were gradually replaced by reef complexes constructed of crustose red algae, calcareous sponges and/or coelenterates (Golubic, 1994)

The study of microbialites has been extensive, yet many aspects about their growth and internal morphology remain elusive. Even after more than a century of research their definition, and origin are still debated. Today most accept that microbialites are biogenically influenced even if only 1% of preserved samples have evidence of so (Grotzinger and Knoll, 1999). Furthermore, growth mechanisms and morphology of microbialites changed throughout their history. While most Archean microbialites were formed through the precipitation of calcium carbonate, growth through the trapping and binding of detrital sediments would become more predominant later in the Proterozoic and throughout (Allwood et al., 2006; Altermann, 2008; Allwood et al., 2009). Morphologically extant and ancient microbialites differ significantly, and an understanding of formation has yet to be reached.

Laguna Bacalar is a unique site as it is one of the few surface water features in the Yucatan Peninsula, but also because it is where we find large microbialites. Freshwater karstic waters surfacing at the Xul-Ha sinkhole become supersaturated with regards to calcium carbonate, which feed Laguna Bacalar, promote the growth of microbialites. The two different locations where microbialites are found in conjunction with the different internal morphologies each displayed, allow us to assess the different factors that control their growth and internal textrue. Such findings can further shed light into our understanding of fossil microbialites, their growth, and the factors that might have controlled their abundance and diversity.

3.2. Study Area

Laguna Bacalar is located in the south-east corner of Quintana Roo, Mexico (Fig.1). It is ~2km wide, and ~50km long, (Gischler et al., 2008), with an area of ~3.1 km^2 (Bauer-Gottwein et al., 2011), and encompassing both a lake and a river system.

Bedrock outcrops around Bacalar and Rio Hondo (further south) are predominantly Miocene in age (Díaz, 2005). Laguna Bacalar, and Xul-Ha (sinkhole) occupy a down-faulted basin, formed between the Late Cretaceous and Pliocene and is aligned with the southern Caribbean coast (Isphording, 1975; Lara, 1993; Díaz, 2005; Lopez-Garcia et al., 2005).

Laguna Bacalar is fed with fresh karstic water by a river system that connects the lake with the Xul-Ha sinkhole. At the time of this study, the river was observed as having an average current speed of 1.8km/h northwards (location 2; Fig. 1), whereas currents in the lake were dependent on wind, and time of day, but normally having a westerly direction. Microbialites are observed on both banks of the river, and predominantly on the western shores of the lake (location 3-9, Fig. 1), along ca. 10 km. No microbialites are observed north of the Bacalar town (location 10; Fig. 1) or in Xul-Ha (location 1; Fig. 1).

3.3. Methods

3.3.1. Sample collection

Microbialite samples were collected from Laguna Bacalar during the summer of 2011, and winter of 2012. Samples were collected from both the lake and the river. They vary in size and morphology (from few cm to several dm) and show variable morphology. Lake sediment and skeletons of macrofauna (bivalves, and gastropods) were also collected for analyses.

3.3.2. Water Samples

Water samples were collected from the lake, the river (connecting Laguna Bacalar with the Xul-Ha sinkhole), Cenote Azul sinkhole, and a spring that fed into the lake. Samples were collected using 60 mL syringes, filtered through a 0.2 μm micropore filter, and stored in polycarbonate sample bottles and immediately refrigerated. Samples were collected in duplicate, one treated with analytical grade HNO_3 (8 N) to a final concentration of 10% v/v for cation analysis. The other sample was used for anion analysis. *In situ* pH measurements were taken with Beakman Φ 295 pH-meter fitted with a Thermo Scientific Oron pH probe.

3.3.3. River Profile and Velocity

Two detailed profiles of the river system were produced. The profiles included length and width of the river, as well as the distribution of microbialites; illustrations were digitized and annotated (Fig. 2). Water velocity was determined by recording the travel time of a stick on a given distance (30 m)

3.3.4. Aqueous Geochemistry

3.3.4.1. SO_4^{2-} and Cl^- Ion Chemistry

Analyses of both SO_4^{2-} and Cl^- ions of the lake and river samples were obtained using a Dionex DX600 Ion Chromatograph (IC) at the University of Alberta.

3.3.4.2. Major and trace elemental concentrations

Water samples were obtained in the field and acidified, and subsequently analyzed at the University of Alberta with a Perkin-Elmer Elan6000 quadrupole ICP-MS. The parameters used were: RF power 1200 W, peak hopping acquisition, 50 ms dwell time. Results were calibrated against a standard containing 10ppm of Br, In, and Sc. The relative standard deviations (2σ) were between 3% for Na and Fe, 0.35% for Al and Zn, and between 0.005 and 0.06% for most analyzed elements. Detection limits were between 0.0009 ppm (e.g. Ti) and 0.31 ppm (e.g. Ca)

3.3.4.3. Water Hardness, Calcium

Water hardness was determined using a Hatch Digital Titrator Model 16900. For each location, 2 mL of Hardness 1 Buffer Solution was added to 50-20 mL water samples. Once the solution was completely mixed the contents of one ManVer® 2 Hardness Indicator Powder Pillow was added. The solution was then titrated with EDTA and the total volume for the solution to change from red to blue was noted.

Subsequently, such volume was used in order to determine mg/L of Total hardness as Ca.

3.3.5. Solid phase mineralogical/geochemical analyses

All solid phase mineralogical and geochemical analyses were conducted at the University of Albert

3.3.5.1. Bulk element geochemistry

Individual samples weighing 10 mg powdered and dissolved in screw-top Teflon® bombs (Savillex®) using HF and HNO_3. Samples were react at 130ºC for 48 hours. Subsequently, the temperature was increased to 140ºC, allowing for samples to dry completely. Samples were then treated with HCL and HNO_3 for 24 hours at 130ºC, and re-dried at 140ºC. Samples was then treated with HNO_3 and allowed to react for two hours at 130ºC. Samples were then analyzed using a Perkin-Elmer Elan 6000 quadrupol ICP-MS.

3.3.5.2 XRD Analysis

Six different microbialite samples and associated sediment and skeletal fragments from various locations within the lake and the river were analyzed for their mineral composition. Samples were powdered using an agar mortar and pestle, to a size less than 10 μm. From each sample 1-2 g of powder were placed on holders and analyzed using a Rigaku Ultima IV X-ray diffractometer. Data was processed and minerals identified using JADE 9.1 software and the ICDD and ICSD databases.

3.3.5.3. Scanning electron microscopy (SEM)

Microbialite, and sediment samples were grain mounted and sputter coated with gold, and analyzed using a Zeiss EVO MA 15 and JEOL630F. The analyses were performed at accelerating voltages of 5 and 20kV and a working distance ranging from 6 to 19mm (see individual image for specifics). For microbialite samples textural relationship between the extracellular polymeric substance (EPS), and authigenic mineral phases were noted, as well as types of organisms present, grain types and size. For sediment samples, grain size and morphology were recorded.

3.3.6. Petrography

Petrographic thin sections of the various microbialites samples (river and lake), displaying stromatolitic and thrombolitic textures were prepared and examined using transmitted light microscopy. Grain type and size were noted, as well as the mineral composition and texture. The interaction between the organisms present within microbialites, and the mineral composition were noted.

3.3.7. Bacteria culturing and identification

Microbialite samples from six different locations were collected and kept viable in 250 mL Nalgene bottles. Samples containing visible bacteria were collected from each sample and grown photoautotrophically on a rotary shaker (150 rpm) at 30ºC in BG-11 medium. Illumination was provided by fluorescent lamps at 150 microeinsteins m^{-2} s^{-1}. Bacteria were grown and transferred every 7 days in order to purify samples and to remove any sediment present. Bacteria cultures were then identified through the use of a light microscope.

3.4. Results

3.4.1. Water Chemistry

The complete geochemistry of the water samples is provided in Table 1. The sample locations are shown in Figure 1. Measured pH values of the surface waters throughout Laguna Bacalar ranged between 7.4 and 8.2 mmol/g, the adjacent Cenote Azul sinkhole has a value of 8.2 mmol/g. The dominant cation is Ca^{2+}, which is present in the highest concentrations in Cenote Azul sinkhole (9.6 mml/g) is followed by water samples collected from the spring (8.7 mmol/g)(Fig. 1). The river system contains the highest concentrations of Ca^{2+} and a decrease occurs from the river towards and into the main lake. The other dominant cation in Laguna Bacalar is Mg^{2+} with values 3.0 mmol/g to 3.6 mmol/g. No downstream gradient is observed regarding Mg^{2+} distribution. The average Cl concentration is 42 mg/L and appears to be lowest at the river; SO_4 concentrations average 1073 mg/L and dissolved organic carbon (DOC) values average 0.97 mg/L. From the water hardness measurements it is calculated that the lake water ranges from 636 to 522 mL of Ca, and no trend in distribution is observed.

3.4.2. River current velocity

The first river location (Site 2) is closest the Xul-Ha sinkhole and has an average velocity of 0.6 m/s, whereas the second location (Site 3) is further north and has slower current velocities, averaging 0.5 m/s.

3.4.3. Microbialite composition and microstructures

Microbialites in Laguna Bacalar are categorized into two distinct groups based on their internal fabric, regardless of size: (1) thrombolitic-stromatolites, having both internal lamination (stromatolitic mesostructures) and clotting (thrombolitic mesostructures), and (2) stromatolites, having internal lamination.

3.4.3.1. Thrombolitic-stromatolites

Thrombolitic-stromatolites are predominantly found in the main lake, whereas in the river thrombolitic-stromatolites are observed in sheltered areas and on the banks, where water velocity is moderate. Thrombolitic-stromatolites reach up to meters in height and width, displaying domal morphology, a smooth (Fig. 3 A & B) or pitted exterior (Fig. 3C), and largely seen coalescing with each other. Underwater samples typically display light cream coloration, similar to that of the lake sediment. Sub-aerially exposed samples have a much darker coloration (dark gray). Thrombolitic-stromatolites grow on various substrates, and they are observed growing on mangrove roots, glass bottles, and plant matter (Fig. 3 D-F). Most samples have bivalves embedded on their outer surface (Fig. 3G).

Internally, thrombolitic-stromatolites display both stromatolitic and thrombolitic mesostructures (Fig. 4). Lamination consists of alternating dark and light lamina (see arrow with 'l'; Fig. 4). Laminae are present within all samples, predominantly on the uppermost part of the sectioned samples, and to various degrees in the interior sections of the samples (see arrow with 'l'; Fig. 4B). Photosynthetic cyanobacteria are observed in a 1-2cm thick layer, found ~2-5 cm beneath the outer most mineralized zone, i.e. growth occurs endolithically (see arrow with 'e'; Fig. 4A). Where lamination is not present internal clotting developed throughout. Bivalves are also found cemented within the interior of the samples; no evidence of burrowing or boring was observed (see arrow with 'b'; Fig. 4). Porosity is associated with the mesostructures observed: lesser porosity is seen in areas that have stromatolitic textures compared to sections composed of thrombolitic textures, which are characterized by having greater porosity (Fig. 5 A & B).

3.4.3.1.1 Thrombolitic-stromatolite petrography

Thrombolitic-stromatolites are composed entirely of calcium carbonate, of microsparite (~5 μm), and micrite size crystals (< 1 μm). Laminated stromatolitic texture contain cyanobacterial filaments with widths of up to ~30 μm (Fig. 5C). Individual filaments are surrounded by micrite (Fig. 5C) forming microbial molds; internal structures of filaments are locally preserved (see arrows; Fig. 5D).

As the filaments begin to decompose, the void is infilled by microsparite (Fig. 5D). The individual molds are cemented together by microsparite. Stromatolitic lamination is the result of higher abundance of bacterial filaments/moulds (designated as P-laminae, after Konhauser et al., 2004), preceded by laminae containing higher porosity and few bacterial filaments/moulds (designated as U-lamina)(Fig. 5A). Thrombolitic macrostructures predominantly comprise rounded detrital micritic peloids of various sizes, cemented together by microsparite (Fig. 5B). Similar grain composition is observed in the lake sediment (Fig. 5E). Cyanobacterial filaments are not as readily observed in the clotted sections of the thrombolitic-stromatolite. Also present are bioclasts (bivalves) cemented into the structure by micrite, with no evidence of burrowing (Fig. 5F).

3.4.3.1.2 Thrombolitic-stromatolite SEM

SEM analyses of thrombolitic-stromatolites display the various interactions between the cyanobacteria filaments and calcite grains (Fig. 6). At the surface of samples where growth is endolithic, a high abundance of filaments can be observed (Fig. 6A). Also present are bacterial molds formed by the calcite, molds are void of cyanobacteria (Fig. 6B). Calcite grains are micrite (<4 μm)(Fig. 6C) and microsparite (>4 μm)((Fig. 6D) in size, and in association with smooth EPS sheets (see arrows with 'e', Figs. 6C & D). Individual cyanobacterial filaments are also observed in association with EPS, which appear to coat the calcite and the filaments (Figs. 6E & F)

3.4.3.2 Stromatolites

Stromatolites are predominantly observed growing on the surface of coalescing thrombolitic-stromatolites (Fig. 7A), and at the bottom of the river channel (see arrow with ‘s’, Fig. 7B). These have a darker gray coloration compared to thrombolitic-stromatolites, and displayed a smooth domal morphology (Fig. 7C). Samples found in the river channel are distinguished by the presence of EPS (Fig. 7C & D). Internally the filamentous cyanobacteria can be observed comprising the different laminae resulting in the internal lamination (Fig. 7E).

3.4.3.2.1 Stromatolite petrography

Similar to thrombolitic-stromatolites, stromatolites are composed of micrite and microsparite size grains, and cyanobacterial filaments and their mineralogy is calcite (Fig. 8A). As previously observed the individual filaments are surrounded by micrite. As the bacteria within the mold begin to decompose, secondary microsparite begins to inwardly infill the void. The molds are cemented together by microsparite (Fig. 8B). Stromatolites were found to have very few detrital peloids, and bioclasts, and in some cases are devoid of both. Laminae are defined by layers that containing a high abundance of cyanobacterial filaments (P-laminae) versus those having greater and fewer filaments (U-laminae)(Fig. 8C).

3.4.3.2.2 Stromatolite SEM

Cyanobacterial filaments are abundant (Fig. 9A), and highly calcified (Fig. 9B). Calcite grains surrounding the individual filaments are micrite (<4 μm)(see arrow with ‘m’, Fig. 9B), and microsparite (>4 μm)(see arrow with ‘s’, Fig. 9B) in size. Cyanobacterial molds are also observed; filaments are seen still present in some (see arrow with ‘f’, Fig. 9C) while others are completely void. The presence of EPS can still be observed, appearing to bind grains between the molds (see arrow with ‘e’, Fig. 9C). Molds are internally composed of micrite and surrounded by microsparite (Fig. 9D and E). Calcite grains appear to have either a dumbbell or rod morphology (Fig. 9F-H), with some seen covered by EPS (see arrows, Fig. 9G).

3.4.4 Microbial Geochemistry and Solid Phase Mineralogy

3.4.4.1 Geochemistry

Geochemically both microbialites are similar in composition. Trace element patterns constructed from LA-ICP-MS and bulk ICP-MS analysis show similar elemental concentrations, however, thrombolitic-stromatolites appear to have lower concentrations compared to those of stromatolites (Rapids and Bac 4). Geochemical differences were also observed due to the analytical technique utilized (bulk vs. laser ablation). Stromatolite sample from the rive and the lake appear to closely correlate to each other (Fig. 10)

3.4.4.2 XRD Analyses

XRD results for microbialites samples show that the mineral composition of all six samples were carbonate and calcite in nature.

3.5. Discussion

3.5.1. Laguna Bacalar Environmental Settings

The water from Laguna Bacalar is supersaturated with regards to calcium carbonate. The supersaturation is the result of the change in partial pressure of CO_2 as a consequence of the degassing of underground water reaching the surface. This is evident from the total water hardness concentrations (mg/L total hardness as $CaCO_3$), where both the Cenote Azul sinkhole, and the spring water displayed the highest values, and where water concentrations for Laguna Bacalar decreased northwards as they flowed further away from the Xul-Ha sinkhole (Table 1). A similar gradient can be observed with regards to the calcium cation concentrations, from our analyzed water samples, however, when compared to those analyzed by Gischler et al. (2011) the northward decrease in concentration was no longer apparent. Bicarbonate values do however displayed a northward decrease in concentration similar to that observed from the total water hardness, while having its greatest concentration at the Cenote Azul sinkhole. It is clear that the source of calcium carbonate in Laguna Bacalar is the surfacing underground water, and as such concentrations decrease with distance from the source (sinkhole).

3.5.1 Microbialites textures

Laguna Bacalar microbialites display two distinct mesostructures resulting from the growth mechanism employed by the cyanobacteria present. Stromatolitic mesostructures show distinct fabric caused by interlaminations containing high concentrations of cyanobacterial filaments/molds (P-lamina) and lamina with higher porosity and fewer cyanobacteria (U-lamina)(Fig. 8). In contrast thrombolitic mesostructures displaying clotting, are composed predominantly of detrital peloids bound by microspar (Fig. 5D), and displaying less cyanobacteria.

Stromatolitic textures are the result of precipitation of calcite by cyanobacteria. The uptake of CO_2 during photosynthesis causes an increase in the pH and bicarbonate ions facilitating the precipitation of calcium carbonate (Simkiss and Wilbur, 1989; Castanier et al., 1999; Castanier et al., 2000; Riding, 2000; Altermann et al., 2006; Riding, 2006; Planavsky et al., 2009). As seen petrographically, micrite precipitates on the outer surface of the bacteria, forming a mold. Secondary precipitation of microspar binds the molds together while inwardly infilling the void after the decomposition of cyanobacterial filaments (Fig. 8). SEM shows the presence of EPS and calcite grains displaying dumbbell and rod morphologies (Fig. 9 F-H), which preferentially form in the presence of EPS (Buczynski and Chafetz, 1991; Buczynski and Chafetz, 1993). Collectively, a lack of detrital peloids, in conjunction with the precipitation of micrite and microspar with distinct morphology suggests that growth occurs solely through the precipitation of calcite, and mediated by the cyanobacteria present.

Thrombolitic textures are the result of the trapping and binding of detrital peloids, which are cementation through the precipitation of calcite facilitated by the degradation of EPS. Cyanobacterial filaments are not are readily observed (Fig. 5 A-B), however their influence on thrombolitic textures have been previously linked to microbial mediated processes based on distinct geochemical signatures (Castro-Contreras et al., 2014). Detrital peloids and bioclasts are deposited on the surface of microbialites, which are then trapped, and bound by the cyanobacteria (Fig. 5 D-F). The decrease of photosynthetic active radiation (PAR) will cause the migration and/or re-colonization of cyanobacteria. The residual EPS, observed in SEM images (Fig. 6A), provides textural support for the bound grains, while its degradation allows the release of previously absorbed Ca^{2+} and HCO_3^-, further supersaturating the water, and facilitating the precipitation of microspar and the cementing of the bound grains (Decho, 1990; Golubic et al., 2000; Visscher et al., 2000; Paerl et al., 2001; Dupraz and Visscher, 2005; Dupraz et al., 2009). Similar growth mechanisms have been suggested for fossil microbialites where lithification was concluded to only be possible if cyanobacteria were present, even if not preserved (Grotzinger, 1990; Grotzinger and Knoll, 1999; Allwood et al., 2006). The predominant peloidal composition of the thrombolitic textures, the lack of abundant cyanobacterial molds, and the lithification of the overall structure is evidence that growth occurred through binding and trapping, and preceded by precipitation upon the migration of cyanobacteria.

3.5.3. Environmental effects on microbialite textures

Given the importance of binding and trapping and allochem availability in determining the textures discussed above, these microbialites can be associated to sedimentary processes as well as biogeochemical regimes. Stromatolites (internally laminated) and thrombolitic-stromatolites (internally clotted and laminated) are both found within the lake and the river of Laguna Bacalar. Gischler et al., (2011) attributes the shape of the microbialites to the shoreline topography and relief, and observed that each distinct types of microbialite contained a differing cyanobacterial type. Our study does not disprove their findings but rather suggests that other factors, including current velocity, sediment transport and sedimentation also contributes to the type of internal textures observed in the Bacalar microbialites.

Stromatolites are constantly found in the main river channel (Figs. 2 & 7C) and on the surface of thrombolitic-stromatolites (Fig. 7A) within the lake. As previously stated stromatolitic textures are the result of calcite precipitation, void of detrital input, as they are somewhat scarce of allochems. The supersaturated water of the Xul-Ha sinkhole flows through the river and into the main lake. Even though sediment transport was observed in the river, the stromatolites are unable to bind the sediment before being removed due to the high water velocity. In contrast, are the subaerialy-exposed stromatolites in the lake, were the water velocity is severely dampened by the presence of larger thrombolitic-stromatolites, causing a lack of sediment to be available for trapping and binding by the stromatolites. It is thus evident that stromatolite growth is slow as it is dependent entirely on precipitation of $CaCO_3$ from the lake and river water.

Thrombolitic-stromatolites are observed on the riverbanks (Fig. 3B) and on the western shores of the lake (Fig. 3A). As supersaturated waters transporting sediment flow through the river, away from thalweg, currents are lower and further baffled by the thrombolitic-stromatolites growing on the banks. This promotes the deposition of the sediment on the microbialite surface, allowing it to be trapped and bound by cyanobacteria, generating the clotted thrombolitic texture. Within the lake, conditions vary from calm to turbulent. Westward currents allow the transport of sediment and deposition on the surface of microbialites. Similarly to its river counterparts, this results in clotted fabric. However, the presence of stromatolitic textures suggests changes in sediment transport, and the ability for growth to solely occur through calcite precipitation. Changes can be attributed to calm lake conditions, or by the microbialites themselves providing more wave shelter in their immediate area. The size of the coalescing samples, and a lack of burrowing, or boring from the bivalves imbedded within their structure (see arrow with 'b'; Fig. 4), it can be suggested that growth through trapping and binding is much faster, than that of stromatolites. As such the two distinct growth phases are controlled by sediment deposition, where high and low energy environments in which deposition is restricted form stromatolitic textures, while moderate energy environments allowing sediment deposition allows the formation of thrombolitic textures.

3.6. Conclusions

The supersaturation of the water with regards to calcium carbonate allows the formation of microbialites. Such growth is facilitated by the presence of cyanobacteria, however it is sediment deposition that dictates the type of growth, and texture. Supersaturation of the water is the result of degassing at the Xul-Ha sinkhole, which feeds the river and lake of Laguna Bacalar. Sediment is unable to be deposited on microbialites under high, and low energy settings, allowing growth to occur slowly through the precipitation of calcite. Moderate energy settings allow the transports and deposits of sediment, allowing cyanobacteria to trap, and bind them, and subsequently cementing them into the structure resulting it the formation of clotted textures and faster growth. Further work should be conducted in order to determine the effect sediment deposition had on the distribution of cyanobacteria found in the different microbialites of Laguna Bacalar, as observed by Gischler et al., (2011).

Aitken, J.D., 1967, Classification and environmental significance of cryptalgal limestones and dolomites with illustrations from Cambrian and Ordovician of southwestern Alberta: Journal of Sedimentary Petrology, v. 37, p. 1163-1178.

Allwood, A.C., Grotzinger, J.P., Knoll, A.H., Burch, I.W., Anderson, M.S., Coleman, M.L., and Kanik, I., 2009, Controls on development and diversity of Early Archean stromatolites: Proceedings of the National Academy of Sciences of the United States of America, v. 106, p. 9548-9555, doi: 10.1073/Pnas.0903323106.

Allwood, A.C., Walter, M.R., Kamber, B.S., Marshall, C.P., and Burch, I.W., 2006, Stromatolite reef from the Early Archaean era of Australia: Nature, v. 441, p. 714-718, doi: Doi 10.1038/Nature04764.

Altermann, W., 2008, Accretion, trapping and binding of sediment in Archean stromatolites - Morphological expression of the antiquity of life: Space Science Reviews, v. 135, p. 55-79, doi: Doi 10.1007/S11214-007-9292-1.

Altermann, W., Kazmierczak, J., Oren, A., and Wright, D.T., 2006, Cyanobacterial calcification and its rock-building potential during 3.5 billion years of Earth history: Geobiology, v. 4, p. 147-166, doi: 10.1111/J.1472-4669.2006.00076.X.

Awramik, S.M., 1971, Precambrian columnar stromatolite diversity - reflection of metazoan appearance: Science, v. 174, p. 825-827.

Awramik, S.M., 1991, Archaean and Proterozoic stromatolites, *in* Riding, R., ed., Calcareous Alae and Stromatolites: Springer-Verlag, New York, p. 571.

Awramik, S.M., 1992, The History and Significance of Stromatolites, *in* Schidlowski, M., Golubic, S., Kimberley, M.M., McKirdy, D.M., and Trudinger, P.A., eds., Early Organic Evolution: Springer Berlin Heidelberg, p. 435-449.

Awramik, S.M., and Grey, K., 2005, Stromatolites: biogenicity, biosignatures, and bioconfusion, in Hoover, R.B., Levin, G.V., Rozanov, A.Y., and Gladstone, G.R. eds.: SPIE, San Diego, CA, USA, p. 59060P-9.

Awramik, S.M., and Sprinkle, J., 1999, Proterozoic stromatolites: The first marine evolutionary biota: Historical Biology, v. 13, p. 241-253, doi: 10.1080/08912969909386584.

Bauer-Gottwein, P., Gondwe, B., Charvet, G., Marin, L., Rebolledo-Vieyra, M., and Merediz-Alonso, G., 2011, Review: The Yucatan Peninsula karst aquifer, Mexico: Hydrogeology Journal, v. 19, p. 507-524, doi: 10.1007/s10040-010-0699-5.

Beukes, N.J., 1987, Facies relations, depositional-environments and diagenesis in a major early Proterozoic stromatolitic carbonate platform to basinal sequence, Campbellrand Subgroup, Transvaal Supergroup, Southern-Africa: Sedimentary Geology, v. 54, p. 1-46, doi: Doi 10.1016/0037-0738(87)90002-9.

Buck, S.G., 1980, Stromatolite and ooid deposits within the fluvial and lacustrine sediments of the Precambrian Ventersdorp Supergroup of South-Africa:

Precambrian Research, v. 12, p. 311-330, doi: 10.1016/0301-9268(80)90033-9.

BUCZYNSKI, C., and CHAFETZ, H.S., 1991, Habit of bacterially induced precipitates of calcium-carbonate and the influence of medium viscosity on mineralogy: Journal of Sedimentary Petrology, v. 61, p. 226-233.

BUCZYNSKI, C., and CHAFETZ, H.S., 1993, Habit of bacterially induced precipitates of calcium carbonate: examples from laboratory experiments and recent sediments, *in* Rezak, R., and Lavoie, D.L., eds., Carbonate Microfabrics: Springer-Verlag, New York, p. 105-116.

BURNE, R.V., and MOORE, L.S., 1987, Microbialites: organosedimentary deposits of benthic microbial communities: Palaios, v. 2, p. 241-254.

BYERLY, G.R., LOWER, D.R., and WALSH, M.M., 1986, Stromatolites from the 3,300-3,500-Myr Swaziland Supergroup, Barberton Mountain Land, South-Africa: Nature, v. 319, p. 489-491, doi: Doi 10.1038/319489a0.

CASTANIER, S., LE METAYER-LEVREL, G., and PERTHUISOT, J.-P., 2000, Bacterial roles in the precipitation of carbonate minerals: Microbial sediments, p. 32-39.

CASTANIER, S., LE METAYER-LEVREL, G., and PERTHUISOT, J.P., 1999, Ca-carbonates precipitation and limestone genesis - the microbiogeologist point of view: Sedimentary Geology, v. 126, p. 9-23.

CASTRO-CONTRERAS, S.I., GINGRAS, M.K., PECOITS, E., AUBET, N.R., PETRASH, P., CASTRO-CONTRERAS, S.M., DICK, G., PLANAVSKY, N., and KONHAUSER, K.O., 2014, Textural and geochemical features of freshwater microbialites from Laguna Bacalar, Quintana Roo, Mexico: Palaios.

DECHO, A.W., 1990, Microbial Exopolymer Secretions in Ocean Environments - Their Role(S) in Food Webs and Marine Processes: Oceanography and Marine Biology, v. 28, p. 73-153.

DÍAZ, J.E.H., 2005, Decreto por el cual se establece el programa de ordenamineto ecologico territorial de al región de Laguna Bacalar, Quintana Roo, México, Periodico Oficial, p. 126.

DUPRAZ, C., REID, R.P., BRAISSANT, O., DECHO, A.W., NORMAN, R.S., and VISSCHER, P.T., 2009, Processes of carbonate precipitation in modern microbial mats: Earth-Science Reviews, v. 96, p. 141-162, doi: 10.1016/J.Earscirev.2008.10.005.

DUPRAZ, C., and VISSCHER, P.T., 2005, Microbial lithification in marine stromatolites and hypersaline mats: Trends in Microbiology, v. 13, p. 429-438.

FISCHER, A.G., 1965, Fossils early life and atmospheric history: Proceedings of the National Academy of Sciences of the United States of America, v. 53, p. 1205-1213.

GISCHLER, E., GIBSON, M.A., and OSCHMANN, W., 2008, Giant Holocene freshwater microbialites, Laguna Bacalar, Quintana Roo, Mexico: Sedimentology, v. 55, p. 1293-1309.

GISCHLER, E., GOLUBIC, S., GIBSON, M., OSCHMANN, W., and HUDSON, J.H., 2011, Microbial mats and microbialites in the freshwater Laguna Bacalar, Yucatan Peninsula, Mexico, Advances in Stromatolite Geobiology: Springer Berlin Heidelberg, p. 187-205.

GOLUBIC, S., 1994, The continuing importance of cyanobacteria, *in* Bengtson, S., ed., Nobel Symposium; Early life on earth, p. 334-340.

GOLUBIC, S., SEONG-JOO, L., and BROWNE, K.M., 2000, Cyanobacteria: architects of sedimentary structures: Microbial sediments, p. 57-67.

GROTZINGER, J.P., 1990, Geochemical model for Proterozoic stromatolite decline: American Journal of Science, v. 290A, p. 80-103.

GROTZINGER, J.P., and KNOLL, A.H., 1999, Stromatolites in Precambrian carbonates: evolutionary mileposts or environmental dipsticks?: Annual Review of Earth and Planetary Sciences, v. 27, p. 313-358.

HOFMANN, H.J., 1973, Stromatolites: characteristics and utility: Earth-Science Reviews, v. 9, p. 339-373.

HOFMANN, H.J., 1977, On Aphebian Stromatolites and Riphean Stromatolite Stratigraphy: Precambrian Research, v. 5, p. 175-205.

HOFMANN, H.J., GREY, K., HICKMAN, A.H., and THORPE, R.I., 1999, Origin of 3.45 Ga coniform stromatolites in Warrawoona Group, Western Australia: Geological Society of America Bulletin, v. 111, p. 1256-1262, doi: 10.1130/0016-7606(1999)111<1256:oogcsi>2.3.co;2.

ISPHORDING, W.C., 1975, The physicl geology of Yucatan: Trans Gulf Coast Assoc Geol Soc, v. 25, p. 231-262, doi: 10.1306/A1ADD8E6-0DFE-11D7-8641000102C1865D.

KALKOWSKY, E., 1908, Oolith und stromatolith im norddeutschen Buntsandstein: Zeitschrift der deutschen geologischen Gesells-chaft, v. 60, p. 68-125.

KONHAUSER, K.O., JONES, B., PHOENIX, V., FERRIS, G., and RENAUT, R., 2004, The microbial role in hot spring silicification: Ambio, v. 33, p. 552-558, doi: 10.1639/0044-7447(2004)033[0552:Tmrihs]2.0.Co;2.

LARA, M.E., 1993, Divergent Wrench Faulting in the Belize Southern Lagoon - Implications for Tertiary Caribbean Plate Movements and Quaternary Reef Distribution: Aapg Bulletin-American Association of Petroleum Geologists, v. 77, p. 1041-1063.

LOPEZ-GARCIA, P., KAZMIERCZAK, J., BENZERARA, K., KEMPE, S., GUYOT, F., and MOREIRA, D., 2005, Bacterial diversity and carbonate precipitation in the giant microbialites from the highly alkaline Lake Van, Turkey: Extremophiles, v. 9, p. 263-274, doi: Doi 10.1007/S00792-005-0457-0.

LOWE, D.R., 1980, Stromatolites 3,400-Myr old from the archean of western-australia: Nature, v. 284, p. 441-443.

MCNAMARA, K.J., and AWRAMIK, S.M., 1992, Stromatolites - a key to understanding the early evolution of life: Science Progress, v. 76, p. 345-364.

PAERL, H.W., STEPPE, T.F., and REID, R.P., 2001, Bacterially mediated precipitation in marine stromatolites: Environmental Microbiology, v. 3, p. 123-130.

PLANAVSKY, N.J., REID, R.P., LYONS, T.W., MYSHRALL, K.L., and VISSCHER, P.T., 2009, Formation and diagenesis of modern marine calcified cyanobacteria: Geobiology, v. 7, p. 566-576, doi: 10.1111/J.1472-4669.2009.00216.X.

PRATT, B.R., 1982, Stromatolite decline - a reconsideration: Geology, v. 10, p. 512-515.

RIDING, R., 1997, Stromatolite decline: a brief reassessment: Facies, v. 36, p. 227-230.

RIDING, R., 1999, The term stromatolite: towards an essential definition: Lethaia, v. 32, p. 321-330.

RIDING, R., 2000, Microbial carbonates: the geological record of calcified bacterial-algal mats and biofilms: Sedimentology, v. 47, p. 179-214.

RIDING, R., 2006, Cyanobacterial calcification, carbon dioxide concentrating mechanisms, and Proterozoic-Cambrian changes in atmospheric composition: Geobiology, v. 4, p. 299-316, doi: 10.1111/J.1472-4669.2006.00087.X.

RIDING, R., 2011, The nature of stromatolites: 3,500 million years of histroy and a century of research, *in* Reitner, J., Quéric, N-VB, Arp, G., ed., Advances in Stromatolite Geobiology: Springer, Heidelberg, p. 29-74.

SCHIEBER, J., 1999, Microbial mats in terrigenous clastics: the challenge of identification in the rock record: Palaios, v. 14, p. 3-12, doi: 10.2307/3515357.

SCHOPF, J.W., KUDRYAVTSEV, A.B., CZAJA, A.D., and TRIPATHI, A.B., 2007, Evidence of archean life: stromatolites and microfossils: Precambrian Research, v. 158, p. 141-155, doi: 10.1016/J.Precamres.2007.04.009.

SHAPIRO, R.S., 2000, A comment on the systematic confusion of thrombolites: Palaios, v. 15, p. 166-169.

SIMKISS, K., and WILBUR, K.M., 1989, Biomineralization : cell biology and mineral deposition: Academic Press, San Diego, xiv, 337 p.

VISSCHER, P.T., REID, R.P., and BEBOUT, B.M., 2000, Microscale observations of sulfate reduction: Correlation of microbial activity with lithified micritic laminae in modern marine stromatolites: Geology, v. 28, p. 919-922, doi: Doi 10.1130/0091-7613(2000)28<919:Moosrc>2.0.Co;2.

WALTER, M.R., BUICK, R., and DUNLOP, J.S.R., 1980, Stromatolites 3,400-3,500 Myr Old from the North-Pole Area, Western-Australia: Nature, v. 284, p. 443-445, doi: 10.1038/284443a0.

WALTER, M.R., and HEYS, G.R., 1985, Links between the rise of the metazoa and the decline of stromatolites: Precambrian Research, v. 29, p. 149-174.

WRAY, J.L., 1977, Calcareous algae: Developments in paleontology and stratigraphy: Elsevier Scientific Pub. Co., New York, xiv, 185 p.

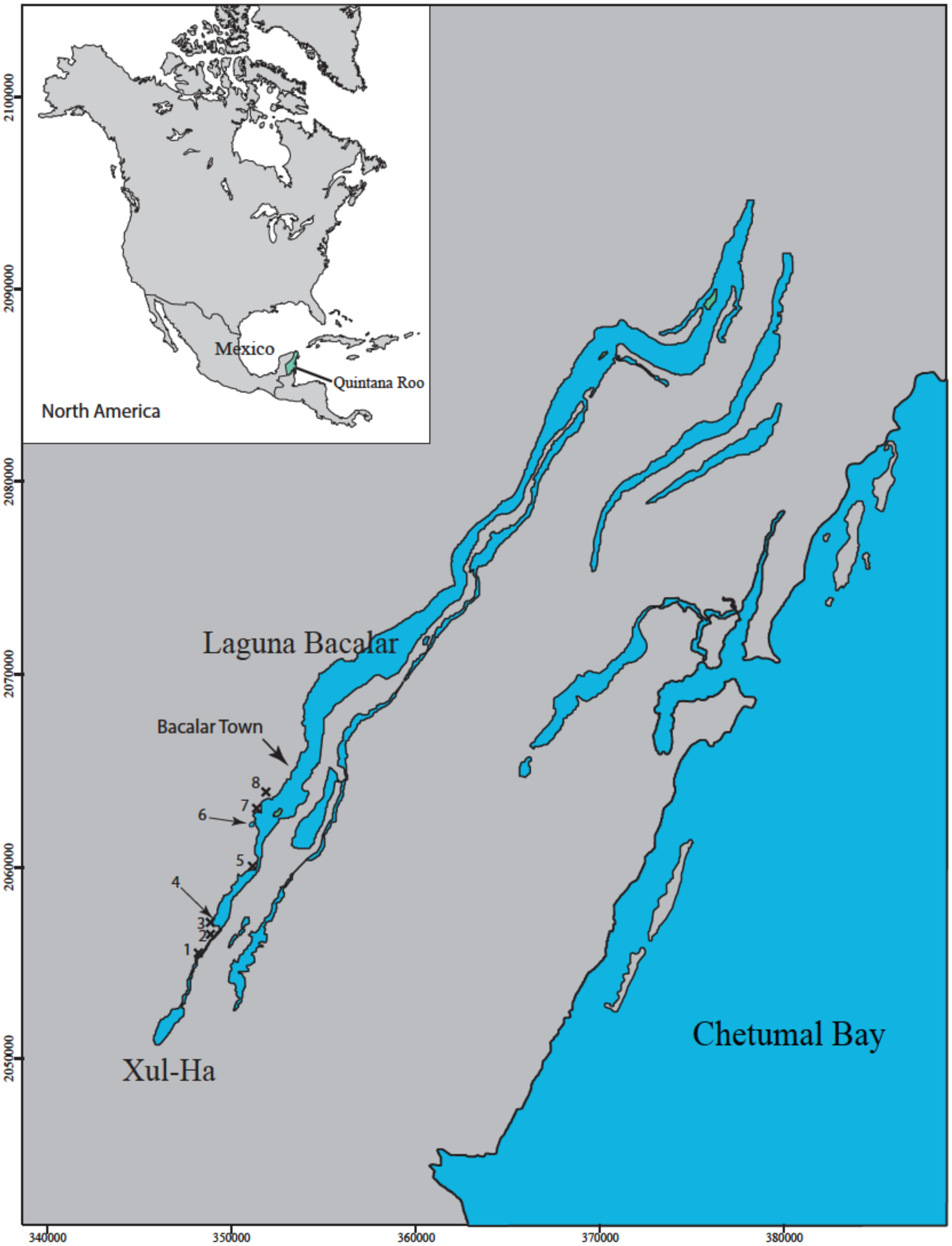
Mexico
Quintana Roo
North America
Laguna Bacalar
Bacalar Town
8
7
6
5
4
3
2
1
Xul-Ha
Chetumal Bay
2100000
2090000
2080000
2070000
2060000
2050000
340000
350000
360000
370000
380000

FIGURE 3.1 – Map of study area, Laguna Bacalar located in Quintana Roo, Mexico. Water flows from the Xul-Ha sinkhole into Laguna Bacalar. Water and microbialite samples were taken from each 8 different locations. (1-8).

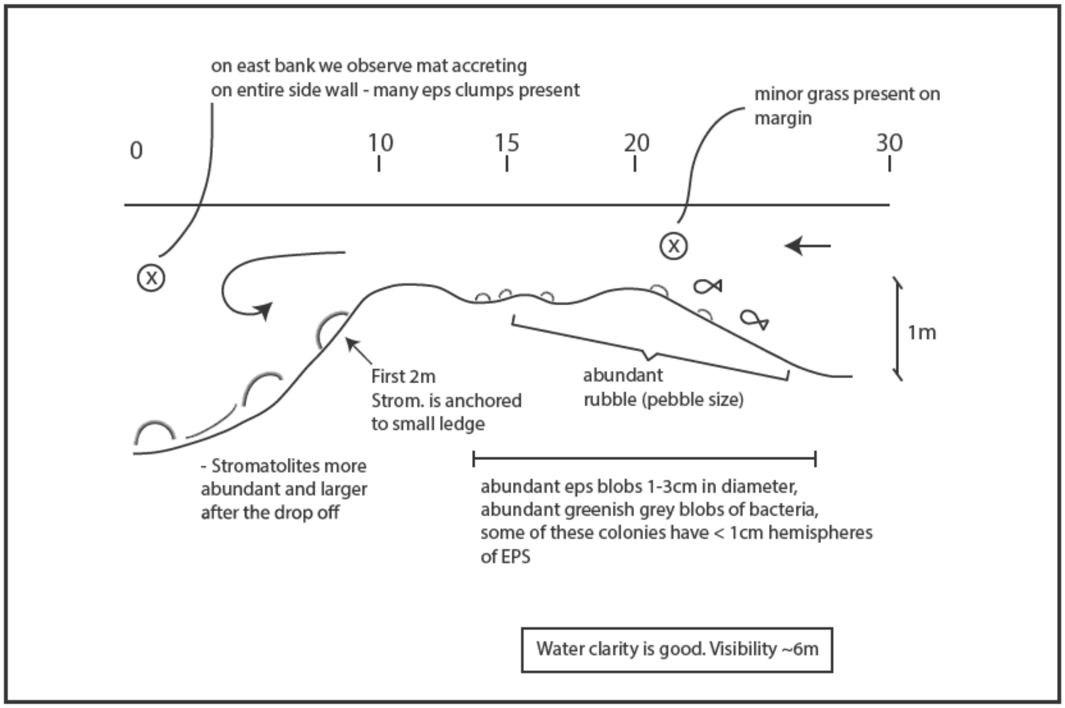
on east bank we observe mat accreting
on entire side wall - many eps clumps present
minor grass present on
margin
0
10
15
20
30
1m
First 2m
Strom. is anchored
to small ledge
abundant
rubble (pebble size)
- Stromatolites more
abundant and larger
after the drop off
abundant eps blobs 1-3cm in diameter,
abundant greenish grey blobs of bacteria,
some of these colonies have < 1cm hemispheres
of EPS
Water clarity is good. Visibility ~6m

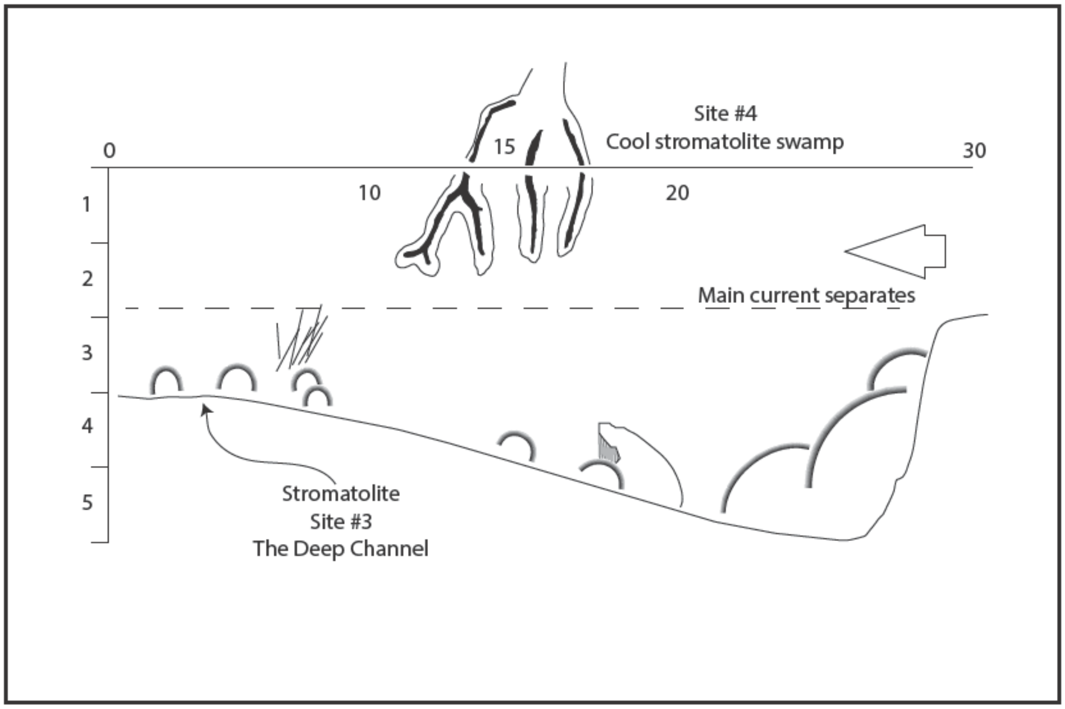
Site #4
Cool stromatolite swamp
0
15
30
10
20
1
2
3
4
5
Main current separates
Stromatolite
Site #3
The Deep Channel

FIGURE 3.2 – River profiles with distribution of microbialites and flow direction. Thirty-meter sections were used in order to determine current velocity. (A) Profile of location 2. (B) Profile of location 3.


A
B
C
D
E
F

FIGURE 3.3 – Thrombolitic-stromatolites from Laguna Bacalar. (A) Large sample found in the lake, displaying domal morphology with a smooth exterior, coalescing with adjacent samples. (B) Large domal samples found in the river, having similar smooth exterior and coalescing with other samples. (C) Sample displaying domal morphology, with a pitted exterior. (D) Mangrove roots covered by thrombolitic-stromatolite, both submerged and sub-aerially exposed. Samples were also seen coalescing. (E) Beer bottle encrusted by thrombolitic-stromatolite. (F) Sample containing bivalves encrusted on its outer surface.

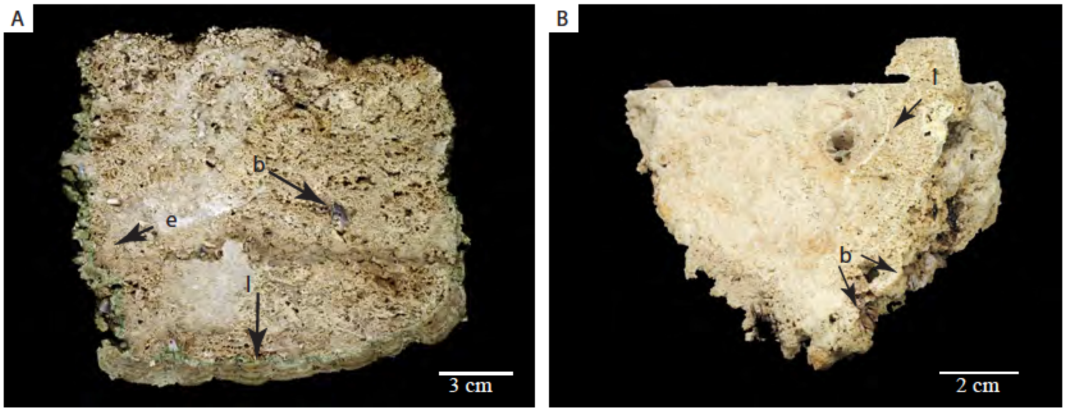

FIGURE 3.4 – Hand samples of thrombolitic-stromatolites. (A) Dome shaped sample, having an endolithic bacterial mat (see arrow with ‘e’), and having both laminations (see arrow with ‘l’), and clotting. Imbedded bivalves were also present (see arrow with ‘b’). (B) Sample also displaying imbedded bivalves (see arrow with ‘b’); texture composed of internal lamination (see arrow with ‘b’) and clotting.

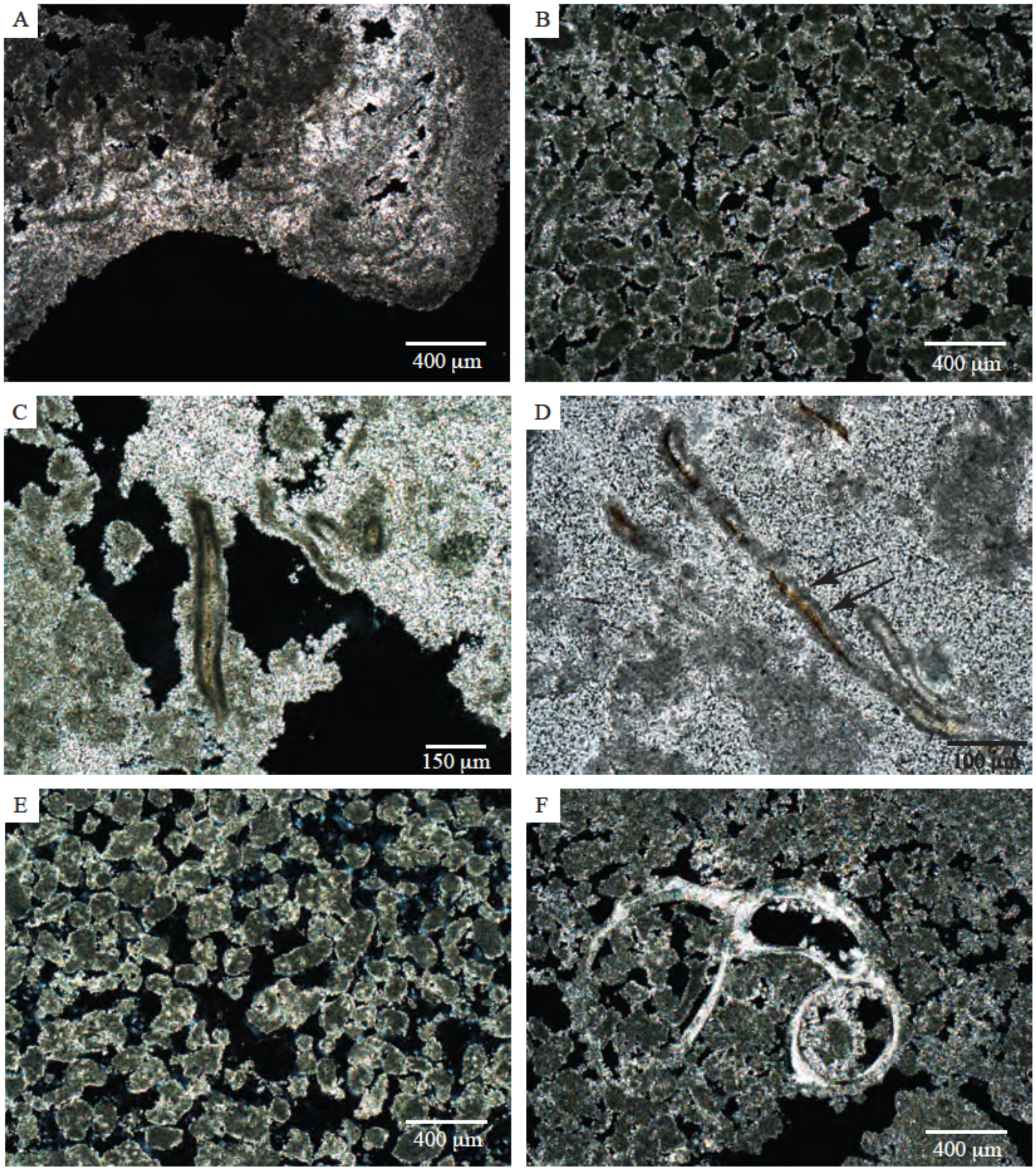
A
400 µm
B
400 µm
C
150 µm
D
100 µm
E
400 µm
F
400 µm

FIGURE 3.5 – Petrographic images of thrombolitic-stromatolites, and sediment. (A) Petrographic image of microbial mold under cross-polarized light (XPL). Bacterial filament having a brown coloration is surrounded by micrite (displaying a grey translucent appearance, individual grains indistinguishable). Mold is seen to be cemented by microspar size calcite. (B) Bacterial mold under plain-polarized light (PPL). Internal structure is still visible (see arrows). Micrite is once again seen to surround the filaments. (C) Faint lamination under XPL Lamina are composed of micrite. (D) Peloids composed of micrite cemented together by microspar cement, image under XPL (E) Peloid grains under XPL from lake sediment, and also composed of micrite. (F) Bioclasts cemented by microspar, and surrounded by micritic peloids. Image taken under XPL.

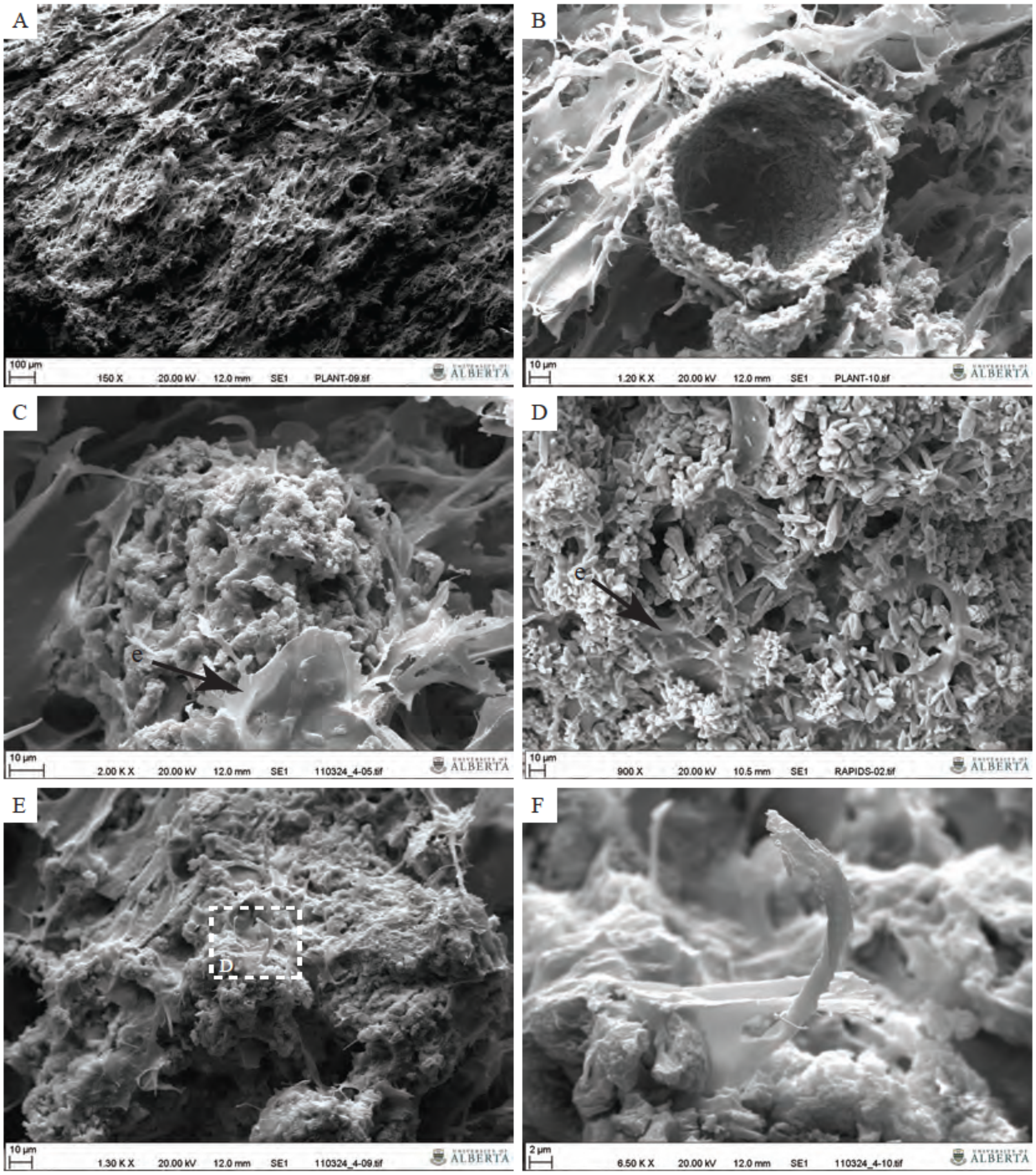
A
100 µm 150 X 20.00 kV 12.0 mm SE1 PLANT-09.tif
UNIVERSITY OF ALBERTA
B
10 µm 1.20 K X 20.00 kV 12.0 mm SE1 PLANT-10.tif
UNIVERSITY OF ALBERTA
C
e
10 µm 2.00 K X 20.00 kV 12.0 mm SE1 110324_4-05.tif
UNIVERSITY OF ALBERTA
D
e
10 µm 900 X 20.00 kV 10.5 mm SE1 RAPIDS-02.tif
UNIVERSITY OF ALBERTA
E
D
10 µm 1.30 K X 20.00 kV 12.0 mm SE1 110324_4-09.tif
UNIVERSITY OF ALBERTA
F
2 µm 6.50 K X 20.00 kV 12.0 mm SE1 110324_4-10.tif
UNIVERSITY OF ALBERTA

FIGURE 3.6 – SEM images of thrombolitic-stromatolites. (A) Abundant cyanobacterial filaments having calcite surrounding them, in the presence of EPS. (B) Micrite size calcite. (C) Individual cyanobacterial filaments in association with EPS and calcite grains. (D) cyanobacteria filaments in the presence of EPS. EPS appears to coat the calcite grains. (F) Presence of bacterial molds. (G) Close look at bacterial mold, surrounded by calcite.


A
B
S
C
D
E

FIGURE 3.7 – Stromatolites form the lake and river of Laguna Bacalar. (A) Dome shaped stromatolites growing on the surface of larger thrombolitic-stromatolites. Stromatolites were darker in color and coalescing together. At times subaerialy exposed. (B) Stromatolites (see arrow with 's') found in the main river channel. (C) Stromatolites from the river channel as well as EPS nodules (see arrow). (D) EPS nodules from the river. (E) domal stromatolite displaying internal lamination and a fibrous texture.

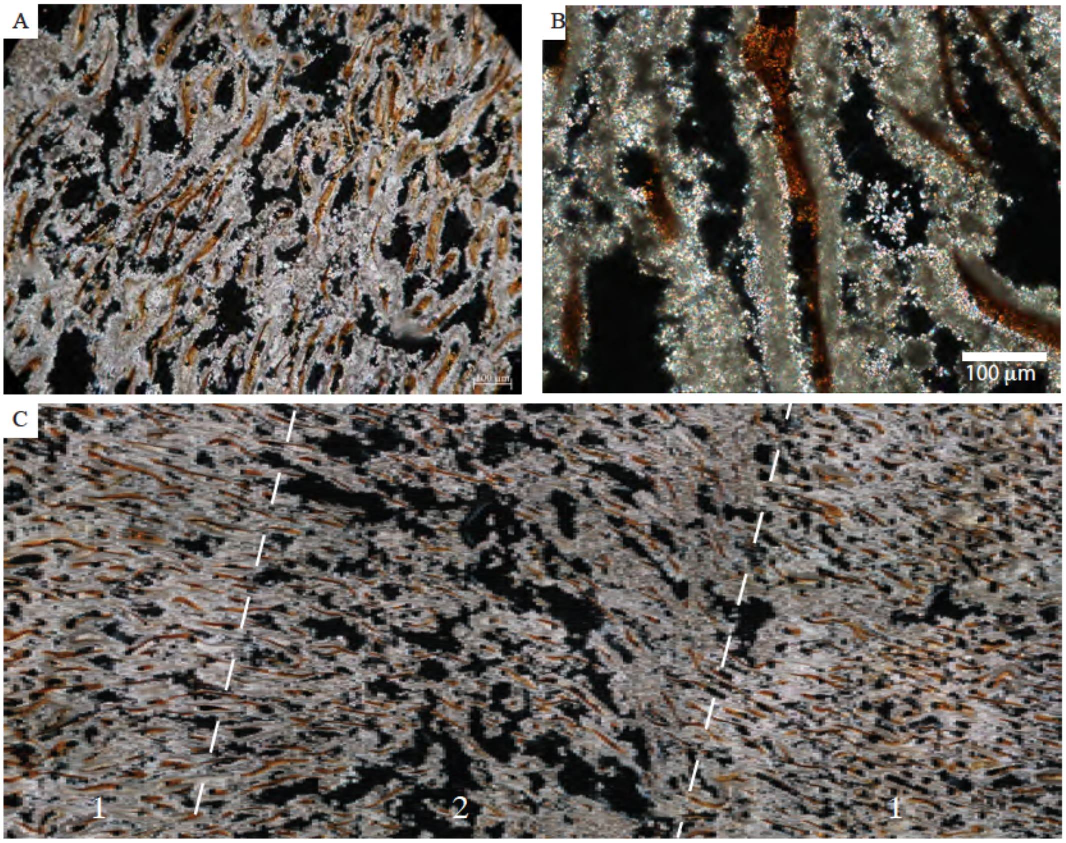

FIGURE 3.8 – Petrographic images of stromatolites all taken under XPL. (A) Cyanobacteria filaments having brown coloration, surrounded by microspar (fain, translucent appearance), and cemented together by microspar. (B) Micrite surrounding bacterial filament, forming a mold. As cyanobacteria decomposes void is infilled by microspar, even while cyanobacteria still present. Molds are cemented together by microspar. (C) Transect of stromatolites, having two P-lamina (indicated with '1') with high abundance of cyanobacteria filaments/ molds, and a U-laminae (indicated with '2') separating them. U-lamina displayed a higher degree of porosity.

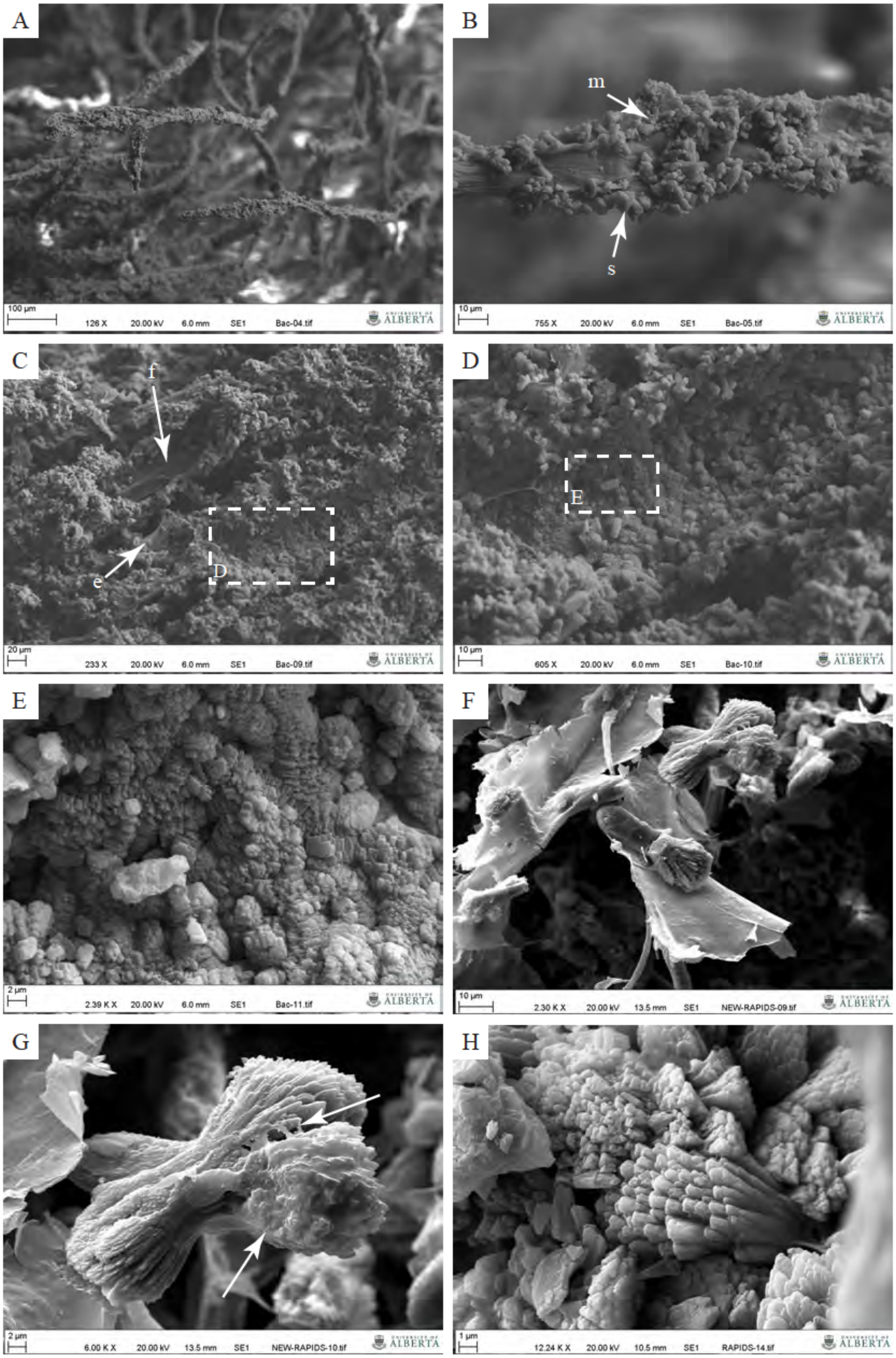
A
100 µm
126 X 20.00 kV 6.0 mm SE1 Bac-04.tif
UNIVERSITY OF ALBERTA
B
m
s
10 µm
755 X 20.00 kV 6.0 mm SE1 Bac-05.tif
UNIVERSITY OF ALBERTA
C
f
e
D
20 µm
233 X 20.00 kV 6.0 mm SE1 Bac-09.tif
UNIVERSITY OF ALBERTA
D
E
10 µm
605 X 20.00 kV 6.0 mm SE1 Bac-10.tif
UNIVERSITY OF ALBERTA
E
2 µm
2.39 K X 20.00 kV 6.0 mm SE1 Bac-11.tif
UNIVERSITY OF ALBERTA
F
10 µm
2.30 K X 20.00 kV 13.5 mm SE1 NEW-RAPIDS-09.tif
UNIVERSITY OF ALBERTA
G
2 µm
6.00 K X 20.00 kV 13.5 mm SE1 NEW-RAPIDS-10.tif
UNIVERSITY OF ALBERTA
H
1 µm
12.24 K X 20.00 kV 10.5 mm SE1 RAPIDS-14.tif
UNIVERSITY OF ALBERTA

FIGURE 3.9 – SEM images of stromatolites. (A) cyanobacterial filaments encrusted with calcite. (B) Filament encrusted by micrite (see arrow with 'm') and microspar (see arrow with 's'). (C) Two microbial molds, one still containing a cyanobacterial filament (see arrow with 'f'), and the other void. Also present between the molds is EPS (see arrow with 'e'). (D) Mold no longer having filament, completely composed of calcite. (E) Micrite found within the mold. (F) calcite grains in the presence of EPS. (G). Dumbbell shaped calcite with EPS surrounding it (see arrows). (H) Calcite grains displaying a rod morphology.

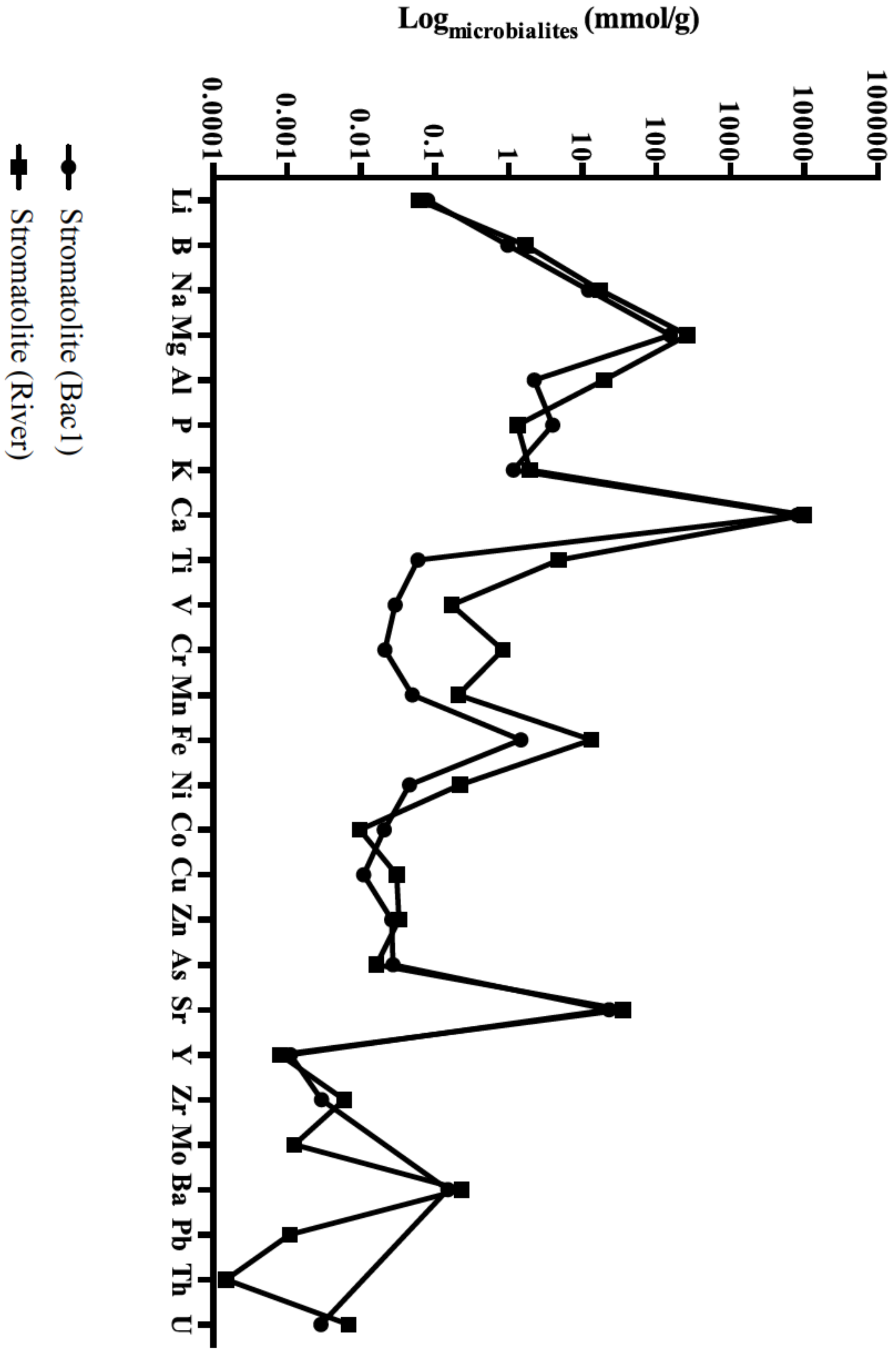
Log$_{microbialites}$ (mmol/g)
100000
10000
1000
100
10
1
0.1
0.01
0.001
0.0001
Li
B
Na
Mg
Al
P
K
Ca
Ti
V
Cr
Mn
Fe
Ni
Co
Cu
Zn
As
Sr
Y
Zr
Mo
Ba
Pb
Th
U
Stromatolite (Bac1)
Stromatolite (River)

FIGURE 3.10 - Elemental graph comparing stromatolite from the lake (Bac 1) to those found in the river.

Location	pH	Ca^{2+} (mmol/g)	Mg^{2+} (mmol/g)	DOC (ppm)
Cenote Azul	8.2	9.6	3.3	0.5
Spring	7.4	8.7	3.2	1.2
Carrera Ranch – Vent	8.1	8.5	3.1	0.7
River – Location4	8.2	8.5	3.0	0.6
River– Location 2	7.9	8.4	3.1	0.7
River – Location 3	8.2	8.3	3.1	0.9
River– Location 1	8.1	8.3	3.3	0.7
Carrera Ranch – RM2	7.8	8.1	3.3	0.8
Dock	8.0	8.0	3.6	
Carrera Ranch – RM1	7.9	7.9	3.3	2.6

Location	mg/L Total Hardness as Ca
Cenote Azul	626
Spring	552
River (Average from the 4 locations)	545
Carrera Rancho – Vent	540
Carrera Rancho (Average from 2 locations)	536

TABLE 3.1 – Ion concentrations, pH, dissolved inorganic carbon, and total water hardness as Ca concentrations for the various locations in the Laguna Bacalar.

Location 2

Velocity (s/m)	**Velocity (m/s)**
61s/30m	0.49
51s/30m	0.59
52s/30m	0.58
Average:	0.55

Location 3

Velocity (s/m)	**Velocity (m/s)**
72s/30m	0.41
61s/30m	0.49
59s/30m	0.51
Average:	0.47

TABLE 3.2 – Current velocities for location 2 and 3 located in the Laguna Bacalar river.

CHAPTER 4: SUMMARY AND CONCLUSION

From the studies of the Laguna Bacalar microbialites, several observations have furthered our understanding of the various factors controlling microbialite growth, and internal fabric. These observations can also be utilized to broaden our understanding of fossil microbialites.

The effects that grazing and burrowing organisms have on microbialite growth and preservation has been a major point of ongoing research. As stated in the introduction of this thesis, some researchers have attributed the genesis of metazoans during the Phanerozoic to the drastic decline of microbialite communities. As such, the ability to assess the interaction between grazing organisms, such as gastropods and microbialites, has the potential to shed light on the possible effects they pose on microbialites. The freshwater conditions of Laguna Bacalar, allows for gastropods to co-exist with microbialites, without exerting a significant influence on microbialite growth. Thus, the vast growth of microbialites, and developments of differing internal fabric appears to be dominantly influenced by factors other than grazing organisms.

Changes in ocean chemistry during the Proterozoic are thought to have had a significant impact on microbialite growth and may potentially be the reason for their drastic decline. Within Laguna Bacalar, water chemistry appears to be an important factor controlling the vast microbialite growth. As the underground karstic water surfaces at the Xul-Ha sinkhole, its degassing reduces the partial pressure of the CO_2 and induces the immediate supersaturation of the water, with respect to calcium carbonate. As the water flows northwards through the river channel connecting Laguna Bacalar to Xul-Ha, and further away from its source, a decrease in saturation (with respect to HCO_3^- and water harness) is observed. As cyanobacteria utilize calcite in the formation of the microbialites, it correspondingly decreases the concentration of Ca^{2+} and HCO^{3-}. This was evident by a distinct absence of microbialites formations beyond the Bacalar town, where saturation levels are no longer high enough for calcification to occur. As such it is clear that the water chemistry has a direct and significant impact on the growth of microbialites.

While the saturation state of HCO_3^- in the water allows for microbialite growth, the internal fabric of each of the different morphologies was controlled by sediment deposition and the energy regime of their locality. It was found that internal lamination (stromatolitic mesostructures) was the result of calcite precipitation. The stromatolites formed by such growth are affected by either a high or low energy setting. In the river channel, where water velocity is high, sediment is prevented from remaining on the surfaces of stromatolites and becoming incorporated into their structure. Conversely, stromatolites found in the lake grow predominantly on the surface of thrombolitic-stromatolites or in sheltered areas, where water velocity was low, and sediment transport was limited or absent.

Larger microbialite samples are observed having both laminated (stromatolitic) and clotted (thrombolitic) mesostructures growing in locations where the current is varying. During periods where current velocity is strong enough to deposit sediment onto the microbialites, trapping and binding by cyanobacteria resulted in both clotted fabric and a much faster growth rate. Lamination will thus occur only when growth through precipitation is possible, such as during periods were current velocity is low, and incapable of transporting sediment. Therefore, sediment transport, and the resultant type of growth directly control the internal mesostructrue of the Laguna Bacalar microbialites.

Geochemically, microbialites are observed to have similar elemental patterns and linked to the presence of cyanobacteria within the structure. The presence of cyanobacteria are much more prominent in stromatolitic textures than in thrombolitic where cyanobacterial filaments are rare. However, it was determined that even though cyanobacterial filaments may not be present, they still mediate stromatolite growth. Such evidence comes from the comparison of essential elements (e.g.. Mg, Si, Ni, Mo) needed by cyanobacteria for growth and synthesis of enzymes, in thrombolitic and stromatolitic sections. The elemental patterns were similar, yet differed in their concentration. It was concluded that the concentrations reflect the type of growth the different microbialites employ. During stromatolitic growth, cyanobacteria remain longer in a specific location leading to higher concentrations of essential elements to be sequestered. However, thrombolitic growth forces cyanobacteria to migrate at a faster rate in order to obtain the necessary photosynthetic active radiation (PAR), resulting in a shortened period of filament presence, and a corresponding decrease in essential element concentrations.

The conclusions reached in chapters 3 and 4 provide a better understanding of the various factors that control the growth and internal fabric of these microbialites. However, it also provides further knowledge that can allow us to better interpret their fossil counterparts. If the growth of fossil microbialites were affected in the same manner as those found in Bacalar, the controlling factor which affected their growth would have been the saturation of the water with respect to calcium carbonate. It would also signify that the presence of ancient grazing and burrowing organisms would have little or no effect on growth, as microbialites can grow at a faster rate than grazing and burrowing organisms can affect them. If postulated changes in the Proterozoic/Phanerozoic ocean chemistry caused a decrease in available calcium carbonate, microbialite formation would have been hampered. This may have, in turn, been amplified by the competition for substrate and nutrients with eukaryotic organisms. This would result in the inability for cyanobacteria to form microbialites, resulting in a lack of protection and subsequent exposure to grazing organisms. As such, it appears that while microbialite growth in Laguna Bacalar is mediated by the $CaCO_3$ concentration in the water, there is still much to be determined to conclusively explain the sudden decline in fossil microbialites during the Proterozoic/Phanerozoic. It does, however, seem plausible that the decrease in the calcium carbonate saturation state of the water could be the initial trigger in the decline, from which other factors may have contributed or amplified the decline.

4.1. Future Work

The microbialites of Laguna Bacalar provide an excellent setting to study modern microbialite growth and have demonstrated a high potential as an analogue for understanding fossil microbialite growth. However, work still needs to be done in order to better understand fossil microbialites and the environments in which they formed. The Archean and Proterozoic were characterized by environmental conditions much different than at present. The atmosphere was anoxic and as a result, an ozone layer was non-existent. This, in turn, allowed unabated UV radiation to reach the surface of the Earth. Such high intensities of UV radiation would have had profound physiological impact on the early biosphere, likely damaging DNA, RNA, proteins and lipids. In order to survive, ancient microorganisms would have had to be capable of protecting themselves either through physical means (sheltering) and/or physiological adaptations (e.g., the ability to repair damaged DNA). As such early organisms were limited to areas were they could overcome such extreme factors. The ability for water to absorb UV radiation, as well as the effect suspended sediment might have on UV attenuation, are important factors that could further contribute to our current understanding of early Precambrian ecosystems and microorganism evolution. As such, future research should thus focus on characterizing the effects that UV radiation had on microbialites, and the ability for these to overcome such extreme conditions.

Through the use of optical remote sensing, biochemistry and molecular microbiology, future research should aim to address the following. First, determine how UV and PAR are attenuated in the water column as a function of depth, and how this may be applied to the understanding of the photic zone in which ancient photosynthetic microorganisms could have survived exposure to damaging UV radiations. Second, the impact sediment and dissolved solids in the upper water column would have had regarding the attenuation and depth of penetration of UV radiation and PAR. Third, determining other potentially non-marine aquatic settings that would have allowed photosynthetic organisms to survive intense UV irradiance. Fourth, how calcium carbonate being trapped, bound, and/or precipitated during the formation of stromatolites impacted the attenuation of UV radiation, thereby providing further shielding that may have allowed them to colonize areas where UV radiation might not have otherwise been filtered out, such as shallow coastal waters and epicontinental alkaline lakes. Fifth, assess the physiological impacts that UV radiation has on these microorganisms through some genomic and proteomic analyses. And sixth, determine in situ UV and PAR radiation reaching underwater microbialites from various modern settings (e.g., Laguna Bacalar, Cuatro Cienegas, Bahamas, Kelley Lake), to assess the impact of both the distribution and the differing microorganisms present in each microbialite.

BIBLIOGRAPHY

ABED, R.M.M., GOLUBIC, S., GARCIA-PICHEL, F., CAMOIN, G.F., and SPRACHTA, S., 2003, Characterization of microbialite-forming cyanobacteria in a tropical lagoon: Tikehau Atoll, Tuamotu, French Polynesia: Journal of Phycology, v. 39, p. 862-873.

AITKEN, J.D., 1967, Classification and environmental significance of cryptalgal limestones and dolomites with illustrations from Cambrian and Ordovician of southwestern Alberta: Journal of Sedimentary Petrology, v. 37, p. 1163-1178.

ALLWOOD, A.C., GROTZINGER, J.P., KNOLL, A.H., BURCH, I.W., ANDERSON, M.S., COLEMAN, M.L., and KANIK, I., 2009, Controls on development and diversity of Early Archean stromatolites: Proceedings of the National Academy of Sciences of the United States of America, v. 106, p. 9548-9555, doi: 10.1073/Pnas.0903323106.

ALLWOOD, A.C., WALTER, M.R., BURCH, I.W., and KAMBER, B.S., 2007, 3.43 billion-year-old stromatolite reef from the Pilbara Craton of Western Australia: Ecosystem-scale insights to early life on Earth: Precambrian Research, v. 158, p. 198-227, doi: http://dx.doi.org/10.1016/j.precamres.2007.04.013.

ALLWOOD, A.C., WALTER, M.R., KAMBER, B.S., MARSHALL, C.P., and BURCH, I.W., 2006, Stromatolite reef from the Early Archaean era of Australia: Nature, v. 441, p. 714-718, doi: Doi 10.1038/Nature04764.

ALTERMANN, W., 2008, Accretion, trapping and binding of sediment in Archean stromatolites - Morphological expression of the antiquity of life: Space Science Reviews, v. 135, p. 55-79, doi: Doi 10.1007/S11214-007-9292-1.

ALTERMANN, W., KAZMIERCZAK, J., OREN, A., and WRIGHT, D.T., 2006, Cyanobacterial calcification and its rock-building potential during 3.5 billion years of Earth history: Geobiology, v. 4, p. 147-166, doi: 10.1111/J.1472-4669.2006.00076.X.

ANDRES, M.S., and PAMELA REID, R., 2006, Growth morphologies of modern marine stromatolites: A case study from Highborne Cay, Bahamas: Sedimentary Geology, v. 185, p. 319-328.

ARP, G., REIMER, A., and REITNER, J., 1999, Calcification in cyanobacterial biofilms of alkaline salt lakes: European Journal of Phycology, v. 34, p. 393-403, doi: Doi 10.1017/S0967026299002292.

ARP, G., REIMER, A., and REITNER, J., 2001, Photosynthesis-induced biofilm calcification and calcium concentrations in phanerozoic oceans: Science, v. 292, p. 1701-1704, doi: 10.1126/Science.1057204.

ARP, G., REIMER, A., and REITNER, J., 2003, Microbialite formation in seawater of increased alkalinity, Satonda crater lake, Indonesia: Journal of Sedimentary Research, v. 73, p. 105-127.

AWRAMIK, S.M., 1971, Precambrian columnar stromatolite diversity - reflection of metazoan appearance: Science, v. 174, p. 825-827.

AWRAMIK, S.M., 1991, Archaean and Proterozoic stromatolites, *in* Riding, R., ed., Calcareous Alae and Stromatolites: Springer-Verlag, New York, p. 289-304.

AWRAMIK, S.M., 1992, The History and Significance of Stromatolites, *in* Schidlowski, M., Golubic, S., Kimberley, M.M., McKirdy, D.M., and Trudinger, P.A., eds., Early Organic Evolution: Springer Berlin Heidelberg, p. 435-449.

AWRAMIK, S.M., 1992, The Oldest Records of Photosynthesis: Photosynthesis Research, v. 33, p. 75-89.

AWRAMIK, S.M., and GREY, K., 2005, Stromatolites: biogenicity, biosignatures, and bioconfusion, in Hoover, R.B., Levin, G.V., Rozanov, A.Y., and Gladstone, G.R. eds.: SPIE, San Diego, CA, USA, p. 59060P-9.

AWRAMIK, S.M., and MARGULIS, L., 1974, Definiton of stromatolite, Stromatolite Newsletter, p. 5.

AWRAMIK, S.M., SCHOPF, J.W., and WALTER, M.R., 1983, Filamentous Fossil Bacteria from the Archean of Western Australia, *in* B. Nagy, R.W.J.C.G., and Schidlowski, M., eds., Developments in Precambrian Geology: Elsevier, p. 249-266.

AWRAMIK, S.M., and SPRINKLE, J., 1999, Proterozoic stromatolites: The first marine evolutionary biota: Historical Biology, v. 13, p. 241-253, doi: 10.1080/08912969909386584.

BAPTISTA, M.S., and VASCONCELOS, M.T., 2006, Cyanobacteria metal interactions: requirements, toxicity, and ecological implications: Critical Reviews in Microbiology, v. 32, p. 127-137, doi: 10.1080/10408410600822934.

BEUKES, N.J., 1987, Facies relations, depositional-environments and diagenesis in a major early Proterozoic stromatolitic carbonate platform to basinal sequence, Campbellrand Subgroup, Transvaal Supergroup, Southern-Africa: Sedimentary Geology, v. 54, p. 1-46, doi: Doi 10.1016/0037-0738(87)90002-9.

BLACK, M., 1933, The algal sediments of Andros Island, Bahamas: Philosophical Transactions of the Royal Society of London Series B-Containing Papers of a Biological Character, v. 222, p. 165-U50.

BODISELITSCH, B., KOEBERL, C., MASTER, S., and REIMOLD, W.U., 2005, Estimating duration and intensity of Neoproterozoic snowball glaciations from Ir anomalies: Science, v. 308, p. 239-242.

BOSAK, T., LIANG, B., WU, T.D., TEMPLER, S.P., EVANS, A., VALI, H., GUERQUIN-KERN, J.L., KLEPAC-CERAJ, V., FRIEDMAN, J., SIM, M.S., and MUI, J., 2013, Cyanobacterial diversity and activity in modern conical microbialites (vol 10, pg 384, 2012): Geobiology, v. 11, p. 100-100, doi: Doi 10.1111/Gbi.12016.

BRAITHWAITE, C.J.R., CASANOVA, J., FREVERT, T., and WHITTON, B.A., 1989, Recent stromatolites in landlocked pools on Aldabra, Western Indian ocean: Palaeogeography, Palaeoclimatology, Palaeoecology, v. 69, p. 145-165.

BRAITHWAITE, C.J.R., and ZEDEF, V., 1994, Living hydromagnesite stromatolites from Turkey: Sedimentary Geology, v. 92, p. 1-5.

BRAITHWAITE, C.J.R., and ZEDEF, V., 1996, Hydromagnesite stromatolites and sediments in an alkaline lake, Salda Golu, Turkey: Journal of Sedimentary Research, v. 66, p. 991-1002.

BUCK, S.G., 1980, Stromatolite and ooid deposits within the fluvial and lacustrine sediments of the Precambrian Ventersdorp Supergroup of South-Africa: Precambrian Research, v. 12, p. 311-330, doi: 10.1016/0301-9268(80)90033-9.

BUCZYNSKI, C., and CHAFETZ, H.S., 1991, Habit of bacterially induced precipitates of calcium-carbonate and the influence of medium viscosity on mineralogy: Journal of Sedimentary Petrology, v. 61, p. 226-233.

BUCZYNSKI, C., and CHAFETZ, H.S., 1993, Habit of bacterially induced precipitates of calcium carbonate: examples from laboratory experiments and recent sediments, *in* Rezak, R., and Lavoie, D.L., eds., Carbonate Microfabrics: Springer-Verlag, New York, p. 105-116.

BURNE, R.V., 1995, Microatoll microbialites of Lake Clifton, Western-Australia - the morphological analogs of cryptozoon Proliferum Hall, the first formally named stromatolite - reply: Facies, v. 32, p. 257-257.

BURNE, R.V., and MOORE, L.S., 1987, Microbialites: organosedimentary deposits of benthic microbial communities: Palaios, v. 2, p. 241-254.

BYERLY, G.R., LOWER, D.R., and WALSH, M.M., 1986, Stromatolites from the 3,300-3,500-Myr Swaziland Supergroup, Barberton Mountain Land, South-Africa: Nature, v. 319, p. 489-491, doi: Doi 10.1038/319489a0.

CAMOIN, G.F., GAUTRET, P., MONTAGGIONI, L.F., and CABIOCH, G., 1999, Nature and environmental significance of microbialites in Quaternary reefs: the Tahiti paradox: Sedimentary Geology, v. 126, p. 271-+.

CASTANIER, S., LE METAYER-LEVREL, G., and PERTHUISOT, J.-P., 2000, Bacterial roles in the precipitation of carbonate minerals: Microbial sediments, p. 32-39.

CASTANIER, S., LE METAYER-LEVREL, G., and PERTHUISOT, J.P., 1999, Ca-carbonates precipitation and limestone genesis - the microbiogeologist point of view: Sedimentary Geology, v. 126, p. 9-23.

CASTRO-CONTRERAS, S.I., GINGRAS, M.K., PECOITS, E., AUBET, N.R., PETRASH, P., CASTRO-CONTRERAS, S.M., DICK, G., PLANAVSKY, N., and KONHAUSER, K.O., 2014, Textural and geochemical features of freshwater microbialites from Laguna Bacalar, Quintana Roo, Mexico: Palaios.

CHARPYROUBAUD, C.J., CHARPY, L., and CREMOUX, J.L., 1990, Nutrient budget of the lagoonal waters in an open central South-Pacific atoll (Tikehau, Tuamotu, French-Polynesia): Marine Biology, v. 107, p. 67-73.

CONAGUA, 2002, Determinación de la disponibilidad de agua en el acuífero Peninsula de Yucatán, estado de Yucatán: Gerencia de Aguas Subterráneas p. 1-20.

DECHO, A.W., 1990, Microbial Exopolymer Secretions in Ocean Environments - Their Role(S) in Food Webs and Marine Processes: Oceanography and Marine Biology, v. 28, p. 73-153.

DEFARGE, C., TRICHET, J., MAURIN, A., and HUCHER, M., 1994, Kopara in polynesian atolls - early stages of formation of calcareous stromatolites: Sedimentary Geology, v. 89, p. 9-23.

DÍAZ, J.E.H., 2005, Decreto por el cual se establece el programa de ordenamineto ecologico territorial de al región de Laguna Bacalar, Quintana Roo, México, Periodico Oficial, p. 126.

DILL, R.F., SHINN, E.A., JONES, A.T., KELLY, K., and STEINEN, R.P., 1986, Giant subtidal stromatolites forming in normal salinity waters: Nature, v. 324, p. 55-58.

DUANE, M.J., and AL-ZAMEL, A.Z., 1999, Syngenetic textural evolution of modern sabkha stromatolites (Kuwait): Sedimentary Geology, v. 127, p. 237-245.

DUPRAZ, C., REID, R.P., BRAISSANT, O., DECHO, A.W., NORMAN, R.S., and VISSCHER, P.T., 2009, Processes of carbonate precipitation in modern microbial mats: Earth-Science Reviews, v. 96, p. 141-162, doi: 10.1016/J.Earscirev.2008.10.005.

DUPRAZ, C., and VISSCHER, P.T., 2005, Microbial lithification in marine stromatolites and hypersaline mats: Trends in Microbiology, v. 13, p. 429-438.

FENCHEL, T., 1998, Formation of laminated cyanobacterial mats in the absence of benthic fauna: Aquatic Microbial Ecology, v. 14, p. 235-240.

FERRIS, F.G., THOMPSON, J.B., and BEVERIDGE, T.J., 1997, Modern Freshwater Microbialites from Kelly Lake, British Columbia, Canada: Palaios, v. 12, p. 213-219.

FISCHER, A.G., 1965, Fossils early life and atmospheric history: Proceedings of the National Academy of Sciences of the United States of America, v. 53, p. 1205-1213.

FROST, J.G., 1974, Subtidal algal stromatolites from Florida backreef environment: Journal of Sedimentary Petrology, v. 44, p. 532-537.

GAMBOA-PEREZ, H.C., and SCHMITTER-SOTO, J.J., 1999, Distribution of cichlid fishes in the littoral of Lake Bacalar, Yucatan Peninsula: Environmental Biology of Fishes, v. 54, p. 35-43.

GARRETT, P., 1970, Phanerozoic stromatolites: noncompetitive ecologic restriction by grazing and burrowing animals: Science, v. 169, p. 171-173.

GAUTRET, P., CAMOIN, G., GOLUBIC, S., and SPRACHTA, S., 2004, Biochemical control of calcium carbonate precipitation in modern lagoonal microbialites, Tikehau atoll, French Polynesia: Journal of Sedimentary Research, v. 74, p. 462-478.

GINSBURG, R.N., 1955, Recent Stromatolitic Sediments from South-Florida: Journal of Paleontology, v. 29, p. 723-724.

GISCHLER, E., GIBSON, M.A., and OSCHMANN, W., 2008, Giant Holocene freshwater microbialites, Laguna Bacalar, Quintana Roo, Mexico: Sedimentology, v. 55, p. 1293-1309.

GISCHLER, E., GOLUBIC, S., GIBSON, M., OSCHMANN, W., and HUDSON, J.H., 2011, Microbial mats and microbialites in the freshwater Laguna Bacalar, Yucatan Peninsula, Mexico, *in* Reitner, J., Trauth, M.H., Stüwe, K., and Yuen, D., eds., Advances in Stromatolite Geobiology: Springer Berlin Heidelberg, p. 187-205.

GOLUBIC, S., 1994, The continuing importance of cyanobacteria, *in* Bengtson, S., ed., Nobel Symposium; Early life on earth, p. 334-340.

GOLUBIC, S., and FOCKE, J.W., 1978, Phormidium-Hendersonii Howe - identity and significance of a modern stromatolite building microorganism: Journal of Sedimentary Petrology, v. 48, p. 751-764.

GOLUBIC, S., SEONG-JOO, L., and BROWNE, K.M., 2000, Cyanobacteria: architects of sedimentary structures: Microbial sediments, p. 57-67.

GREINERT, J., BOHRMANN, G., and ELVERT, M., 2002, Stromatolitic fabric of authigenic carbonate crusts: result of anaerobic methane oxidation at cold seeps in 4,850 m water depth: International Journal of Earth Sciences, v. 91, p. 698-711.

GROTZINGER, J.P., 1989, Facies and evolution of Precambrian carbonate depositional systems: emergence of the modern platform archetype.

GROTZINGER, J.P., 1990, Geochemical model for Proterozoic stromatolite decline: American Journal of Science, v. 290A, p. 80-103.

GROTZINGER, J.P., 1994, Trends in Precambrian carbonate sediments and their implication for understanding evolution, *in* Bengtson, S., ed., Nobel Symposium; Early life on earth, p. 245-258.

GROTZINGER, J.P., and KNOLL, A.H., 1999, Stromatolites in Precambrian carbonates: evolutionary mileposts or environmental dipsticks?: Annual Review of Earth and Planetary Sciences, v. 27, p. 313-358.

HIPS, K., and HAAS, J., 2006, Calcimicrobial stromatolites at the Permian-Triassic boundary in a western Tethyan section, Bukk Mountains, Hungary: Sedimentary Geology, v. 185, p. 239-253, doi: Doi 10.1016/J.Sedgeo.2005.12.016.

HODELL, D.A., QUINN, R.L., BRENNER, M., and KAMENOV, G., 2004, Spatial variation of strontium isotopes (Sr-87/Sr-86) in the Maya region: a tool for tracking ancient human migration: Journal of Archaeological Science, v. 31, p. 585-601, doi: 10.1016/j.jas.2003.10.009.

HOFMANN, H., 2000, Archean stromatolites as microbial archives, *in* Riding, R.A., S. M., ed., Microbial sediments: Springer Verlag, New York, p. 315-327.

HOFMANN, H.J., 1973, Stromatolites: characteristics and utility: Earth-Science Reviews, v. 9, p. 339-373.

HOFMANN, H.J., 1977, On Aphebian Stromatolites and Riphean Stromatolite Stratigraphy: Precambrian Research, v. 5, p. 175-205.

HOFMANN, H.J., GREY, K., HICKMAN, A.H., and THORPE, R.I., 1999, Origin of 3.45 Ga coniform stromatolites in Warrawoona Group, Western Australia: Geological Society of America Bulletin, v. 111, p. 1256-1262, doi: 10.1130/0016-7606(1999)111<1256:oogcsi>2.3.co;2.

ISPHORDING, W.C., 1975, The physicl geology of Yucatan: Trans Gulf Coast Assoc Geol Soc, v. 25, p. 231-262, doi: 10.1306/A1ADD8E6-0DFE-11D7-8641000102C1865D.

JAROSEWICH, E., 2002, Smithsonian microbeam standards: Journal of Research of the National Institute of Standards and Technology, v. 107, p. 681-686.

JAVOR, B.J., and CASTENHOLZ, R.W., 1981, Laminated microbial mats, Laguna Guerrero Negro, Mexico: Geomicrobiology Journal, v. 2, p. 237-273.

JENKINS, G.S., 2003, GCM greenhouse and high ‐ obliquity Solutions for early Proterozoic glaciation and middle Proterozoic warmth: Journal of Geophysical Research: Atmospheres (1984–2012), v. 108.

JONES, B., RENAUT, R.W., and KONHAUSER, K.O., 2005, Genesis of large siliceous stromatolites at Frying Pan Lake, Waimangu geothermal field, North Island, New Zealand: Sedimentology, v. 52, p. 1229-1252.

KALKOWSKY, E., 1908, Oolith und stromatolith im norddeutschen Buntsandstein: Zeitschrift der deutschen geologischen Gesells-chaft, v. 60, p. 68-125.

KAZMIERCZAK, J., and KEMPE, S., 2004, Microbialite formation in seawater of increased alkalinity, Satonda Crater Lake, Indonesia - Discussion: Journal of Sedimentary Research, v. 74, p. 314-317.

KAZMIERCZAK, J., KEMPE, S., LOPEZ-GARCIA, P., TAVERA, R., KREMER, B., & MOREIRA, D., 2008, Modern and sub-recent carbonate microbialites from the alkaline crater lake Alchichica, Mexico, in Reitner, J. ed., Internationales Kalkowsky-Symposium: University of Göttingen, Göttingen, p. 87.

KEMPE, S., and KAZMIERCZAK, J., 1990, Chemistry and stromatolites of the sea-linked Satonda Crater Lake, Indonesia - a recent model for the Precambrian sea: Chemical Geology, v. 81, p. 299-310.

KEMPE, S., KAZMIERCZAK, J., LANDMANN, G., KONUK, T., REIMER, A., and LIPP, A., 1991, Largest known microbialites discovered in Lake Van, Turkey: Nature, v. 349, p. 605-608.

KERSHAW, S., GUO, L., SWIFT, A., and FAN, J.S., 2002, Microbialites in the Permian-Triassic boundary interval in Central China: Structure, age and distribution: Facies, v. 47, p. 83-89, doi: Doi 10.1007/Bf02667707.

KNOLL, A.H., and GOLUBIC, S., 1992, Proterozoic and Living Cyanobacteria, *in* Schidlowski, M., Golubic, S., Kimberley, M.M., McKirdy, D.M., and Trudinger, P.A., eds., Early Organic Evolution: Springer-Verlag, Belin, p. 450-462.

KOBLUK, D.R., and CRAWFORD, D.R., 1990, A modern hypersaline organic mud and gypsum-dominated basin and associated microbialites: Palaios, v. 5, p. 134-148.

KONHAUSER, K.O., JONES, B., PHOENIX, V., FERRIS, G., and RENAUT, R., 2004, The microbial role in hot spring silicification: Ambio, v. 33, p. 552-558, doi: 10.1639/0044-7447(2004)033[0552:Tmrihs]2.0.Co;2.

KONISHI, Y., PRINCE, J., and KNOTT, B., 2001, The fauna of thrombolitic microbialites, Lake Clifton, Western Australia: Hydrobiologia, v. 457, p. 39-47.

LARA, M.E., 1993, Divergent Wrench Faulting in the Belize Southern Lagoon - Implications for Tertiary Caribbean Plate Movements and Quaternary Reef Distribution: Aapg Bulletin-American Association of Petroleum Geologists, v. 77, p. 1041-1063.

LAVAL, B., CADY, S.L., POLLACK, J.C., MCKAY, C.P., BIRD, J.S., GROTZINGER, J.P., FORD, D.C., and BOHM, H.R., 2000, Modern freshwater microbialite analogues for ancient dendritic reef structures: Nature, v. 407, p. 626-629.

LOGAN, B.W., REZAK, R., and GINSBURG, R.N., 1964, Classification and Environmental Significance of Algal Stromatolites: The Journal of Geology, v. 72, p. 68-83.

LÓPEZ, Z.L., LUGO, F.A., PITA, M.R.S., 2005, Chetumal E16-4-7, Carta Geológico-Minera: Servicio Geológico Mexicano

LOPEZ-GARCIA, P., KAZMIERCZAK, J., BENZERARA, K., KEMPE, S., GUYOT, F., and MOREIRA, D., 2005, Bacterial diversity and carbonate precipitation in the giant microbialites from the highly alkaline Lake Van, Turkey: Extremophiles, v. 9, p. 263-274, doi: Doi 10.1007/S00792-005-0457-0.

LOVE, F.G., SIMMONS, G.M., PARKER, B.C., WHARTON, R.A., and SEABURG, K.G., 1983, Modern conophyton-like microbial mats discovered in Lake Vanda, Antarctica: Geomicrobiology Journal, v. 3, p. 33-48.

LOWE, D.R., 1980, Stromatolites 3,400-Myr old from the archean of western-australia: Nature, v. 284, p. 441-443.

LOWE, D.R., 1983, Restricted shallow-water sedimentation of Early Archean stromatolitic and evaporitic strata of the Strelley Pool Chert, Pilbara Block, Western Australia: Precambrian Research, v. 19, p. 239-283, doi: http://dx.doi.org/10.1016/0301-9268(83)90016-5.

MANN, C.J., and NELSON, W.M., 1989, Microbialitic structures in Storr's Lake, San Salvador Island, Bahama Islands: Palaios, v. 4, p. 287-293.

MATA, S.A., and BOTTJER, D.J., 2012, Microbes and mass extinctions: paleoenvironmental distribution of microbialites during times of biotic crisis: Geobiology, v. 10, p. 3-24, doi: Doi 10.1111/J.1472-4669.2011.00305.X.

MCMASTER, R.L., and CONOVER, J.T., 1966, Recent algal stromatolites from Canary Islands: Journal of Geology, v. 74, p. 647-&.

MCNAMARA, K.J., and AWRAMIK, S.M., 1992, Stromatolites - a key to understanding the early evolution of life: Science Progress, v. 76, p. 345-364.

MERZ-PREIFI, M., 2000, Calcification in cyanobacteria, *in* Riding, R., Awramik, S.M., ed., Microbial sediments: Springer-Verlag Berlin Heidelberg, New York, p. 50.

NICHOLSON, J.A.M., STOLZ, J.F., and PIERSON, B.K., 1987, Structure of a microbial mat at Great Sippewissett Marsh, Cape-Cod, Massachusetts: Fems Microbiology Ecology, v. 45, p. 343-364.

PAERL, H.W., STEPPE, T.F., and REID, R.P., 2001, Bacterially mediated precipitation in marine stromatolites: Environmental Microbiology, v. 3, p. 123-130.

PARKER, B.C., SIMMONS, G.M., JR., LOVE, F.G., WHARTON, R.A., JR., and SEABURG, K.G., 1981, Modern stromatolites in Antarctic Dry Valley Lakes: BioScience, v. 31, p. 656-661.

PEREZ, L., BUGJA, R., LORENSCHAT, J., BRENNER, M., CURTIS, J., HOELZMANN, P., ISLEBE, G., SCHARF, B., and SCHWALB, A., 2011, Aquatic ecosystems of the Yucatan Peninsula (Mexico), Belize, and Guatemala: Hydrobiologia, v. 661, p. 407-433, doi: 10.1007/s10750-010-0552-9.

PERRI, E., and SPADAFORA, A., 2011, Evidence of microbial biomineralization in modern and ancient stromatolites, *in* Tewari, V.C., Seckbach, J., ed., Stromatolites: Interaction of Microbes with Sediments: Springer Dordrecht Heidelberg, New York, p. 633-649.

PERRY, E., PAYTAN, A., PEDERSEN, B., and VELAZQUEZ-OLIMAN, G., 2009, Groundwater geochemistry of the Yucatan Peninsula, Mexico: constraints on stratigraphy and hydrogeology: Journal of Hydrology, v. 367, p. 27-40, doi: 10.1016/J.Jhydrol.2008.12.026.

PERRY, E., VELAZQUEZ-OLIMAN, G., and MARIN, L., 2002, The hydrogeochemistry of the karst aquifer system of the northern Yucatan Peninsula, Mexico: International Geology Review, v. 44, p. 191-221.

PETRASH, D.A., GINGRAS, M.K., LALONDE, S.V., ORANGE, F., PECOITS, E., and KONHAUSER, K.O., 2012, Dynamic controls on accretion and lithification of modern gypsum-dominated thrombolites, Los Roques, Venezuela: Sedimentary Geology, v. 245–246, p. 29-47, doi: http://dx.doi.org/10.1016/j.sedgeo.2011.12.006.

PLANAVSKY, N., and GINSBURG, R.N., 2009, Taphonomy of Modern Marine Bahamian Microbialites: Palaios, v. 24, p. 5-17, doi: Doi 10.2110/Palo.2008.P08-001r.

PLANAVSKY, N.J., REID, R.P., LYONS, T.W., MYSHRALL, K.L., and VISSCHER, P.T., 2009, Formation and diagenesis of modern marine calcified cyanobacteria: Geobiology, v. 7, p. 566-576, doi: 10.1111/J.1472-4669.2009.00216.X.

PRATT, B.R., 1979, Early Cementation and Lithification in Inter-Tidal Cryptalgal Structures, Boca Jewfish, Bonaire, Netherlands Antilles: Journal of Sedimentary Petrology, v. 49, p. 379-386.

PRATT, B.R., 1982, Stromatolite decline - a reconsideration: Geology, v. 10, p. 512-515.

PRINGAULT, O., DE WIT, R., and CAMOIN, G., 2005, Irradiance regulation of photosynthesis and respiration in modern marine microbialites built by benthic cyanobacteria in a tropical lagoon (New Caledonia): Microb Ecol, v. 49, p. 604-16, doi: 10.1007/s00248-004-0102-y.

RASMUSSEN, K.A., MACINTYRE, I.G., and PRUFERT, L., 1993, Modern stromatolite reefs fringing a brackish coastline, Chetumal Bay, Belize: Geology, v. 21, p. 199-202.

READ, J.F., 1976, Chapter 3.1 Calcretes and Their Distinction from Stromatolites, *in* Walter, M.R., ed., Developments in sedimentology: Elsevier, p. 55-71.

REID, R.P., JAMES, N.P., MACINTYRE, I.G., DUPRAZ, C.P., and BURNE, R.V., 2003, Shark Bay stromatolites: microfabrics and reinterpretation of origins: Facies, v. 49, p. 299-324.

REID, R.P., MACINTYRE, I.G., BROWNE, K.M., STENECK, R.S., and MILLER, T., 1995, Modern marine stromatolites in the Exuma-Cays, Bahamas - uncommonly common: Facies, v. 33, p. 1-17.

REID, R.P., VISSCHER, P.T., DECHO, A.W., STOLZ, J.F., BEBOUT, B.M., DUPRAZ, C., MACINTYRE, L.G., PAERL, H.W., PINCKNEY, J.L., PRUFERT-BEBOUT, L., STEPPE, T.F., and DESMARAIS, D.J., 2000, The role of microbes in accretion, lamination and early lithification of modern marine stromatolites: Nature, v. 406, p. 989-992.

REITNER, J., 1993, Modern cryptic microbialite/metazoan facies from Lizard Island (Great Barrier Reef, Australia) formation and concepts: Facies, v. 29, p. 3-39.

RICHERT, L., GOLUBIC, S., LE GUEDES, R., HERVE, A., and PAYRI, C., 2006, Cyanobacterial populations that build 'kopara' microbial mats in Rangiroa, Tuamotu Archipelago, French Polynesia: European Journal of Phycology, v. 41, p. 259-279.

RIDGWELL, A., and ZEEBE, R.E., 2005, The role of the global carbonate cycle in the regulation and evolution of the Earth system: Earth and Planetary Science Letters, v. 234, p. 299-315.

RIDING, R., 1991, Classification of microbial carbonates, *in* Riding, R., ed., Calcareous Algae and Stromatolites: Springer-Verlag, Berlin, p. 21-51.

RIDING, R., 1997, Stromatolite decline: a brief reassessment: Facies, v. 36, p. 227-230.

RIDING, R., 1999, The term stromatolite: towards an essential definition: Lethaia, v. 32, p. 321-330.

RIDING, R., 2000, Microbial carbonates: the geological record of calcified bacterial-algal mats and biofilms: Sedimentology, v. 47, p. 179-214.

RIDING, R., 2006, Cyanobacterial calcification, carbon dioxide concentrating mechanisms, and Proterozoic-Cambrian changes in atmospheric composition: Geobiology, v. 4, p. 299-316, doi: 10.1111/J.1472-4669.2006.00087.X.

RIDING, R., 2006, Microbial carbonate abundance compared with fluctuations in metazoan diversity over geological time: Sedimentary Geology, v. 185, p. 229-238, doi: Doi 10.1016/J.Sedgeo.2005.12.015.

RIDING, R., 2011, Microbialites, stromatolites, and thrombolites, in Reitner, J., and Thiel, V. eds., Encyclopedia of Geobiology: Springer, Netherlands, p. 635-654.

RIDING, R., 2011, The nature of stromatolites: 3,500 million years of histroy and a century of research, *in* Reitner, J., Quéric, N-VB, Arp, G., ed., Advances in Stromatolite Geobiology: Springer, Heidelberg, p. 29-74.

RIDING, R., and LIANG, L.Y., 2005, Geobiology of microbial carbonates: metazoan and seawater saturation state influences on secular trends during the Phanerozoic:

Palaeogeography Palaeoclimatology Palaeoecology, v. 219, p. 101-115, doi: Doi 10.1016/J.Palaeo.2004.11.018.

SABATER, S., 2000, Structure and architecture of a stromatolite from a Mediterranean stream: Aquatic Microbial Ecology, v. 21, p. 161-168.

SCHIDLOWSKI, M., 2000, Carbon isotopoes and microbial sediments, *in* Riding, R., and Awramik, S.M., eds., Microbial sediments: Springer-Verlag, Berlin, p. 84-95.

SCHIEBER, J., 1999, Microbial mats in terrigenous clastics: the challenge of identification in the rock record: Palaios, v. 14, p. 3-12, doi: 10.2307/3515357.

SCHOPF, J.W., 1993, Microfossils of the Early Archean Apex Chert - New Evidence of the Antiquity of Life: Science, v. 260, p. 640-646, doi: Doi 10.1126/Science.260.5108.640.

SCHOPF, J.W., 2006, Fossil evidence of Archaean life: Philosophical Transactions of the Royal Society B-Biological Sciences, v. 361, p. 869-885, doi: Doi 10.1098/Rstb.2006.1834.

SCHOPF, J.W., and BLACIC, J.M., 1971, New Microorganisms from the Bitter Springs Formation (Late Precambrian) of the North-Central Amadeus Basin, Australia: Journal of Paleontology, v. 45, p. 925-960, doi: 10.2307/1302822.

SCHOPF, J.W., KUDRYAVTSEV, A.B., CZAJA, A.D., and TRIPATHI, A.B., 2007, Evidence of archean life: stromatolites and microfossils: Precambrian Research, v. 158, p. 141-155, doi: 10.1016/J.Precamres.2007.04.009.

SCHUBERT, J.K., and BOTTJER, D.J., 1992, Early Triassic Stromatolites as Post Mass Extinction Disaster Forms: Geology, v. 20, p. 883-886, doi: Doi 10.1130/0091-7613(1992)020<0883:Etsapm>2.3.Co;2.

SEMIKHATOV, M.A., GEBELEIN, C.D., CLOUD, P., AWRAMIK, S.M., and BENMORE, W.C., 1979, Stromatolite Morphogenesis - Progress and Problems: Canadian Journal of Earth Sciences, v. 16, p. 992-1015.

SHAPIRO, R.S., 2000, A comment on the systematic confusion of thrombolites: Palaios, v. 15, p. 166-169.

SHEN, J.W., and WANG, Y., 2008, Modern microbialites and their environmental significance, Meiji reef atoll, Nansha (Spratly) Islands, South China Sea: Science in China Series D-Earth Sciences, v. 51, p. 608-617.

SILVA, J.J.R.F.S.D., and WILLIAMS, R.J.P., 2001, The biological chemistry of the elements : the inorganic chemistry of life: Oxford University Press, Oxford ; New York, xvii, 575 p. p.

SILVER, S., 1998, Genes for all metals - a bacterial view of the periodic table - the 1996 thom award lecture: Journal of Industrial Microbiology & Biotechnology, v. 20, p. 1-12.

SIMKISS, K., and WILBUR, K.M., 1989, Biomineralization : cell biology and mineral deposition: Academic Press, San Diego, xiv, 337 p.

SMN, 2000, Normales climatógicas de San Felipe Bacalar, Quintana Roo: Servicio Meteorologico Nacional

STAL, L.J., 2000, Cyanobacterial mats and stromatolites, *in* Whitton, B.A., Potts, M., ed., The Ecology of Cyanobacteria Their Diversity in Time and Space: Kluwer Academic Publisher, Dordrecht, p. 61-120.

STOLZ, J.F., 1985, The Microbial Community at Laguna Figueroa, Baja-California Mexico - from Miles to Microns: Origins of Life and Evolution of the Biosphere, v. 15, p. 347-352.

THRAILKILL, J., 1976, Chapter 3.2 Speleothems, *in* Walter, M.R., ed., Developments in sedimentology: Elsevier, p. 73-86.

VASCONCELOS, C., WARTHMANN, R., MCKENZIE, J.A., VISSCHER, P.T., BITTERMANN, A.G., and VAN LITH, Y., 2006, Lithifying microbial mats in Lagoa Vermelha, Brazil: Modern Precambrian relics?: Sedimentary Geology, v. 185, p. 175-183.

VISSCHER, P.T., REID, R.P., and BEBOUT, B.M., 2000, Microscale observations of sulfate reduction: Correlation of microbial activity with lithified micritic laminae in modern marine stromatolites: Geology, v. 28, p. 919-922, doi: Doi 10.1130/0091-7613(2000)28<919:Moosrc>2.0.Co;2.

VISSCHER, P.T., REID, R.P., BEBOUT, B.M., HOEFT, S.E., MACINTYRE, I.G., and THOMPSON, J.A., 1998, Formation of lithified micritic laminae in modern marine stromatolites (Bahamas): the role of sulfur cycling: American Mineralogist, v. 83, p. 1482-1493.

WALTER, M.R., 1976, Chapter 3.3 Geyserites of Yellowstone National Park: An Example of Abiogenic "Stromatolites", *in* Walter, M.R., ed., Developments in sedimentology: Elsevier, p. 87-112.

WALTER, M.R., BUICK, R., and DUNLOP, J.S.R., 1980, Stromatolites 3,400-3,500 Myr Old from the North-Pole Area, Western-Australia: Nature, v. 284, p. 443-445, doi: Doi 10.1038/284443a0.

WALTER, M.R., and HEYS, G.R., 1985, Links between the rise of the metazoa and the decline of stromatolites: Precambrian Research, v. 29, p. 149-174.

WESTALL, F., DE RONDE, C.E.J., SOUTHAM, G., GRASSINEAU, N., COLAS, M., COCKELL, C.S., and LAMMER, H., 2006, Implications of a 3.472-3.333 Gyr-old subaerial microbial mat from the Barberton greenstone belt, South Africa for the UV environmental conditions on the early Earth: Philosophical Transactions of the Royal Society B-Biological Sciences, v. 361, p. 1857-1875, doi: Doi 10.1098/Rstb.2006.1896.

WINSBOROUGH, B.M., and GOLUBIC, S., 1987, The role of diatoms in stromatolite growth - Two examples from modern fresh-water settings: Journal of Phycology, v. 23, p. 195-201.

WRAY, J.L., 1977, Calcareous algae: Developments in paleontology and stratigraphy: Elsevier Scientific Pub. Co., New York, xiv, 185 p. p.

Appendix S1

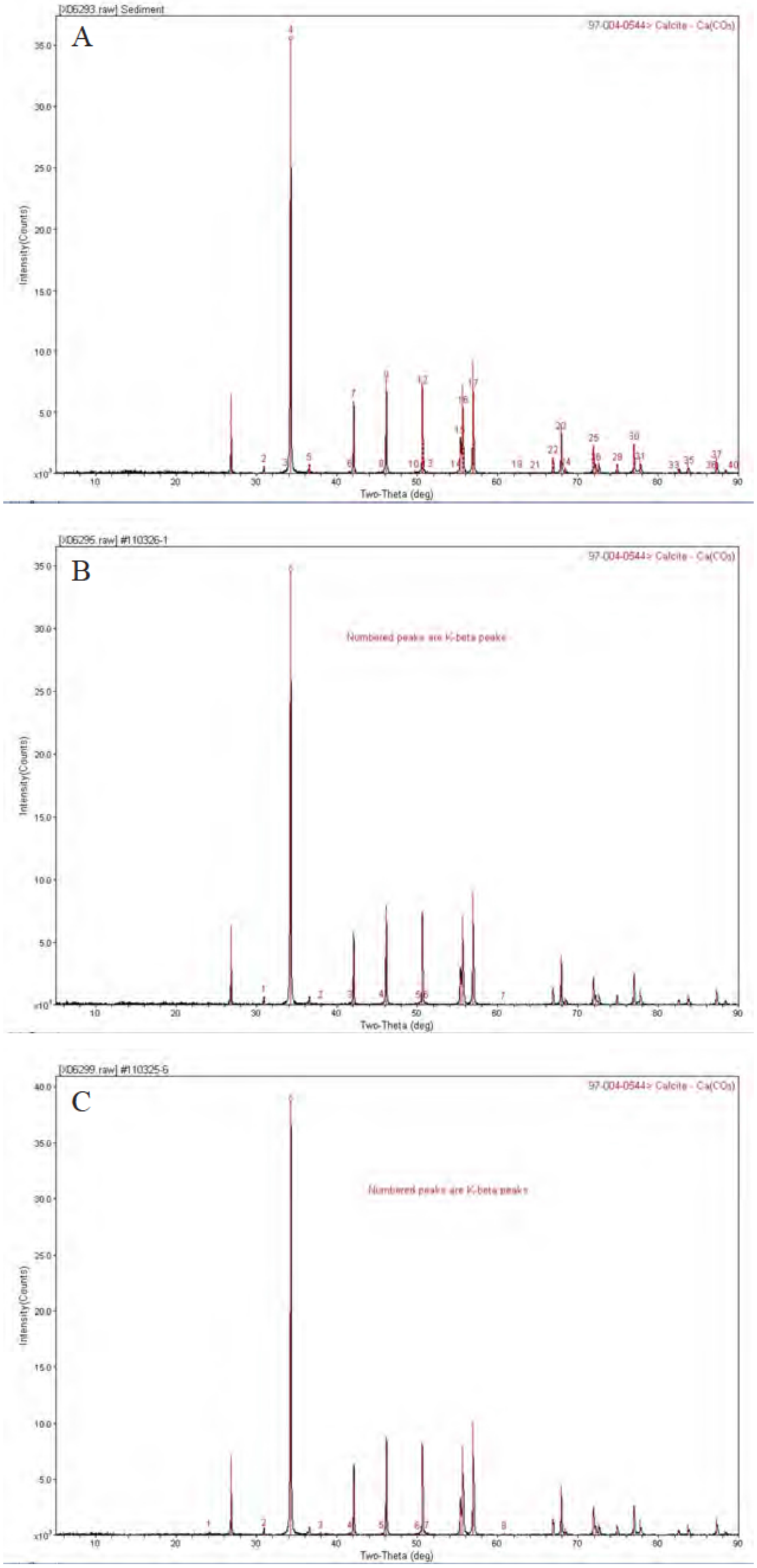
[XD6293.raw] Sediment
A
97-004-0544> Calcite - Ca(CO3)
Intensity(Counts)
x10³
Two-Theta (deg)
[XD6295.raw] #110326-1
B
97-004-0544> Calcite - Ca(CO3)
Numbered peaks are K-beta peaks
Intensity(Counts)
x10³
Two-Theta (deg)
[XD6299.raw] #110325-6
C
97-004-0544> Calcite - Ca(CO3)
Numbered peaks are K-beta peaks
Intensity(Counts)
x10³
Two-Theta (deg)